

DIPLOMARBEIT

**Urban micro-climate implications of Barcelona's Superblock strategy:
A computational assessment**

ausgeführt zum Zwecke der Erlangung des akademischen Grades

eines Diplom-Ingenieurs

unter der Leitung von

Univ.-Prof. Dr. Ardeshir Mahdavi

E 259/3 Abteilung für Bauphysik und Bauökologie

Institut für Architekturwissenschaften

eingereicht an der


Technischen Universität Wien

Fakultät für Architektur und Raumplanung

von

Eduardo Vidal Kume

Matrikelnr. 11713972



Wien, Mai 2020

KURZFASSUNG

Europäische Städte wurden von rekordverdächtigen Hitzewellen heimgesucht und es wird erwartet, dass dieses Phänomen noch häufiger, intensiver und länger auftreten wird. Besonders in südeuropäischen Regionen und in dichten städtischen Gebieten, wo das Auftreten von extremer Hitze durch urbane Wärmeinseln verstärkt wird, sind die Temperaturen angestiegen.

Extrem hohe Temperaturen sind eine der negativen Auswirkungen der Verstädterung, die in Verbindung mit der steigenden Luft- und Lärmbelastung zu einer Verschlechterung der physischen und psychischen Gesundheit der Bewohner führen kann. Die Auswirkungen betreffen nicht nur die Menschen, sondern führen auch zu einem sprunghaften Anstieg des Einsatzes von Klimaanlage, wodurch der Energieverbrauch steigt und zusätzliche Wärme an die unmittelbare Umgebung abgegeben wird.

In der katalanischen Hauptstadt Barcelona haben Stadtplaner das Projekt Superblocks vorgeschlagen, um den Autoverkehr zu verringern, das städtische Mikroklima zu verbessern und den allgemeinen Komfort im angrenzenden öffentlichen Raum zu erhöhen. Durch die Umwandlung von Nebenstraßen in öffentlichen Raum, der vorrangig von Fußgängern genutzt wird, wird der Autoverkehr innerhalb der Superblocks auf ein Minimum reduziert. Der neu geschaffene öffentliche Raum wird durch Grünflächen und städtische Einrichtungen ergänzt, die von den Bewohnern genutzt und genossen werden können.

Die echten Auswirkungen dieser zukunftsweisenden Stadterneuerung auf die gesamte Metropole sind noch nicht zu erkennen, aber die Effekte auf das städtische Mikroklima konnten mithilfe modernster Computersimulationen, insbesondere der CFD-Software ENVI-met, bewertet werden. Das Tool Urban Weather Generator wurde ebenfalls verwendet, um den Einfluss der Implementierung der Superblocks auf das städtische Mikroklima zu bewerten.

Die Methodik der Verwendung dieser beiden Tools wurde beschrieben und hinsichtlich der Bewertung des Mikroklimas in Superblocks bewertet, und die Anwendbarkeit der beiden verwendeten Berechnungsmethoden wurde verglichen.

Stichwörter

Microklima, Stadtklima, bauliche Umwelt, Mittelmeerklima, städtische Wärmeinsel

ABSTRACT

Every summer, European cities have been witnessing record-breaking heatwaves and this phenomenon is expected to be even more frequent, more intense, and with longer duration. The most significant increase in temperatures have in fact been observed in Southern European regions and in dense urban areas, where the occurrence of extreme heat is reinforced by Urban Heat Islands.

Extreme heat is one of the negative impacts of urbanization, which combined with increased air and sound pollution, might cause the deterioration in the physical and mental health of its inhabitants. The impact is not solely on people, but they also produce a surge in the use of air conditioning, increasing energy consumption and the release of extra heat to the immediate environment.

In the city of Barcelona, urban planners proposed the Superblocks project as a mean to decrease car usage, improve urban microclimate and the overall comfort of adjacent public space. By the conversion of side streets into public spaces that prioritize pedestrian use, the traffic of motor vehicles inside the Superblocks is reduced to a minimum. In the new created public spaces, greenery and urban equipment is added for the people to use and enjoyment.

The overall impact of this ground-breaking urban renewal in the metropolitan scale is yet to be seen but the urban microclimate effects could be already evaluated using state-of-the-art computational simulation, specifically the CFD ENVI-met software. The tool Urban Weather Generator was also used to evaluate the influence of the implementation of the Superblocks in the urban microclimate.

The methodology of using these two tools was described and evaluated regarding the assessment of microclimate in Superblock, and the applicability of the two employed computational methods were compared.

Keywords

Microclimate, Urban Climate, Built environment, Mediterranean Climate, Urban Heat Island

CONTENTS

1	Introduction.....	1
1.1	Overview	1
1.2	Motivation	2
1.3	Background	4
1.3.1	Literature Review.....	4
1.3.2	Historical Barcelona Climate.....	5
1.3.3	Barcelona and Climate Change	6
1.3.4	Urban Heat Islands (UHI)	10
1.3.5	Thermal comfort	11
1.3.5.1.	Predicted Mean Vote and Predicted percentage of dissatisfied	12
1.3.5.2.	Physiological Equivalent Temperature (PET)	13
1.3.6	The Superblock Masterplan	14
1.3.7	Description of the Study Area	17
2	Method	25
2.1	Weather data Acquisition	25
2.1.1	Raval Weather Station.....	25
2.1.2	El Prat Weather Station	26
2.1.3	Local Data Acquisition	26
2.2	ENVI-met Software	28
2.2.1	Calibration Simulations	30
2.2.1.1.	Computational Model Resolution Test.....	30
2.2.1.2.	Initial Boundary Condition Warm-up Test	34
2.2.1.3.	Lateral Boundary Condition Calibration Simulation	36
2.2.2	Simulation Conditions	37
2.2.2.1.	Weather data usage.....	37
2.2.2.2.	Solar Radiation adjustment	39
2.2.2.3.	Material Characteristics.....	39
2.2.2.4.	Anthropogenic heat gain	40

2.2.3	Simulation Models – ENVI-met	40
2.2.3.1.	Virtual Sensors.....	43
2.3	Urban Weather Generator	45
2.3.1	Model Set up	46
2.3.2	Area Characteristics	46
2.3.3	Building Characteristics	47
2.3.4	Anthropogenic heat gain: Traffic	47
2.3.5	Anthropogenic heat gain: Air conditioning.....	48
2.3.6	Simulation Models – UWG.....	48
3	Results	51
3.1	Overview	51
3.2	ENVI-met.....	51
3.2.1	2D Results from ENVI-met.....	51
3.2.2	Numerical Results – ENVI-met	71
3.3	Urban Weather Generator	78
4	Discussion	87
4.1	Overview	87
4.2	ENVI-met.....	87
4.2.1	Sant Antoni.....	87
4.2.2	Poblenou	88
4.3	Urban Weather Generator	89
5	Conclusion.....	90
6	Index.....	92
6.1	List of Figures	92
6.2	List of Tables	95
6.3	List of Equations	95
7	Literature	96

1 INTRODUCTION

1.1 Overview

As heat waves in temperate regions become stronger and more frequent, the effect of Urban Heat Island exacerbates it in urban areas and propels the use of air conditioning to unprecedented levels. The International Energy Agency (IEA, 2018) predicts that, by 2050, 5.5 billion households will have air conditioners, rising from under 1.8 billion in 2018.

The growing dependency on active cooling devices and health hazards caused by heat waves have attracted a growing interest of researchers in ways to mitigate these effects on an urban scale (Aleksandrowicz et al., 2017).

In this context, Superblocks (from the Catalan *Superilles*) are the ambitious proposal of Barcelona's urban planners to decrease car usage and improve microclimate and overall urban comfort. The objective is to mitigate some of the negative effects of bearing Europe's most densely populated areas (Eurostat, 2016). Inside the Superblocks, public space devoted to cars is reduced to a minimum and streets are transformed into mixed-use public space, which includes green areas.

The objective of this Master Thesis is to assess the local benefits of these projects in the urban microclimate, which affect the thermal comfort of pedestrians, nearby city-block dwellers and have the potential to influence the metropolitan climate. The research will focus on the modeling and simulation of already implemented Superblocks with the CFD Program ENVI-met, which was developed to investigate microclimate on an urban scale. A second tool, the Urban Weather Generator (UWG), developed by Bueno et al. (2013), was also used to assess the impact of the Superblocks and the influence of anthropogenic heat gains.

1.2 Motivation

The current levels of energy consumption with the present energy mix based mostly on fossil fuels (UNSD, 2018) cause the rise of the concentration of greenhouse gases, which consequently leads to historical high temperatures across the globe (EEA, 2019). According to NASA (2019), 2018 was the fourth hottest year since 1880, with 1.5°C warmer temperatures than the 1951-1980 average as shown in Figure 1.

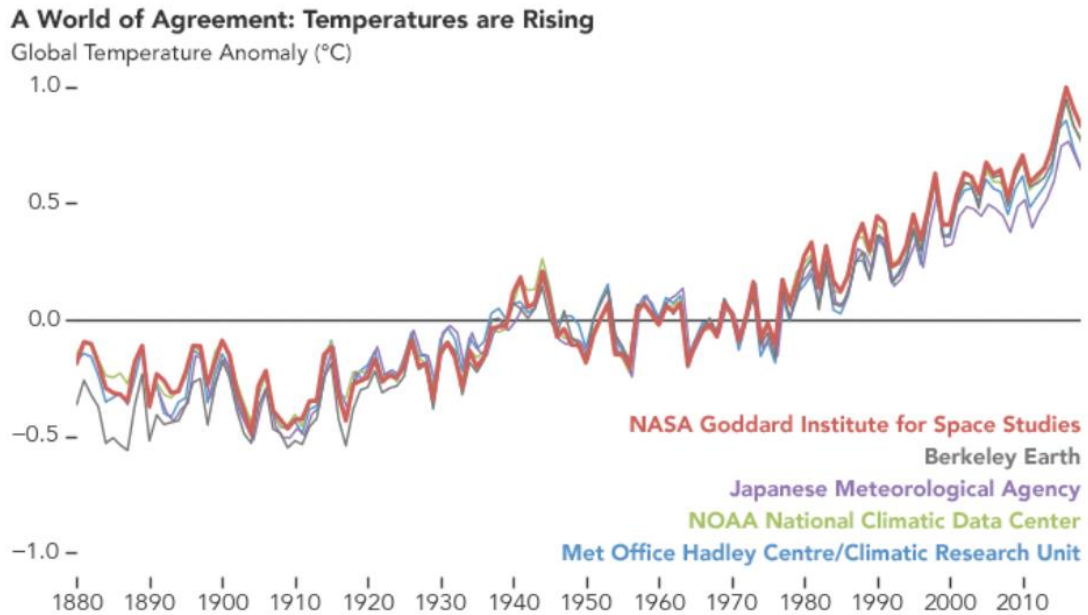


Figure 1. Global temperature anomaly 1880-2018 (NASA, 2019)

As half of the world population live in cities, and closer to three quarters in the developed world, the reduction of the environmental footprint of our urban areas is fundamental to decelerate the concentration of greenhouse gases.

Because of Global Warming, combined with the effects of Urban Heat Island (UHI) and the decrease in prices of manufactured goods, European capitals, and especially Mediterranean metropolis, have seen a rise in the use of air conditioning. According to IEA (2018), an increase of 25% was observed in the last 10 years. It is estimated that the largest annual impact in energy due to climate change and UHI will take place in temperate and mid-latitude climates, as artificial cooling will also be needed during autumn and spring (Salvati et al., 2017).

Additionally, the impact of UHI in energy consumption for cooling in Mediterranean cities might be as high as 24%. In Barcelona, between 18% to 28% of the current cooling loads in residential buildings could be justified by the increased heat due to UHI (Salvati et al., 2017). Besides the increase in energy demand for cooling, the

indiscriminate use of air conditioning exhausts heat to the surroundings, which aggravates the overall discomfort caused by the heat and decrease the efficiency of such cooling devices.

The opening of great avenues and boulevards was a common strategy for expanding European cities in the 19th century combined with the growing concern of universal access to natural sunlight and good urban ventilation. Continuing throughout the 20th century, the car-centric mode of urbanism was prevalent. Having followed this urban expansion model, Barcelona has currently noise pollution as a main concern, as over 40% of its inhabitants are exposed daily to noise over 65 dBA, which is the limit established by WHO (Barcelona, 2016).

Moreover, each of Barcelona's residents have, in average, less than one third of the 9 m² of green area per person recommended by the World Health Organization (WHO). The municipal document *Barcelona's Commitment to Climate* (Barcelona, 2015) reveals that the city plans to increase 1 m² of green space per inhabitant, which will only be possible with the multiple strategies manifested at *The Official Green and Environmental Plan for Barcelona 2020* (Barcelona, 2013): "Decks, roofs, balconies and walls are all elements within reach which are likely to be transformed into gardens or vegetable gardens for use by the community. They may also be converted into spaces for production and for carrying out healthy activities" (page 73).

According to the City of Barcelona (2016), there is an imbalance in the massive space reserved by individual transport in the city, even in its central areas; while representing only 25% of the journeys within the city, cars take up about 50% to 70% of the street space.

The implementation of Superblocks, focuses on mitigating some of the above mentioned issues (Barcelona, 2016). The first phase of the project consists of the incorporation of multiple blocks and the rerouting of car traffic around it. Within the Superblock, more than half of street area is converted to pedestrian and green space; by shadow and evaporative effects and use of less absorbing materials, this could positively affect thermal comfort in warmer days and, consequently, maybe reduce the energy consumption in cooling of the surrounding buildings.

Meanwhile, the comfortable use of the newly generated urban space can only be successful if an acceptable level of thermal comfort is reached. The study of the local impact in the thermal comfort of users and occupants and the reduction of energy consumption in cooling could be a motivating factor, besides the already perceived

noise reduction and expansion of green public space for inhabitants and tourists (Roberts, 2019).

In this regard, the relevance of this study relies on the simulated comparison between the pre and post implementation of the Superblock. Hence, the effect on the urban microclimate and the impact in the thermal comfort for pedestrians and inhabitants around the projects could be assessed.

1.3 Background

1.3.1 Literature Review

The use of CFD simulation and UWG in Mediterranean urban areas

Previous research using the software ENVI-met to calculate the impact of urban typology in the microclimate in the Mediterranean region has been done.

Achour-Younsi and Kharrat (2016) have studied the geometry of the urban street canyon in the city of Tunis. Using three distinct existing urban fabric typologies from distinct areas of Tunis' urban development (Medina, Colonial and Regulated), the calculated thermal comfort on a typical summer day was compared. It was concluded by the simulation that the typology presented on older parts of the city, with a higher height to width ratio of the street canyon, was the cooler and more comfortable to pedestrian. The orientation of the street presented a secondary role, being the North-South the most comfortable.

Tsoka et al. (2017) studied a typical urban street of the Greek city of Thessaloniki by modeling and simulating using ENVI-met. Two strategies to UHI mitigation were used, namely applying cool materials for street surfaces, and adding more trees. Additionally, the two strategies were combined. While both strategies reduced the temperature inside the urban canyon, it was pointed out that the use of materials of higher albedo on the ground might deteriorate thermal comfort as it increases radiative exchange and, consequently, the radiant temperature.

Ambrosini et al. (2014) used the ENVI-met software to simulate a portion of the historical city centre of Teramo and a nearby park. The effect of the UHI is evident both at night and during the day, as the build-up area presents higher temperatures than the park. Furthermore, the strategies of using cooler walls and green roofs were simulated. Higher temperatures were observed in the model with higher albedos than in the base case, as the radiative exchange between building walls increased.

An evaluation of the accuracy of ENVI-met in three internal courtyards of three different buildings in Sevilla, Spain, was performed by López-Cabeza et al. (2018). The results were not satisfactory, with great disparities between measured and simulated temperatures. These errors could come from the small scale of the attempted simulation, which clashed with the limited resolution of the software. The duration of the time frame of the simulation was also limited by computational resources and time.

The creating team of the Urban Weather Generator validated its results themselves for the cities of Bern, Toulouse and Singapore (Bueno et al., 2013). For Mediterranean climate, a validation of this tool was done by Salvati et al. (2016) for the city of Barcelona and Rome. The root mean square error this validations, between calculated and observed temperatures, was within the same range as the work done by Bueno et al. (2013), between 0.5 K and 1.5 K.

Repository on strategies for mitigating UHI

Aleksandrowicz et.al (2017) have created an extensive repository naming the numerous strategies for mitigating overheating in the urban microclimate that were presented in past bibliography between 2009 and 2013. The works within the collected bibliography mainly relied on simulation or monitoring and, more rarely, on both. The most common strategies presented in those studies were the use of cool envelope on buildings and vegetation, both on the ground and on roofs. Furthermore, most of the studies were performed using only one strategy, which would not be very useful for policy makers, who would need to decide between various strategies.

1.3.2 Historical Barcelona Climate

Barcelona presents a Mediterranean climate and, according to the Köppen climate classification, it falls into the Csa category: temperate with a dry or hot summer (Agencia, 2011). Figure 2 and Figure 3 below, from the State-owned Meteorological Agency, show the average and extreme monthly temperatures between 1971-2000 for the Barcelona airport.

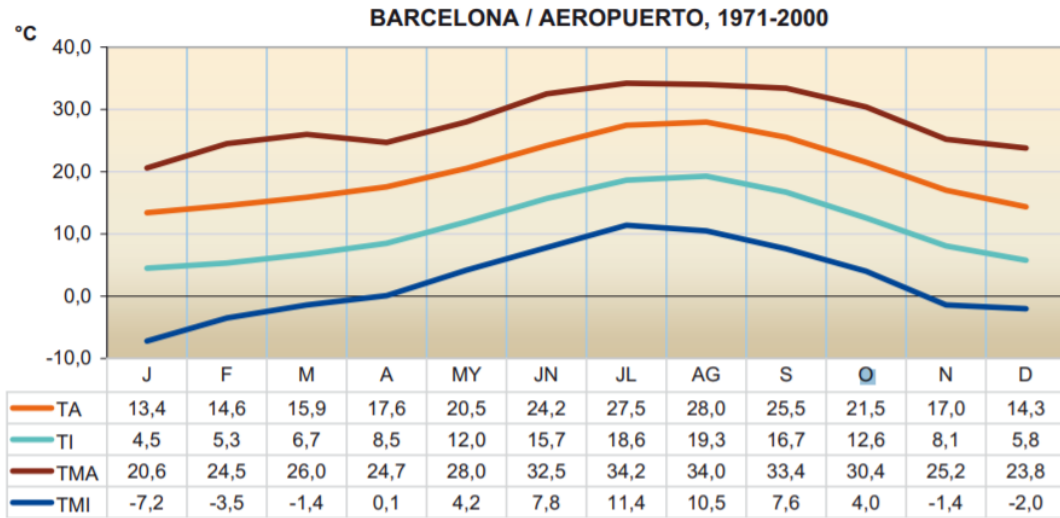


Figure 2. Barcelona average temperatures, 1971-2000 (Agencia, 2011)

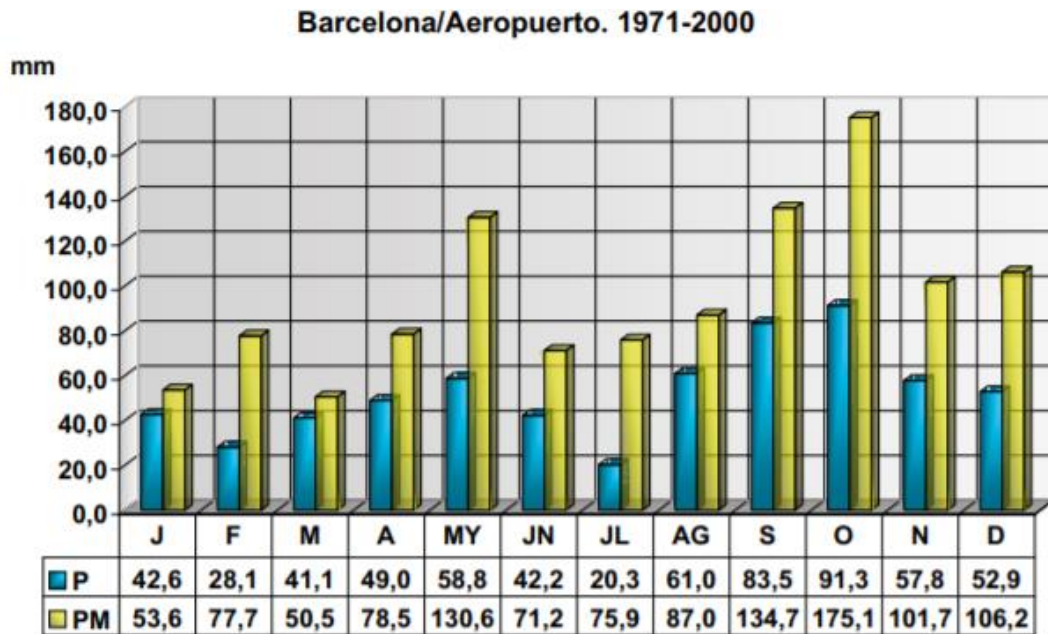


Figure 3. Barcelona average precipitation and maximum daily precipitation, 1971-2000 (Agencia, 2011)

1.3.3 Barcelona and Climate Change

Temperature Change between 1970 and 2019

Using the data set from the Barcelona Airport meteorological station, downloaded from January 1970 to December 2019 (Servei, 2019), we can assess some of the effects of climate change and UHI on the city.

The graphs in Figure 4 shows that, between 1970 and 2019, the number of months that had an average daily temperature above 24°C increased from one to twenty per

decade. Divided by the total number of months in each decade, the percentage value increased from 0.83% in the 1970's to 16.67% in the 2010's.

The graphs in Figure 5 shows that the number of months that had an average high temperature above 29°C increased from three to eleven per decade. Divided by the total number of months in each decade, the percentage value increased from 2.5% in the 1970's to 9.2% in the 2010's.

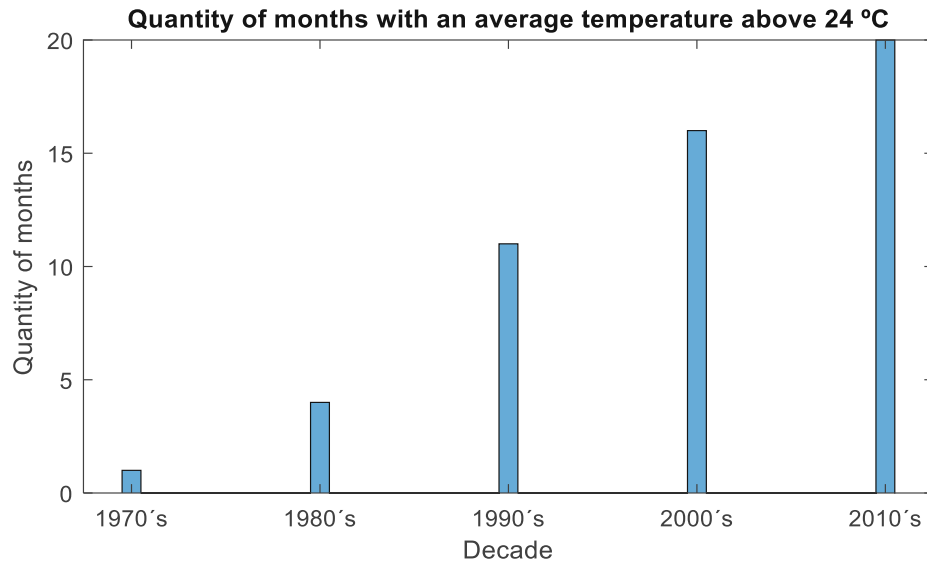


Figure 4. Histogram of the absolute number of months in each decade with an average daily temperature above 24°C

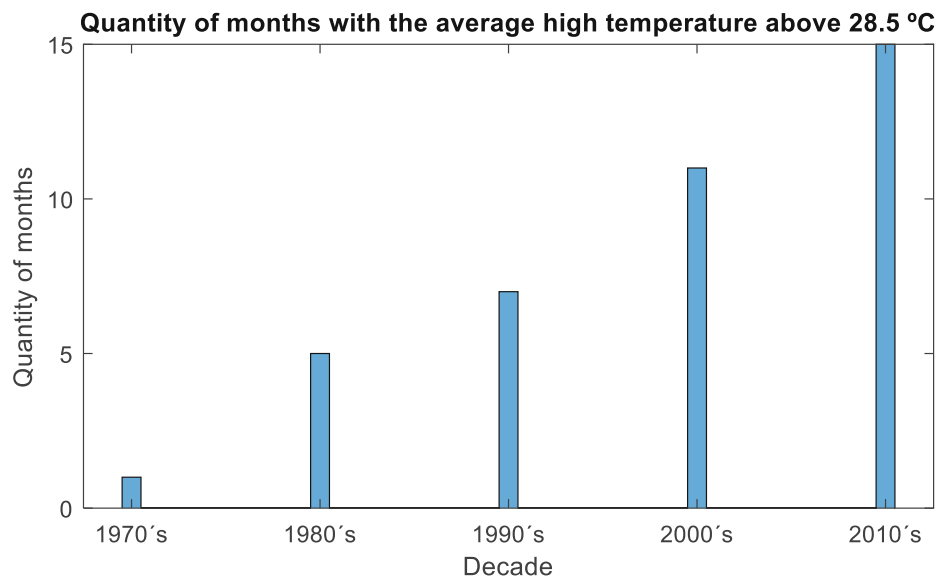


Figure 5. Histogram of the absolute number of months in each decade with an average high temperature above 29°C

The graphs presented in Figure 6 and 7 show cumulative histograms of the average monthly temperature between the decades of 1970's and 2010's. While in Figure 6, containing all the months of the year, there is a clear shift to the right as the decades advance indicates rising temperatures. The graph from Figure 7 shows an even more acute shift when only the months between June and September are analysed.

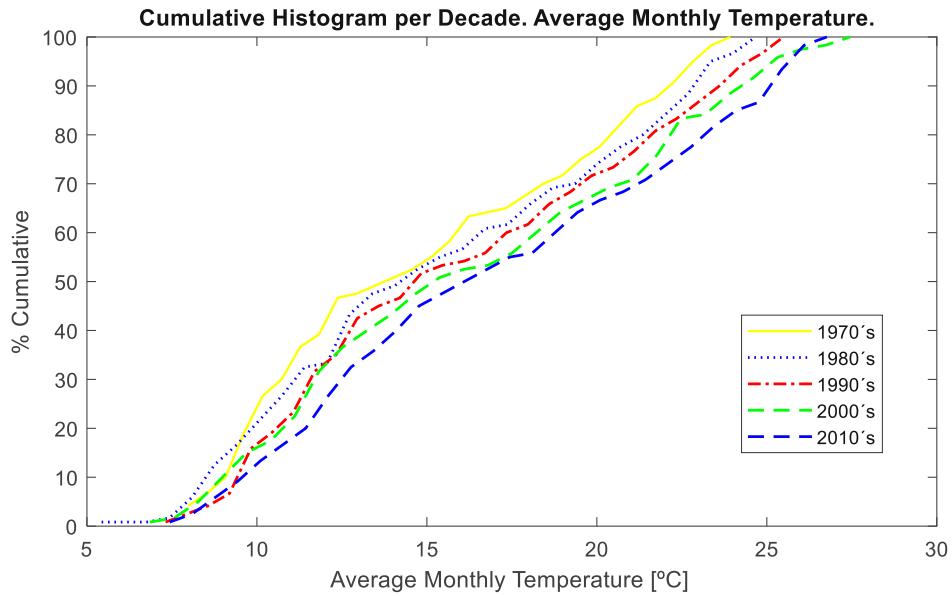


Figure 6. Cumulative Histogram per decade 1970 to 2010 of average monthly temperature

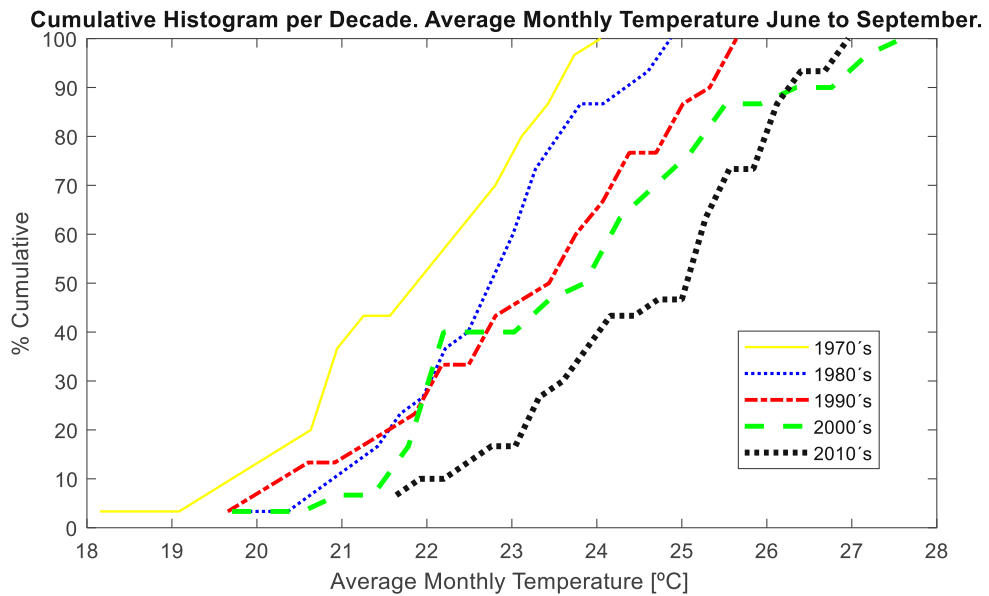


Figure 7. Cumulative Histogram per decade 1970 to 2010 of average monthly temperature.
Months from June to September

Predicted Temperature Increase

The Intergovernmental Panel on Climate Change, or IPCC, which is a body of the United Nations, has adopted standard scenarios that represent the projected concentration of Greenhouse to be used by scientist worldwide for climate modelling and research. The Representative Concentration Pathway (RCP) are named RCP2.6, RCP4.5, RCP6 and RCP8 and the numbers represent the possible values of radiative forcing for the year 2100 in Watts per square meters, and they vary between 2.6 W/m² to 8.0 W/m²; from the most optimist to the most pessimistic (IPCC, 2019).

Based on those scenarios, the Spanish Meteorological Agency (Agencia, 2011) published the predicted temperature increase for all of Spain. The graphs in Figure 8, Figure 9 and Figure 10 contain climatic projections for three of the four scenarios of greenhouse gases emissions, RCP4.5, RCP6.0 and RCP8.5, the base value is the twentieth century average.

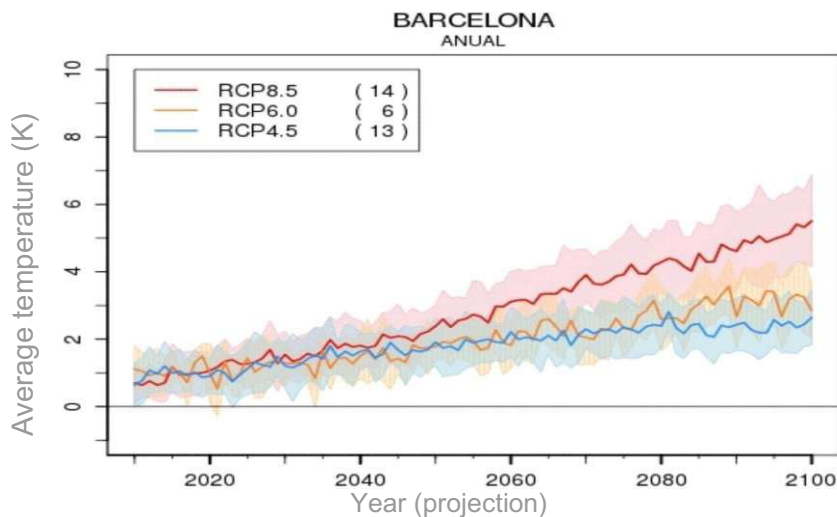


Figure 8. Projection of the average temperature increase [K] for Barcelona (Agencia, 2011)

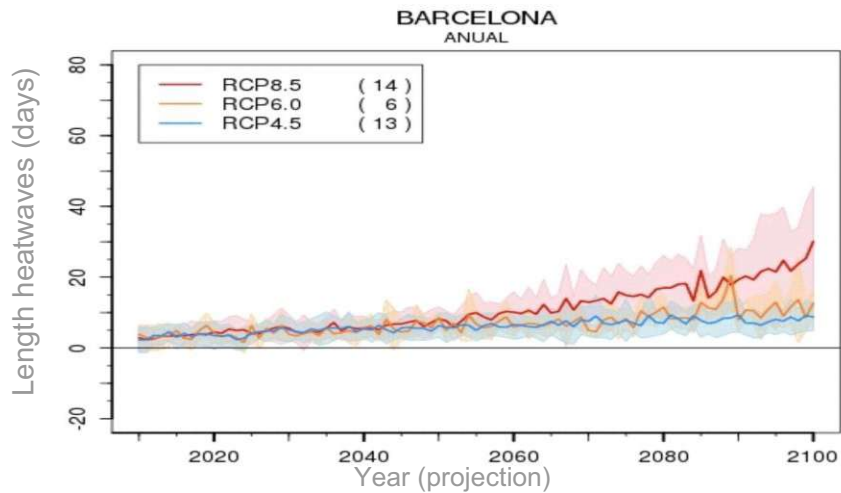


Figure 9. Projection of the length of heatwaves in days for Barcelona (Agencia, 2011)

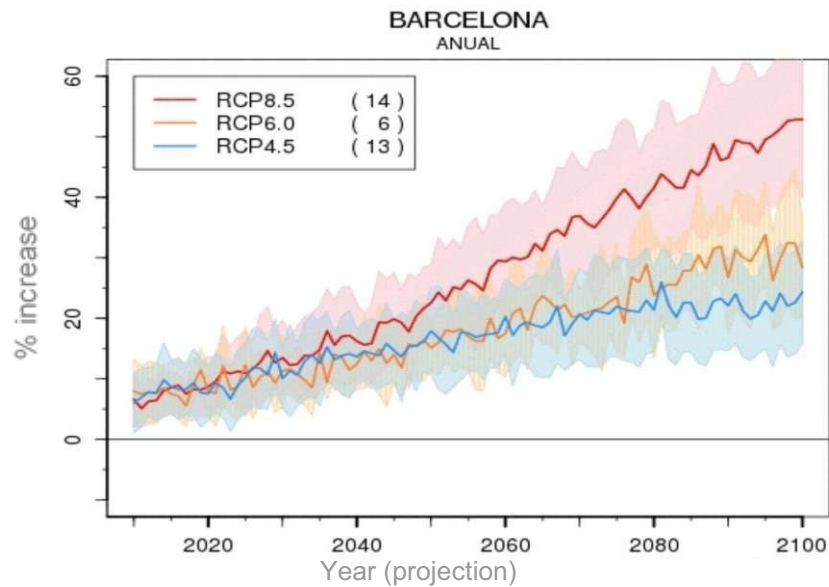


Figure 10. Projection of the increase in warm nights (above 20°C) in percentage for Barcelona (Agencia, 2011)

1.3.4 Urban Heat Islands (UHI)

Urban Heat Islands (UHI) is the phenomenon of higher measured air and surface temperature in city cores compared to the surrounding natural or rural environment. According to American Environmental Protection Agency (2008), UHI causes air temperatures to be around 1 K to 3 K higher in cities than in its surroundings during the day. Surface temperatures tend to be much higher, around 10 K to 15 K higher during the day and 5 K to 10 K higher during the night as dense construction materials have a large thermal capacity. Figure 11 shows the temperature profile of an urban area with its peak, especially during the night, in the denser urban center.

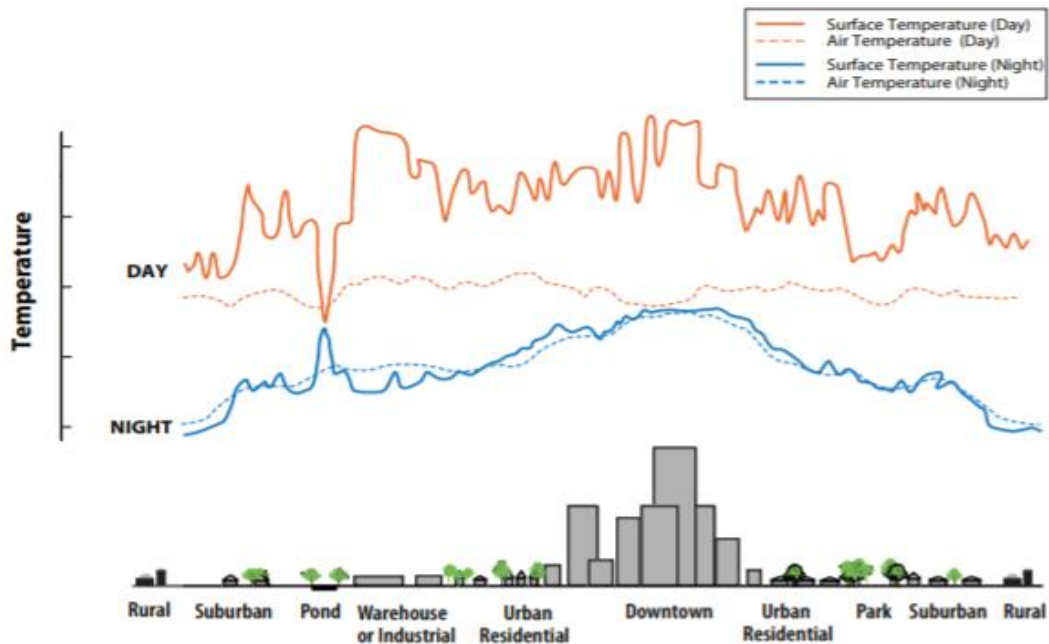


Figure 11. Schematic temperature profile of an urban area showing the UHI effect (EPA, 2008)

UHI measurement in Barcelona

Salvati (2017) evaluated the value of the UHI in Barcelona using the El Prat Airport Weather Station data as reference outside the urban fabric. This data was compared to the data from the station located in dense urban neighborhoods (Raval and Gràcia).

For the reference year of 2014, the peak in UHI was found in December, when a temperature increase of 2.8 K and 2.6 K was observed in Raval and Gràcia, respectively, during the nighttime (22:00 – 08:00 LST). In summer, the in UHI was found to be 1.7 K and 1.3 K at 04:00 LST in Raval and Gràcia, respectively. Explanation to the lower of UHI during the summer months is due to the stronger sea breeze present in hotter days, which helps equalize the urban temperature at roof level to the surrounding areas.

1.3.5 Thermal comfort

According to ASHRAE (2011), thermal comfort is a condition of mind that expresses a person's satisfaction with their thermal environment. It is a result of many variables, some are environmental, such as air temperature, mean radiant temperature, air velocity and relative humidity and others are dependants on the person state, such methaboloc rate and clothing. This variables are resumed in Figure 12.

1.3.5.1. Predicted Mean Vote and Predicted percentage of dissatisfied

Predicted Mean Vote (PMV) is an index that predicts the mean average self reported perception of the thermal conditions by a group of people in an environment. It is expressed in a scale of -3 (Cold) to +3 (Hot); zero being a sought after neutral grade.

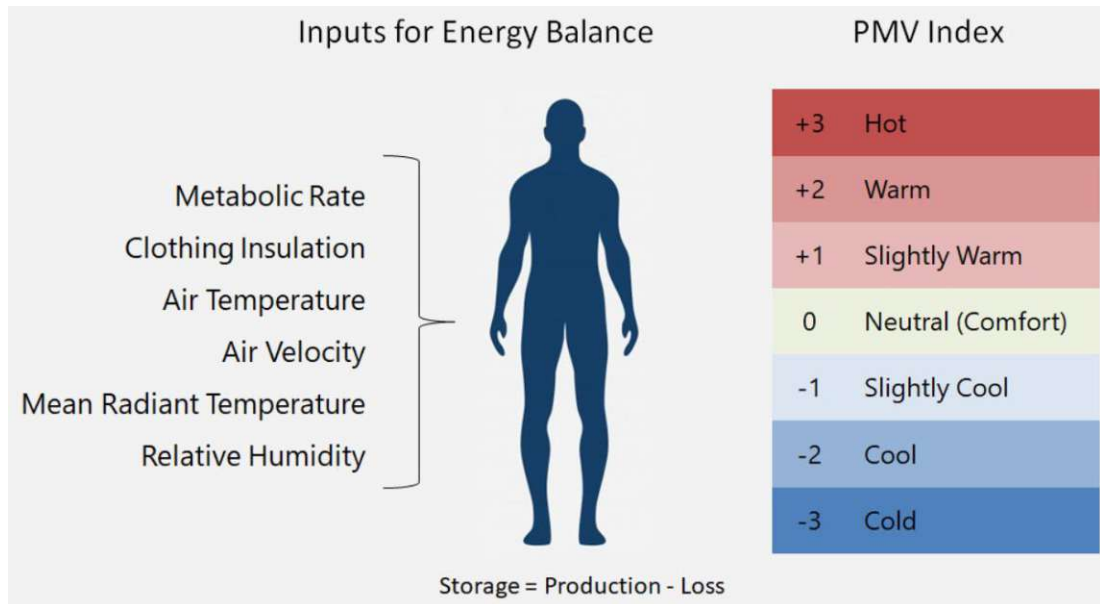


Figure 12. The variables affecting thermal comfort and the PMV scale (Kumar, 2019)

Predicted percentage of dissatisfied (PPD) is an index that predicts, given a thermal comfort condition in a room with a calculated PMV, the percentage of people that will be thermally dissatisfied. Both PDD and PMV have been widely used and their relation can be seen in Figure 13.

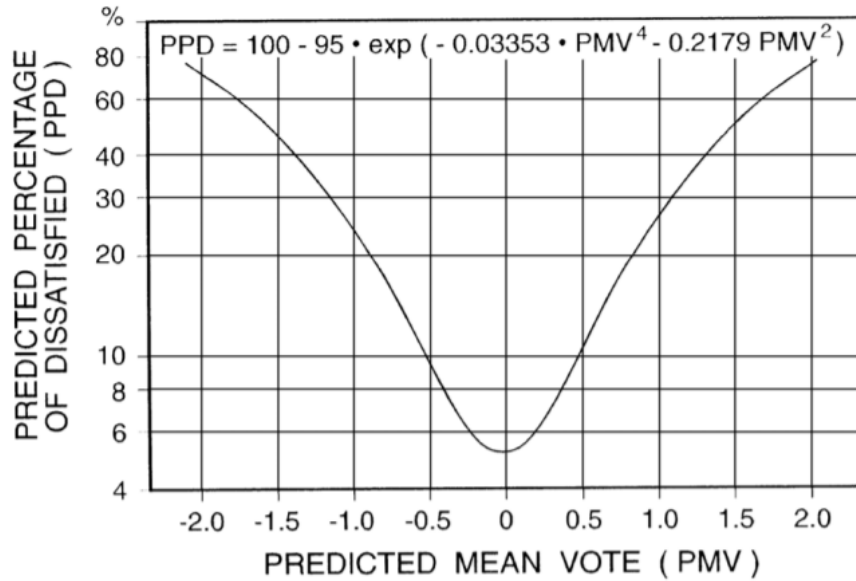


Figure 13. The relation between PPD and PMV (ASHRAE, 2011)

1.3.5.2. Physiological Equivalent Temperature (PET)

The Physiological Equivalent Temperature (PET), described by Höppe (1999) was based on the Munich Energy-balance Model for Individuals by the same author and it is a thermal comfort index that takes into account the complex variables of the external environment and human physiology to calculate an equivalent indoor air temperature at which the body reaches a heat balance of similar core and skin temperatures.

Another way to describe it is the temperature of a reference indoor environment that results in the same physiological response, therefore the same thermal stress to the occupant (Walther and Goestchel, 2018) as shown in Figure 14.

Some arguments that PET would be a more suitable index for outdoor temperature would be the limited use of PMV with radiant temperature outside the range of 10°C to 40°C (Walther and Goestchel, 2018). Secondly, PMV does not account for the direct sunlight and ventilation happening directly in exposed skin, which could be common in external environments during summer. Moreover, the PMV scale from -4 to +4 is too limited given that in a real outside environment those can be easily surpassed and should be assessed (ENVI-met, 2019).

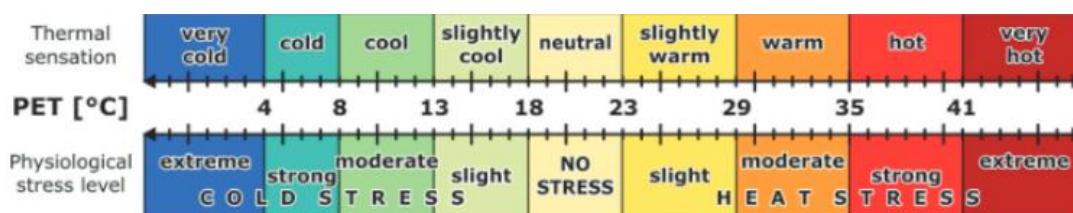


Figure 14. PET index threshold and corresponding sensation categories and levels of physical stress (Kántor, 2016).

1.3.6 The Superblock Masterplan

Challenging the issues of traffic noise and overuse of public space by cars, lack of green spaces and Urban Heat Island, the municipality of Barcelona has started to implement Superblocks. The Superblock is unique structural urban renewal plan that consists in the urban agglutination of traditional squared blocks into big areas in which the internal use of cars is decreased to a minimum, as show in Figure 15.

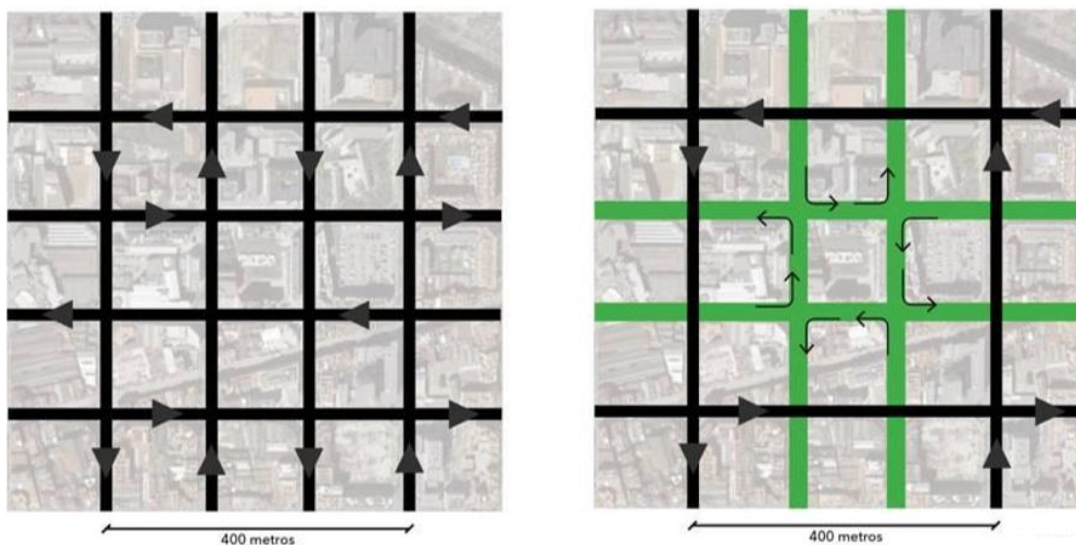


Figure 15. Schematic representation of the street traffic before and after the implementation of Superblocks (Rueda, 2016)

The scale of implementation is gradual, but the objective is that almost all city blocks and streets would be a part of the new street hierarchization as the Superblocks become the unitary blocks that build the new urban road structure. The plan in its full urban scale can be seen in Figure 16 and Figure 17, where the current road structure, with its length in kilometers and area in hectares, is compared to the future city plan.

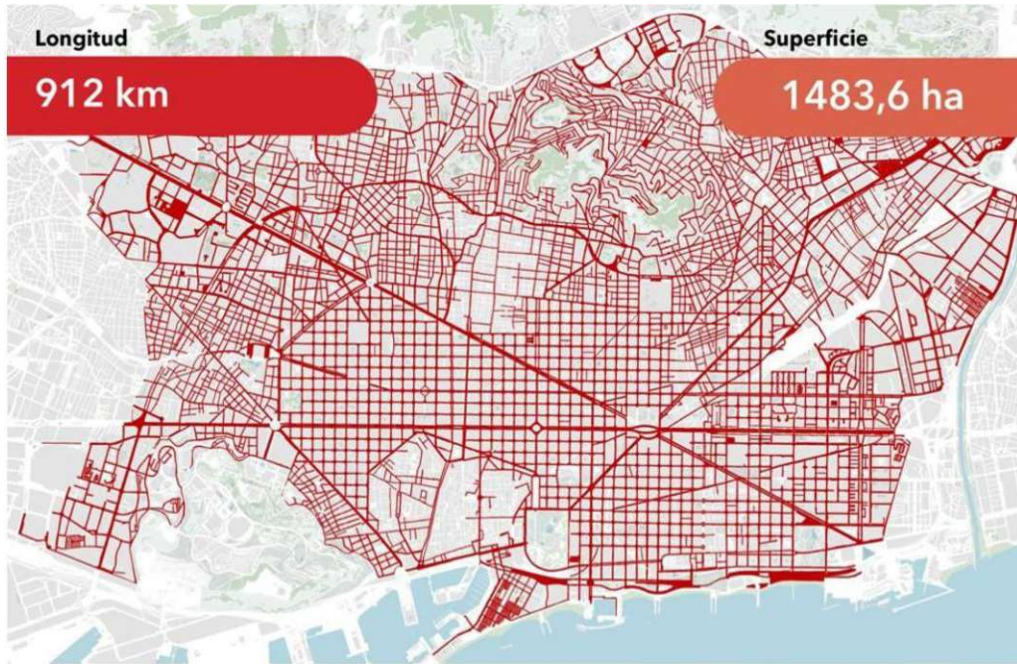


Figure 16. The current street network of Barcelona, with its total length and surface area (Rueda, 2016)

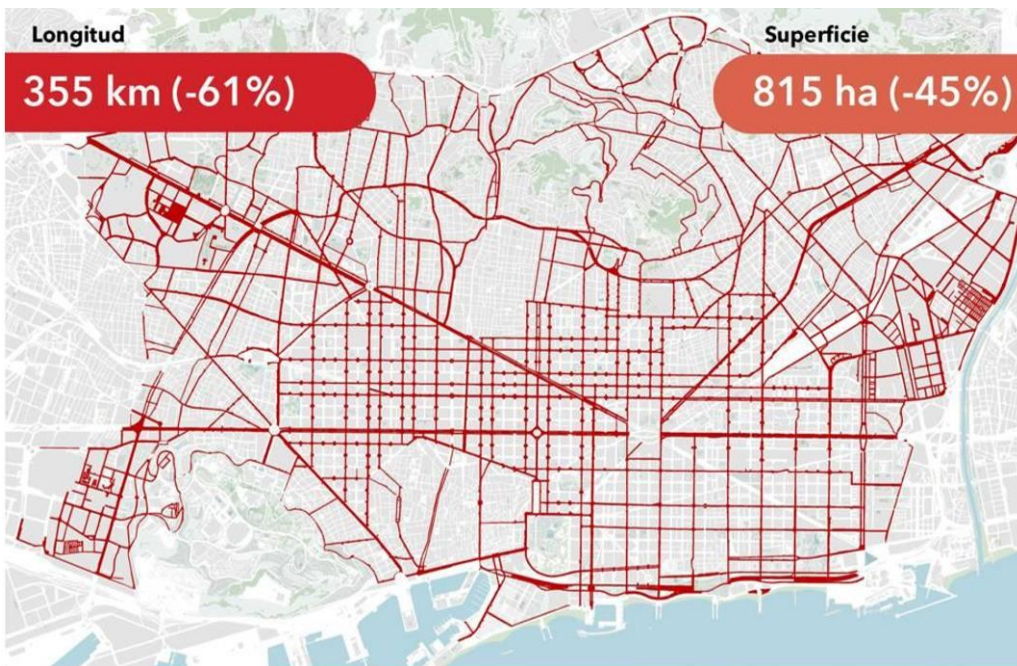


Figure 17. Proposed street network of Barcelona, after the implementation of all planned Superblocks, with its total length and surface area (Rueda, 2016)

All the freed space is allocated to green areas and pedestrian zones, the final projected gain will be of 6 million square meters of public pedestrian and green space. Furthermore, a reduction of 21% in car usage is predicted, encouraged by the

implementation of more public transport lines (Rueda, 2016). This will be a colossal structural change in the way the city works and how the environment is impacted.

The Masterplan from the Superblocks was presented on a strategic plan in 2016 by the Ecology, Urbanism and Mobility Commission of the City of Barcelona, describing it as a change in the urban planning paradigm intended to prepare the city to face new environmental challenges and a great opportunity to improve the quality of life of its inhabitants (Barcelona, 2016). Figure 18 shows a schematic view of an urban intersection, after the implementation of a Superblock where the gain of public and green space can clearly be noted.



Figure 18. Schematic isometric view of an urban intersection, before and after the implementation of a Superblock (Rueda, 2016)

Before 2019, five of the Superblocks had already been implemented, which created 100,000 m² of public space from where asphalt was and three more were to be carried out by the end of 2019, generating more 160,000 m² of new urban space for green area and pedestrians, according to the City of Barcelona (2019b).

Author Juliá studied in his Master Thesis at the School of Engineering of Roads, Bridges and Ports (2017) the financial impact of the Superblocks in traffic. However, the study “did not take into account the positive effect of the habitability index for public space, which is one of the main objectives of Barcelona’s Superblocks Project”. The social aspects of the gain in public space are not scope of this Master Thesis, but the assessment of the immediate microclimate is one of its goals.

1.3.7 Description of the Study Area

Below, in Figure 19, the location of the two Superblocks studied are shown. Sant Antoni is located just adjacent to the old town of Barcelona, while Poblenou is located at about 2.0 km east of the old town, marked red. Both Superblocks are both located about 1.5km from the Mediterranean Sea.



Figure 19. Location of the two studied Superblocks, the old town of Barcelona is highlighted in red (Google Maps, 2020)

Area 1 – Sant Antoni

The Superblock of Sant Antoni is in the district of the same name that extends for less than one square kilometer but accommodates more than 38 thousand inhabitants, with a resulting density of 47,900 inhabitants/km². It is one of the districts that make part of the Eixample area, which was urbanized in the decade of 1850 with the famous regular quadrangular blocks with chamfered corner from Ildefons Cerdà's urban plan. The center point of Sant Antoni area is the Sant Antoni market from 1882, around which the Superblock was developed (Barcelona, 2019b). Figure 20 shows the intervention area of the Superblock, including the block where the Sant Antoni market is located. From the aerial view it can be seen how consolidated this region is, with almost all terrains occupied to their maximum level.



Figure 20. The intervention area of the Sant Antoni Superblock (Google Maps, 2020)

The Superblock is formed by the union of 4 regular urban blocks, one of which contains only the market building and its surrounding open space; all the city blocks are fully developed, with buildings ranging from five to eight floors. During the urban renewal, the two streets separated the four blocks and the area around the market were transformed in pedestrian areas leveled with the sidewalk over an underground garage, covered with a new light gray pavement. It also included many flowerbeds with low and high vegetation. Permanent metal structures that cover temporary usages and events, such as weekend markets, were also built around the market. Figure 21 shows plans of the landscape project for the Sant Antoni Superblock, Figure 22 shows sections comparing the street canyon before and after the interventions.



Figure 21. Urban and landscape project of the Sant Antoni Superblock (Barcelona, 2019b)

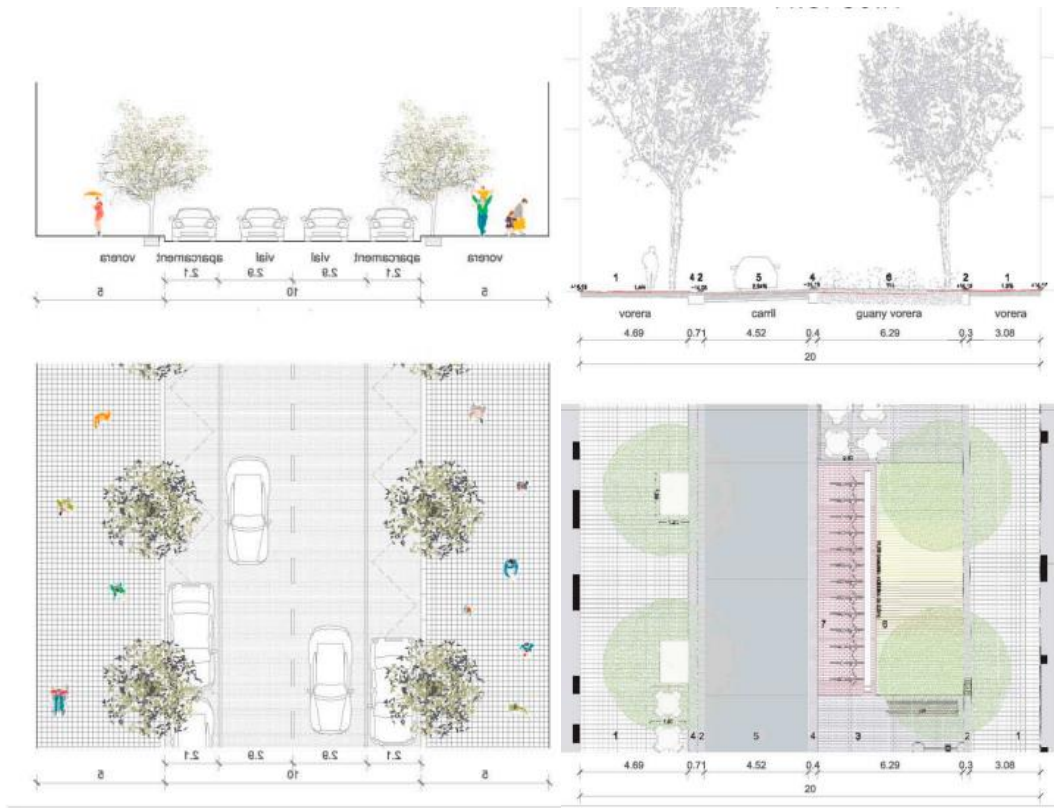


Figure 22. Sections of the street canyon comparing the original situation to the Superblock design (Barcelona, 2019b)

Figure 23 and Figure 24 show Tamarit street before (2013) and after (2019) the implementation of the Sant Antoni Superblock. Figure 25 and Figure 26 show the Sant Antoni market before (2009) and after (2019) the implementation of the same Superblock.



Figure 23. Tamarit Street before the implementation of the Sant Antoni Superblock in 2014
(Google Maps, 2020)



Figure 24. Tamarit Street after the implementation of the Sant Antoni Superblock in 2019



Figure 25. Corner of Tamarit Street and Comte Borrell streets before the implementation of the Sant Antoni Superblock in 2009 (Google Maps, 2020)



Figure 26. Corner of Tamarit Street and Comte Borrell streets after the implementation of the Sant Antoni Superblock in 2019 (Google Maps, 2020)

Area 2 – Poblenou

The Superblock of Poblenou is situated in the district of El Parc i La Llacuna del Poblenou, it houses 15 thousand people and has a populational density of 13,600 inhab./km² and is a part of the Poblenou area. From the XVII until the end the XX century, it had a strong industrial sector. According to the City of Barcelona (2019a), it housed the largest industrial concentration in Spain by the end of the XX century. In the last three decades, the 1992 Olympic Village was built in Poblenou, the technology-oriented Proyecto 22 was implemented in the area which has attracted many tech companies and new young inhabitants. Figure 27 shows the intervention

area of the Superblock, the city block that has the greenest area, which appears on the top part of the highlighted area, is where the Museum Can Framis is located. From the aerial view in Figure 27, it is noticeable that the urban typology is inhomogeneous, and the area is not yet consolidated, with some old industrial buildings still standing next to modern high risers.



Figure 27. The intervention area of the Poblenou Superblock (Google Maps, 2020)

The Superblock is formed by the union of 9 street blocks; being the first built Superblock, it was received with certain doubt and the urban renewal, even though planned to be permanent, was done using solutions of a temporary character. It can be noted how the intervention is less extreme than the Sant Antoni Superblock, the flowerbed and trees planters consist of large plastic pots and the separation between pedestrian and cars was done by painting the asphalt, not leveling the original street path. Figure 28 shows partial details of the Poblenou Superblocks plans.



Figure 28. Details of the implementation of the Poblenou Superblock (Barcelona, 2019b)

Figure 29 and Figure 30 show the corner of Roc de Boronat and Sancho de Ávila streets, before (2014) and after (2019) the implementation of the Poblenou Superblock.



Figure 29. Corner of Roc de Boronat and Sancho de Ávila streets, before the implementation of the Poblenou Superblock in 2014 (Google Maps, 2020)



Figure 30. Corner of Roc de Boronat and Sancho de Ávila streets, after the implementation of the Poble Nou Superblock in 2019

2 METHOD

2.1 Weather data Acquisition

The source of the used weather data was the Catalan Meteorological Service (Servei, 2019) and *in loco* measurement as described in section 2.1.3.

2.1.1 Raval Weather Station

Weather data from an automatic weather was used, situated on a rooftop of an 18-meter-high building in the old town of Barcelona, it is 800 meters from Superblock Sant Antoni and 2,800 meters from the Poblenou Superblock as Figure 31 shows. It is located at an altitude of 33 meter and has coordinates 41.38 N and 2.17 E. (Servei, 2019). The sensor of temperature and relative humidity are 1.7 meters above the terrace floor and the wind sensor is located 12 meters above the terrace floor, or 30 meter above the street level, Figure 32 shows in more detail how it is installed.



Figure 31. Location of the weather station relative to the studied areas (Google Maps, 2020)



Figure 32. More detailed view of the Raval weather station (Salvati et al., 2017)

2.1.2 El Prat Weather Station

The data from weather station at El Prat de Llobregat, located near the Barcelona International Airport, was once used as a rural weather reference by Salvati et al. (2017) to assess the magnitude of UHI in Barcelona. It is located at an altitude of 6 meters and has coordinates 41.28 N and 2.07 E. As Figure 33 shows, the weather station is located outside of the urban fabric.



Figure 33. El Prat de Llobregat weather station (Servei, 2019)

2.1.3 Local Data Acquisition

In the area of Sant Antoni, in a balcony on the Carrer de Tamarit as shown in Figure 34, a sensor/logger was placed to measure and record the temperature and relative humidity throughout a period of three days between 29/07/2019 and 01/08/2019.



Figure 34. Location of the installed sensor-logger (Google Maps, 2020)

The sensor was protected from direct sun radiation and rain with a hard cover, which was covered in aluminium foil, to avoid overheating under the sun. Between the sensor and the cover, an EPS layer was added to avoid heat transfer by direct conduction. The sensor was also shielded with aluminium foil, but two sides were left open for ventilation, as shown in Figure 35. The distance from the façade was about 80 cm and the height from the street level was of about 13 meters. The logger model is Elitech RC-51H, with a working range of -30 to $+70$ °C, with resolution of 0.1 °C in temperature and -1% in relative humidity and with accuracy of ± 0.5 °C in temperature and $\pm 3\%$ in relative humidity. The sensor recorded the data every 10 minutes. During the measured period, the weather was sunny with minimal cloud coverage and the temperatures were between 23.9 °C and 31.3 °C and relative humidity between 35.7% and 82% .



Figure 35. Installation of the sensor-logger

2.2 ENVI-met Software

The ENVI-met software, sold by the German company of the same name, simulates several thermodynamic variables in a three-dimensional microclimate model of an urban environment. Figure 36 shows the variables that influence the computational model of the simulation.

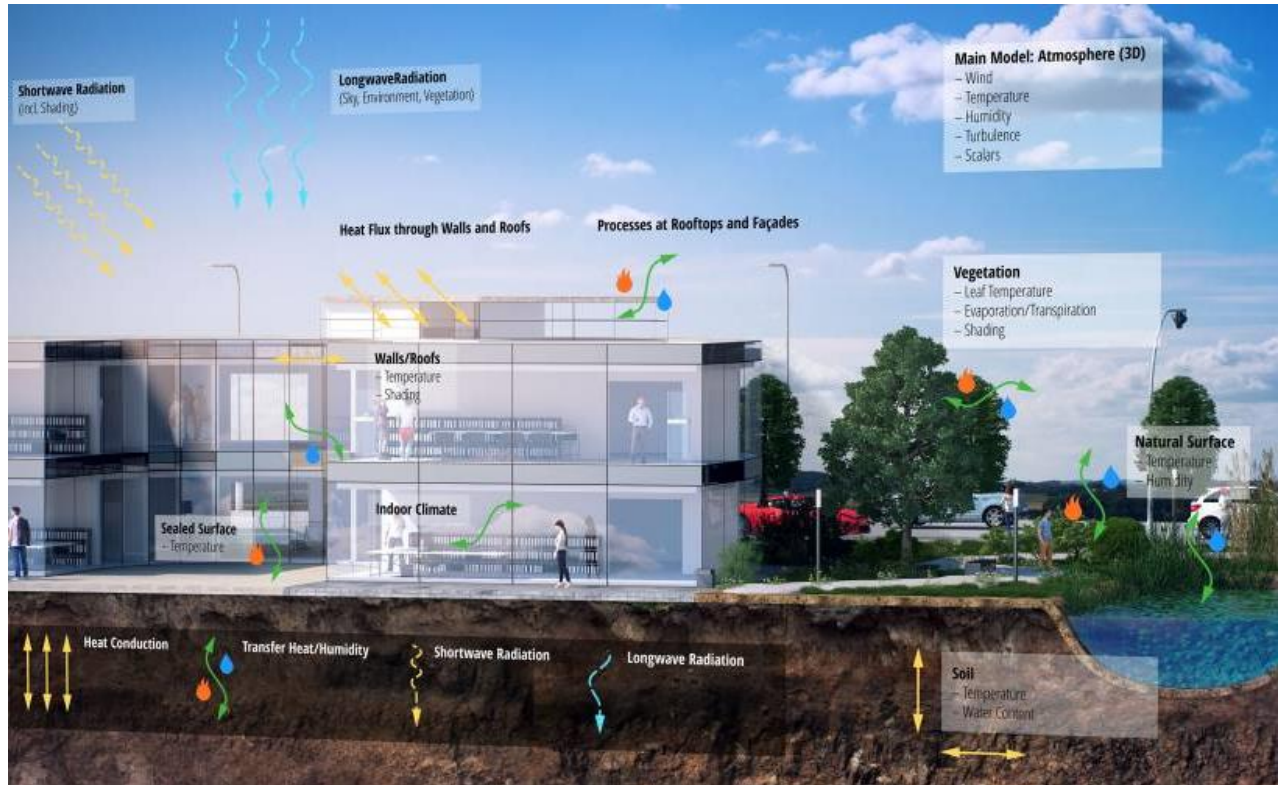


Figure 36. ENVI-met Model Architecture (ENVI-met, 2019)

The main calculation module of the software is the Atmospheric model, which consists of a full 3D Computational Fluid Dynamics (CFD) model that solves Reynolds-averaged non-hydrostatic Navier-Stokes equations for each time step. It calculates the temporal evolution of the atmosphere-plant-surface interaction in a non-hydrostatic model. (ENVI-met, 2019)

An ENVI-met version 4.4.3 with a Student License was used, which has an unlimited model size but a limited computational usage of only one core per simulation, which prolongs greatly the simulation time.

ENVI-met consists of different executable programs that can be opened and run independently but are organized by the main Headquarter module. In this main module projects can be created and saved, main configuration changed and Licenses management. It also serves to open the other Modules. In the ENVIGuide module the simulations are

configured. The ENVI_MET module is the main calculation module, and it checks, runs, and logs the simulations. Monde is used to transform vector-base data such as GIS and Open Street Maps into a grid-based data, to facilitate the creation of 3D ENVI-met models. BioMet module transforms the environmental data simulated results to evaluate thermal comfort by calculating Predicted Mean Vote (PMV), Predicted Percentage Dissatisfied (PPD), Physiological Equivalent Temperature (PET), Universal Thermal Climate Index (UTCI) and Standard Effective Temperature (SET). The LEONARDO module reads the data output of the simulation to create linear, 2D and 3D graphs and it also exports the data for statistical analysis.

In ENVI-met, the initial boundary conditions for air temperature are set the same to all atmospheric layers and the initial temperature is used for the constant reference temperature at 2,500m height. The relative humidity is initiated as a gradient calculated with the values at 2m and 2,500m height.

The lateral boundary conditions (LBC) can be configured in three ways, as Open LBC, in which the values of the next grid point close to the border are copied to the border for each time step, this option is not recommended to be used after version 4 of ENVI-met, as it causes numerical instability in the simulation. Forced (or closed) LBC, in which the values from the forcing data are copied to the border, it is the most stable LBC and is the recommended method in the ENVI-met documentation. Finally, there is the Cyclic LBC, in which the values leaving on one side of the model are copied to the border on the other side. Figure 38 shows a schematic diagram of the inputs and outputs of ENVI-met.

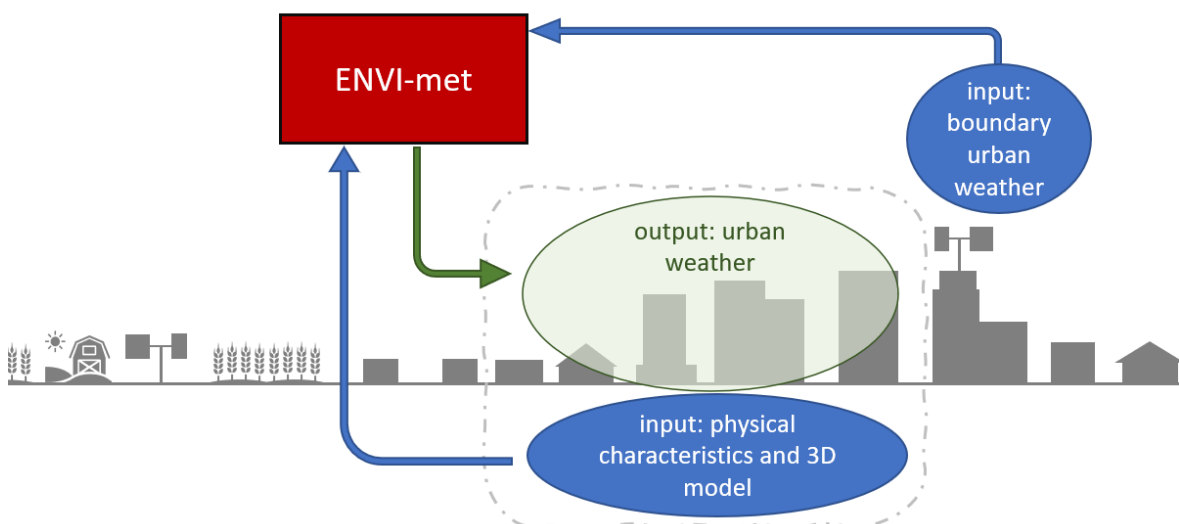


Figure 37. Schematic model of ENVI-met

2.2.1 Calibration Simulations

The area around the superblocks were 3-dimensionally modelled using exported OpenMaps 3D data, together with Google Earth satellite images and Landscape projects from the Barcelona Municipality Website (Barcelona, 2019b).

Before doing the final simulation for data acquisition and comparison, two tests were done to evaluate how the results would be sensitive to using different spatial resolutions and different duration of simulation.

For this test simulations, detailed plants and shading surfaces were not added to the 3D model.

2.2.1.1. Computational Model Resolution Test

According to the ENVI-met technical manual, a typical horizontal resolution for the 3D model should be between 0.5 m and 10 m. CFD simulation needs substantial computational resources, so the grid resolution was determined by comparative simulations in both modeled areas. From the researched literature cited in section 1.3.5, resolution between 2.5 m and 4.0 m was often used. This is a modified version of the method by Tsoka et al. (2017) to simulated in ENVI-met parts of the city of Thessaloniki.

The simulated Sant Antoni area consists of a square of size 340 m by 340 m and the Poblenou area has 400 m by 400 m. Both were simulated using a grid resolution of 2.5 m, 3 m and 4m. A resolution smaller than 2.5 m would result in a grid larger than 160 x 160 which would be too demanding for the available computational resource and the limitations of processor usage with a Student License. Extra cells near the boundaries, around the perimeter of the model should be added for accuracy of the atmospheric calculation, every building should be at a distance from the border of the model of at least its height.

The resolution in each of the 3 spatial coordinates is independent and the vertical grid was kept at 3 m until 21 m, roughly the height of one floor. Over 21 m, which is the average height of the buildings in the studied areas, the grid increased 30% for each cell, the first cell close to the floor is further divided into 5 vertical cells for better calculation at pedestrian level. There should be a free atmospheric space calculated over the buildings roughly the size of the taller building. ENVI-met checks the vertical and horizontal free cells available around the buildings but corrections are done manually.

The materials were not changed and left to the default values in this simulation, nor the vegetation was modeled. A period of 24 hours was simulated, starting at 7:00, as default and suggested by the ENVI-met documentation. The weather configuration was set to

“beginner “, and set to a hot summer day with boundary air temperatures between 22° and 34° with linear variation and average wind speed of 2.5 m/s.

Below, the 3 models with different resolutions (2.5 x 2.5, 3 x 3, and 4 x 4 meters) of each Superblock are shown in Figure 38 and Figure 39.

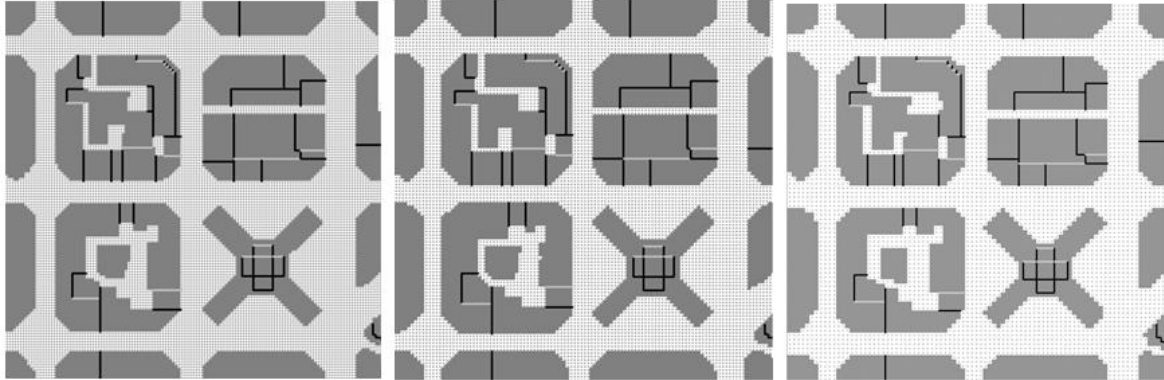


Figure 38. Sant Antoni ENVI-met models with 3 different resolutions

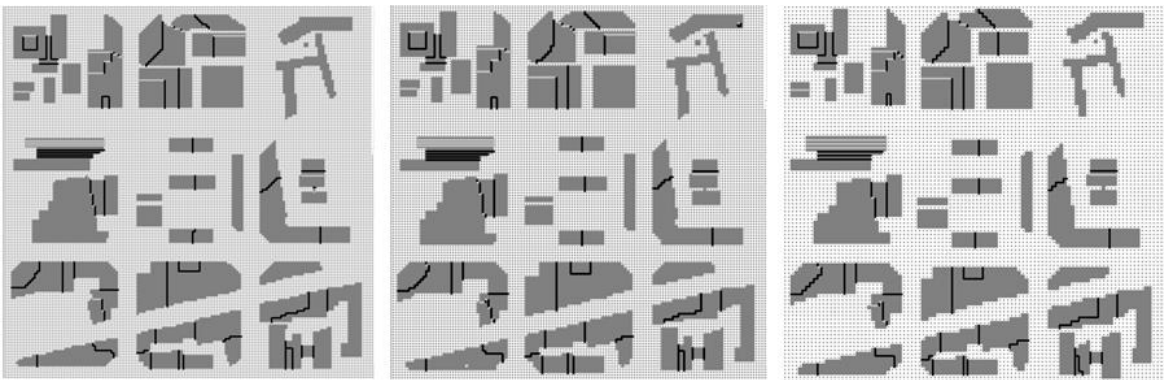


Figure 39. Poblenou ENVI-met models with 3 different resolutions

The simulated temperature at the center of the model at 1.5 m above ground was used for the comparison. The results of the simulations with the medium and largest grid were compared to those of the smallest grid, a scatter graph was plotted, and the root mean square error (RMSE) and coefficient of variation (CV) were calculated, as seen in Equations (1) and (2).

The scatter graph comparing temperatures from the different simulations is shown in Figure 40 and Figure 41. The RSME was calculated and compared between simulation runs. The time needed to run each simulation and the corresponding RSME and CV are shown in Table 1.

$$RMSE = \sqrt{\sum_{i=1}^n \frac{(\hat{y}_i - y_i)^2}{n}} \quad (1) \text{ Root mean square error}$$

$$CV = \frac{\sigma}{\mu} \quad (2) \text{ Coefficient of variation}$$

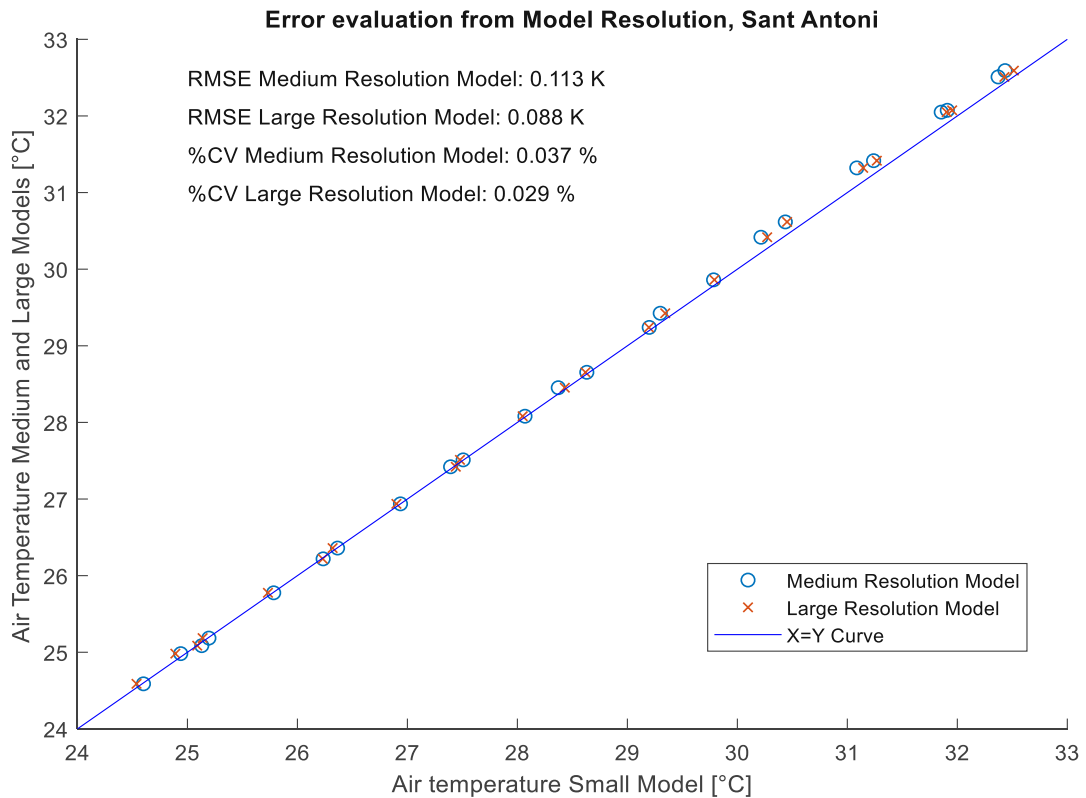


Figure 40. Scatter graph comparing the divergence in simulated air temperatures at 1.5 m between the medium resolution model (3 x 3 meters) and large resolution model (4 x 4 meters) for Sant Antoni

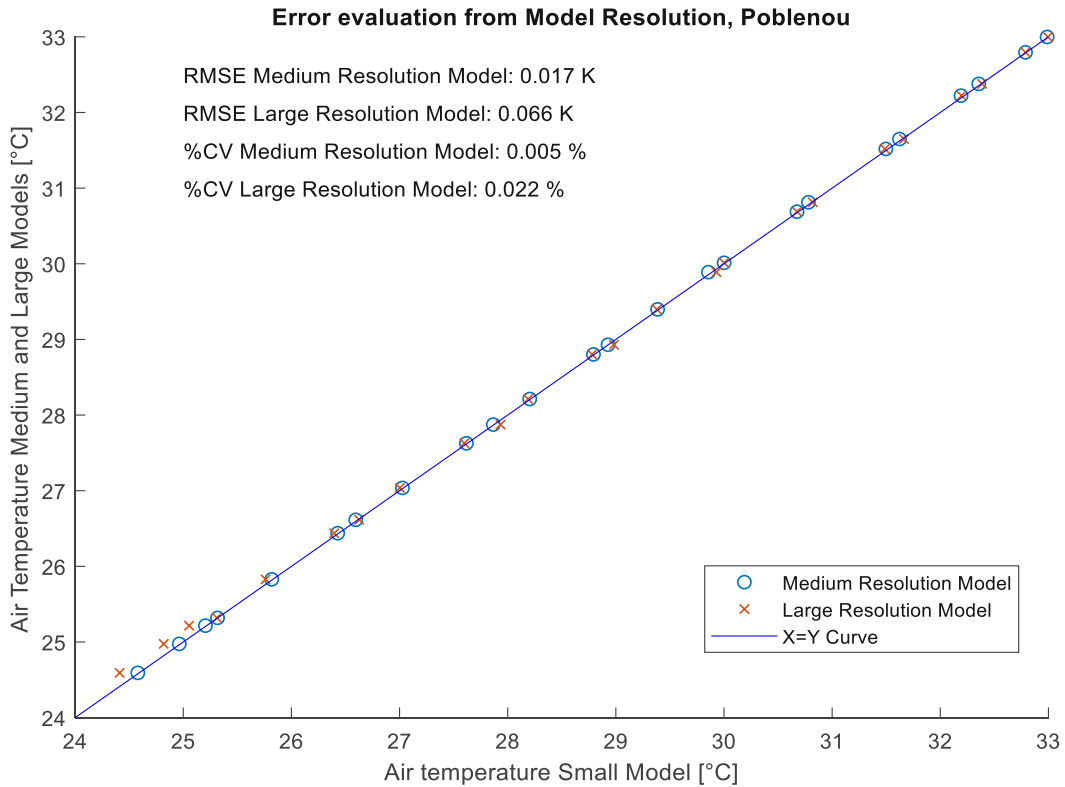


Figure 41. Scatter graph comparing the divergence in simulated air temperatures at 1.5 m between the medium resolution model (3 x 3 meters) and large resolution model (4 x 4 meters) for Poblenu

Table 1. Running time and error of each simulation from the resolution test

Sant Antoni Area		size area: 340 x 340 m		Simulated	Simulation	RMSE	CV
	Resolution	Number of	Period	Duration	air temp.	air temp.	
	[m]	cells	[hh:mm]	[hh:mm]	(K)	(%)	
Smallest Resolution	2.5 x 2.5	136 x 136	24h:00m	103h:12m	Base Simulation		
Medium Resolution	3 x 3	113 x 113	24h:00m	62h:03m	0.113	0.037	
Largest Resolution	4 x 4	85 x 85	24h:00m	36h:10m	0.088	0.029	
Horizontal grid	variable	16					
Poblenu Area		size area: 400 x 400 m		Simulated	Simulation	RMSE	CV
	Resolution	Number of	Period	Duration	air temp.	air temp.	
	[m]	cells	[hh:mm]	[hh:mm]	(K)	(%)	
Smallest Resolution	2.5 x 2.5	160 x 160	24h:00m	121h:33m	Base Simulation		
Medium Resolution	3 x 3	133 x 133	24h:00m	66h:31m	0.017	0.005	
Largest Resolution	4 x 4	100 x 100	24h:00m	61h:00m	0.066	0.022	
Horizontal grid	variable	18					

Given the small divergence in the simulated results in both Sant Antoni and Poblenu areas, the largest being around 0.1 K, and the long duration to run the simulation, which grows exponentially to the length of the model, the 4 x 4 m grid was chosen as it provides sufficiently accurate results.

2.2.1.2. Initial Boundary Condition Warm-up Test

This simulation test was performed to assess the influence of the simulation results from the elapsed time from the start of the simulation. According to the ENVI-met documentation, the typical length for a Simulation should be around 24 to 48 hours. Due to the heat capacity of the simulated materials, such as buildings and soil and due to the change in water content on the air, the longer the simulation, the less dependent on the initial boundary conditions are the results. From the researched literature cited in section 1.3.5, the simulated period was between 24 hours and 72 hours.

To evaluate the influence of the simulation length in the results, four simulations were performed for each area, with duration of 24, 48, 72 and 96 hours, always starting and finishing at 7 AM. As the last 24 hours will be considered, that means zero, 24, 48 and 72 hours of warm up period, respectively. The weather configuration was set to “beginner “and set to a hot summer day with boundary air temperatures between 22° and 34° with linear variation and average wind speed of 2.5 m/s.

The simulated temperature at the center of the model at 1.5 m above ground was used for the comparison. The results of the last day of simulation of the 24, 48 and 72-hours duration simulation were compared to those of the 96-hours simulation. The scatter graph comparing temperature in the different simulations is shown in Figure 42 and in Figure 43. The time need to run each simulation and the corresponding errors RSME and CV are shown in Table 2.

Table 2. Running time and error of each simulation from the warm-up test

Sant Antoni Area	Simulated Period [hh:mm]	Simulation Duration [hh:mm]	RMSE air temp. [K]	CV air temp. [%]
One day	24:00	37h:59m	0.382	0.127
Two days	48h:00m	72h:49m	0.097	0.097
Three days	72h:00m	98h:04m	0.033	0.033
Four days	96h:00m	130h:37m	Base Simulation	
Poble Nou Area	Simulated Period [hh:mm]	Simulation Duration [hh:mm]	RMSE air temp. [K]	CV air temp. [%]
One day	24h:00m	36h:37m	0.447	0.148
Two days	48h:00m	76h:47m	0.189	0.063
Three days	72h:00m	110h:17m	0.043	0.014
Four days	96h:00m	141h:17m	Base Simulation	

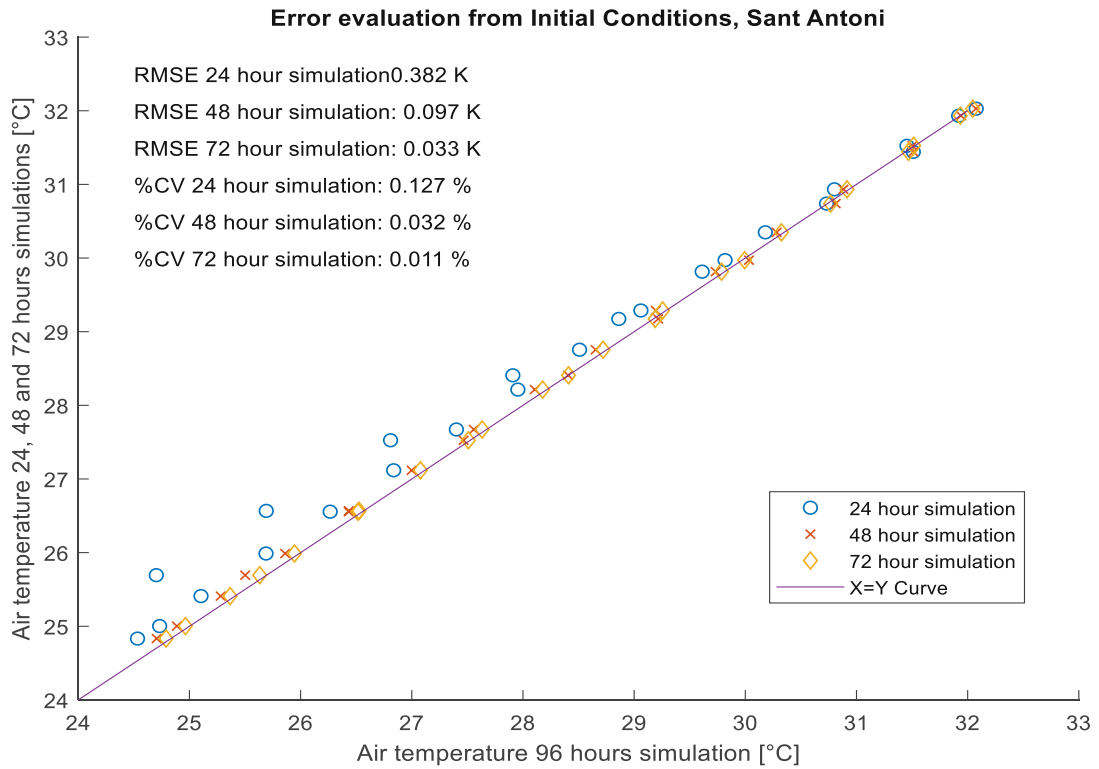


Figure 42. Scatter graph comparing the divergence in simulated air temperatures at 1.5 m according to the duration of the simulation for Sant Antoni

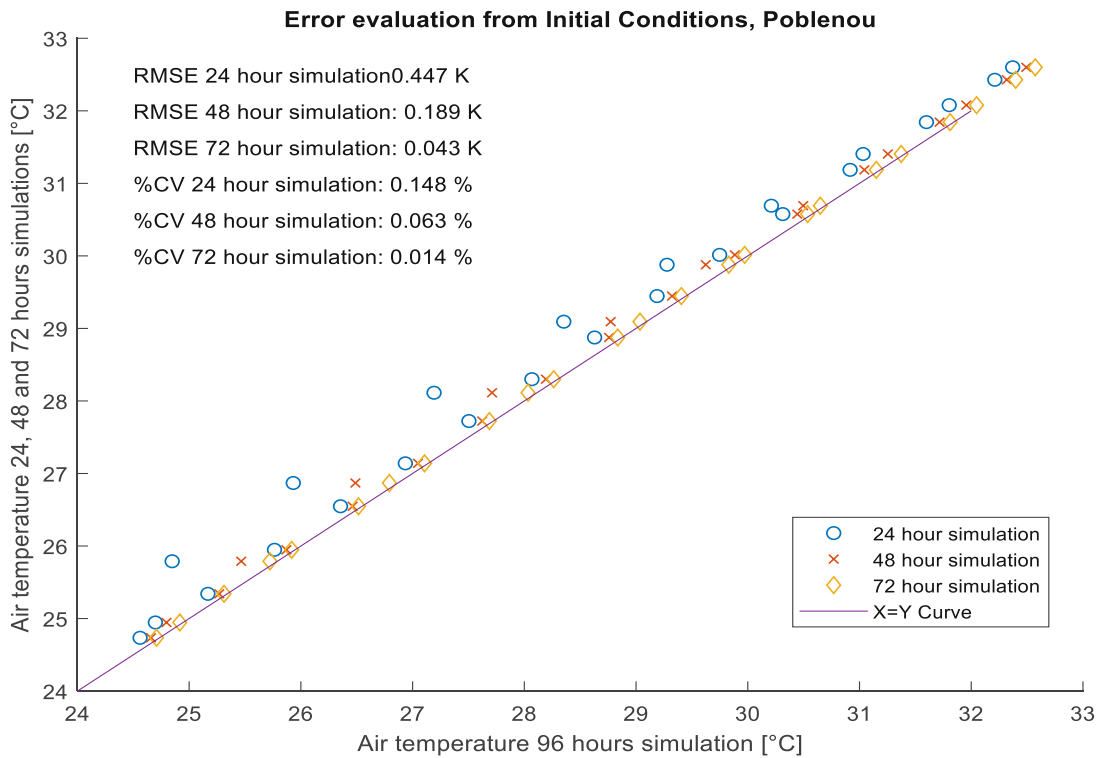


Figure 43. Scatter graph comparing the divergence in simulated air temperatures at 1.5 m according to the duration of the simulation for Poblenou

2.2.1.3. Lateral Boundary Condition Calibration Simulation

The calibration described in this section was performed to evaluate the simulation accuracy regarding the lateral boundary condition input. It is a modified version of the method by Vuckovic et al (2015b). In the mentioned work, the authors compared five different simulated scenarios, altering in each calibration stage the version of ENVI-met, initial temperature, wind speed and method of lateral boundary Input. In this calibration, two different full forcing methods of lateral boundary Input will be compared, equivalent to the two of the tests conducted in (Vuckovic et al., 2015a).

Data from the nearby Raval weather station will be used for forcing the lateral boundary conditions. In one simulation, the maximum and minimum temperatures and relative humidity will be forced, as well as the average wind and direction. In the other simulation, temperature, relative humidity, wind direction and speed will be input every 30 minutes. The solar radiation will be simulated by the date, season, and time by ENVI-met. The solar radiation data from the meteorological station was used to adjust the peak solar radiation. The simulated and measured air temperatures are shown in Figure 44. The scatter graph comparing temperature in the different simulations is shown in Figure 45. The mean square error and the RMSE was calculated.

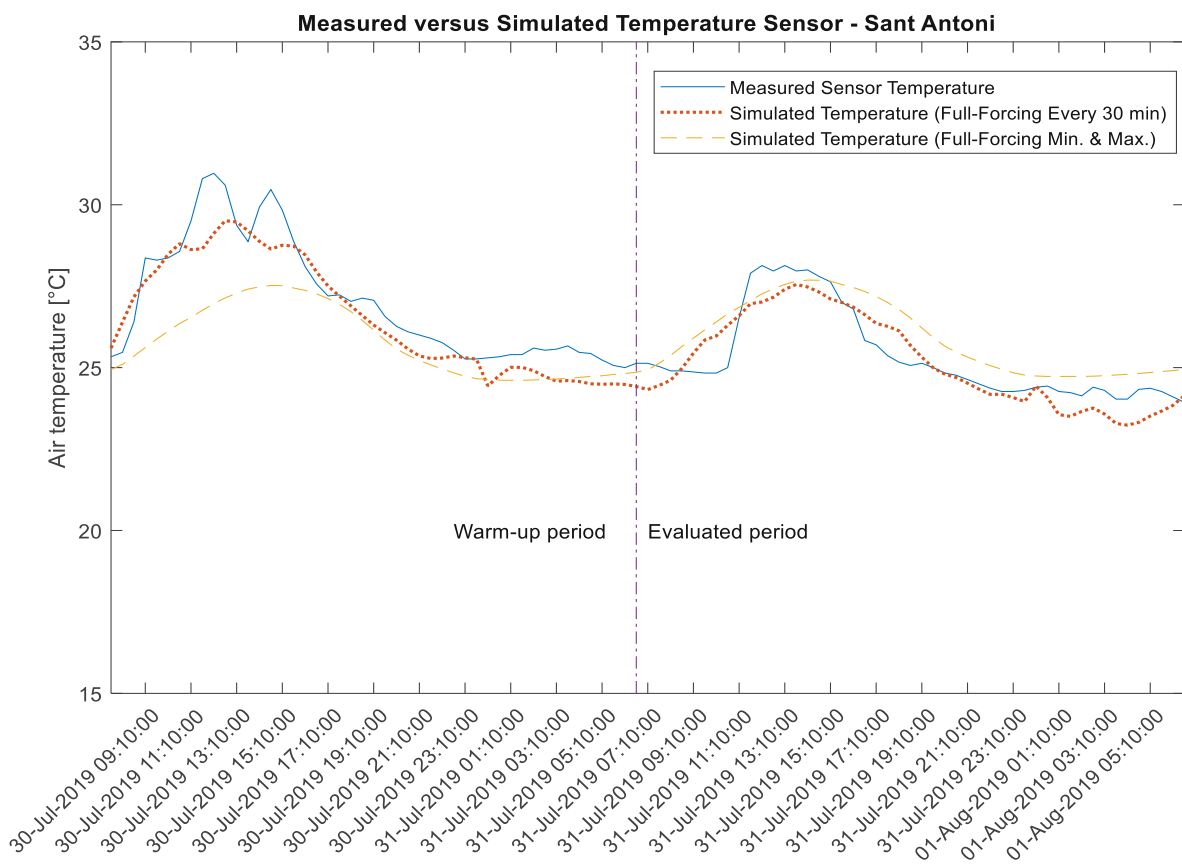


Figure 44. Measured and simulated air temperatures, with two different Full-forcing methods

Measured versus Simulated Temperature Sensor - Sant Antoni

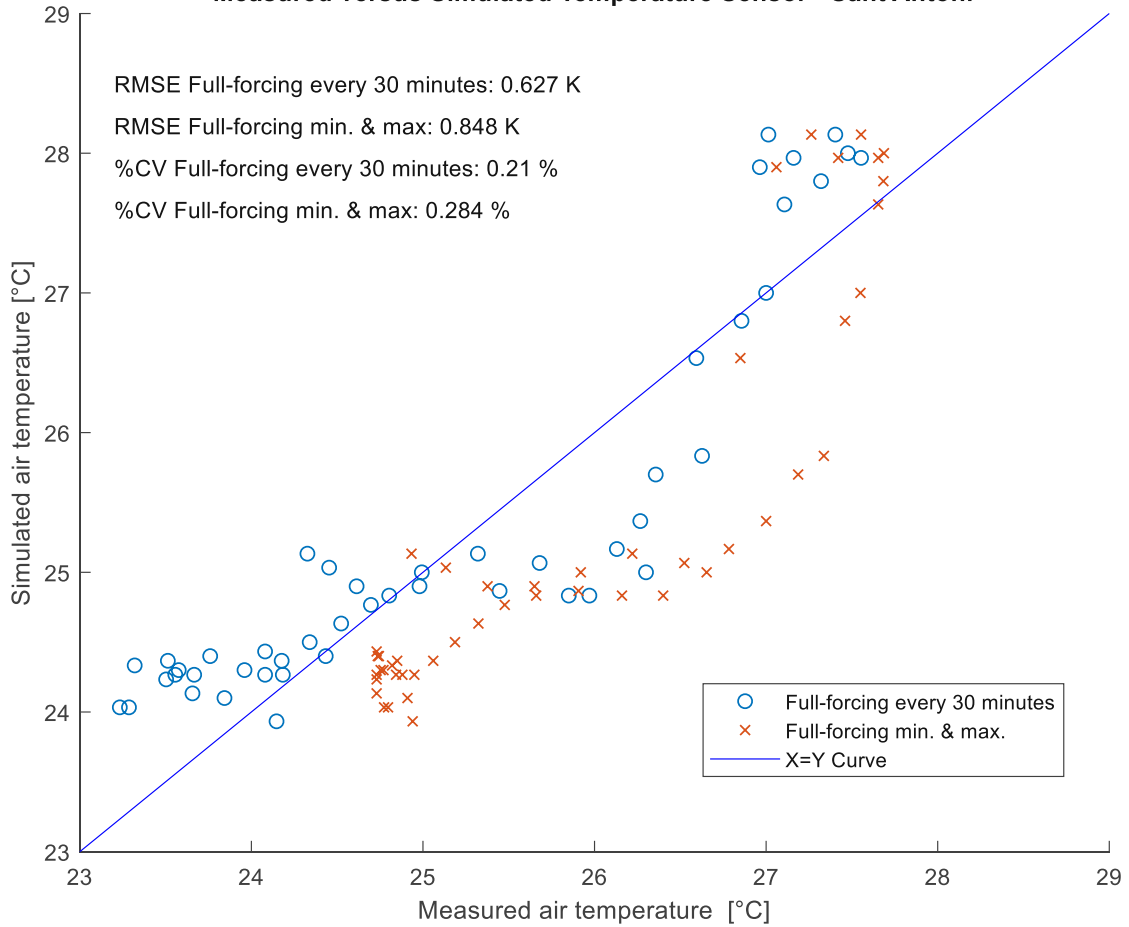


Figure 45. Scatter graph comparing simulated using different Full-forcing methods and measured temperature

2.2.2 Simulation Conditions

In this section the basic condition to all simulated scenarios is described, such as weather, dates, and characteristics of materials.

2.2.2.1. Weather data usage

For the simulations, the chosen period was from 30th of July to 1st of August of 2019, they were sunny days with little to no cloud cover, no precipitation, and maximum temperatures between 26.1 °C and 28.7 °C. They represent average July days in Barcelona, the average temperature in the last decade (2010-2019) for that month was 28.1°C. The meteorological conditions of the simulated days are shown in *Table 3*.

Table 3. Meteorological conditions of the simulated days

Simulated dates	Minimum temperature [°C]	Maximum temperature [°C]	Minimum relative humidity [%]	Maximum relative humidity [%]	Average air speed [m/s]	Peak global solar radiation [W/m ²]	Cloud cover
30/07/2019	25.0	28.8	61.0	83.0	2.2	938.0	Minimal
31/07/2019	23.9	26.5	58.0	69.0	2.0	955.0	Minimal
01/08/2019	23.3	29.2	37.0	68.0	2.9	932.0	Minimal
Average 3 days	24.1	28.2	52.0	73.3	2.4	941.7	Minimal

The weather data were imported into ENVI-met using a 30-minute interval using the Full Forcing Lateral Boundary Conditions method. The information used from the meteorological station was temperature (in Kelvin), relative humidity, wind speed and wind direction. The height of the wind sensor above the street level is necessary for the program to correctly assess the boundary wind speed at different heights. The used weather data during the simulated period is shown in Figure 46.

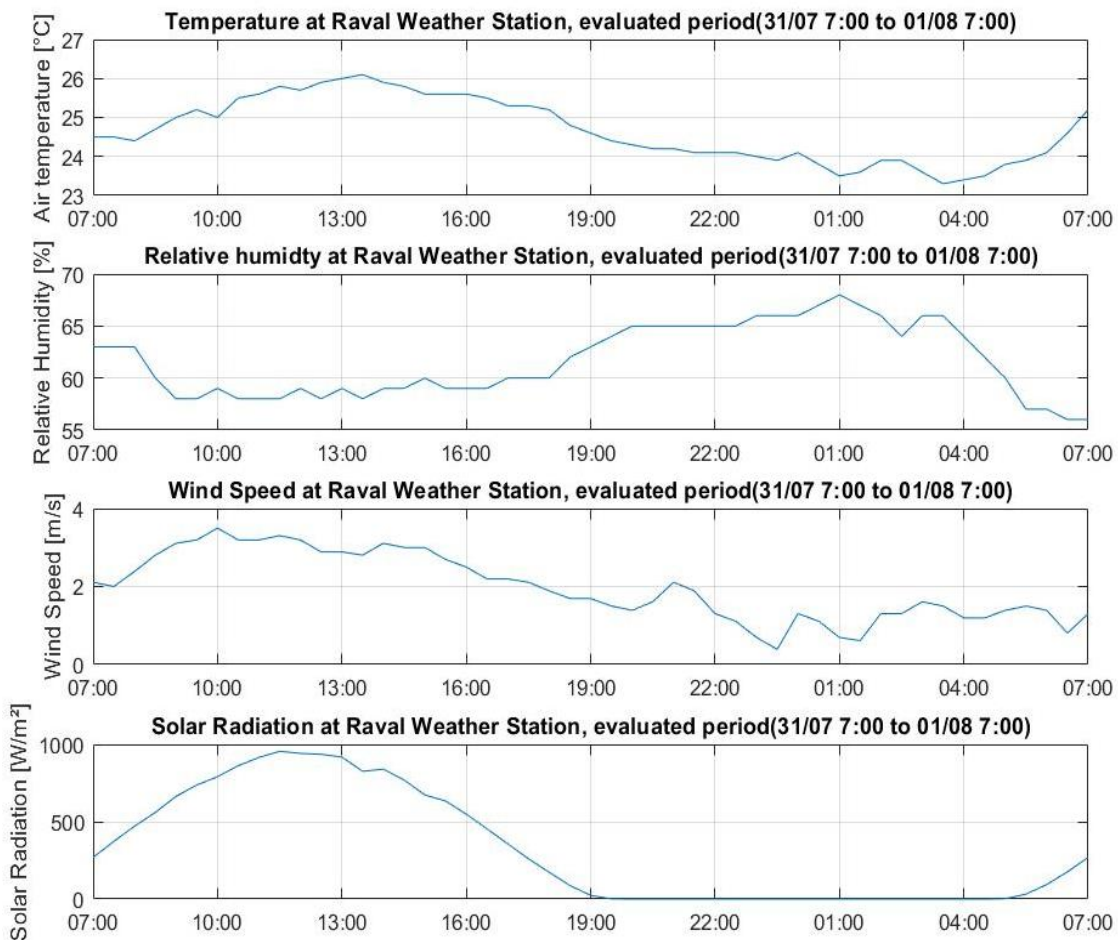


Figure 46. Measured weather station data during the evaluated period

2.2.2.2. Solar Radiation adjustment

The data from the studied meteorological stations only provides information about direct global solar radiation, but not the diffuse and long wave in separate variables as needed for ENVI-met full forcing. For that reason, the solar radiation will be set to be calculated by ENVI-met. Using the global solar radiation measured for at the weather station, the solar radiation adjustment can be calculated by approximating the available data in a second-degree polynomial curve as described by the ENVI-met tutorial by Mendes (2014). The adjustment will be the fraction of the global radiation maximum value given by ENVI-met according to the date and latitude to the maximum of the parabolic curve shown on Figure 47.

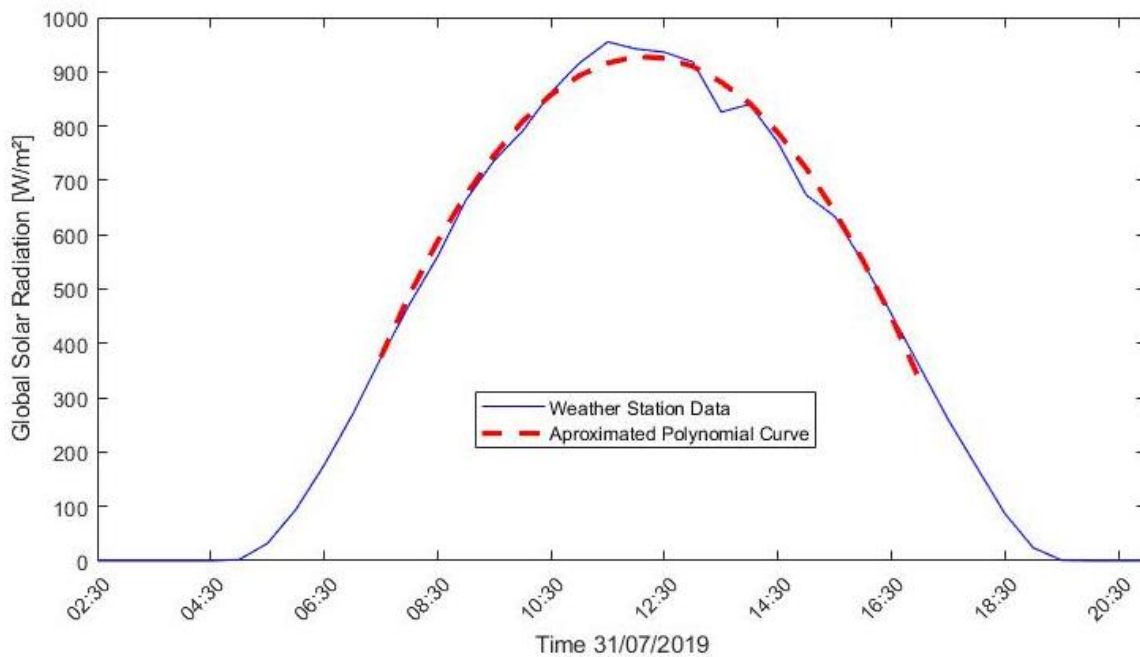


Figure 47. Graph showing the measured direct solar radiation and its approximation to a parabolic curve

2.2.2.3. Material Characteristics

The albedo values from the simulated construction materials were taken from measurements in the work of Prado (2005) and Richard et al. (2015) for the materials listed in Table 4.

Table 4. Material Albedos

Material	Albedo	Source
Painted Asphalt, Gray	0.33	Richard et al. (2015)
Asphalt Road	0.13	Richard et al. (2015)
Concrete Pav. Light	0.29	Richard et al. (2015)
Red Ceramic Pav.	0.53	Prado (2005)
Ceramic Roof	0.53	Prado (2005)
Wall Ocer colour	0.50	Prado (2005)

2.2.2.4. Anthropogenic heat gain

Anthropogenic heat gains, such as those generated by traffic and air conditioning, are not yet implemented in ENVI-met.

2.2.3 Simulation Models – ENVI-met

Each one of the two studied areas were modelled with 3D version that emulated the urban characteristics before and after the implementation of the Superblocks in a total of four models.

Model EM-SA-0: Sant Antoni before Superblock ENVI-met

This 3D model shown in Figure 49 was elaborated with information from old aerial imagery extracted from Google Earth History tool. The main differences from the implemented urban project as seen in Figure 48 are the closing of the streets to cars and the opening of the market's parking space to pedestrians and new green spaces. A dark peripheral roof was taken out and floor covering was substituted for lighter materials, new lighter shading horizontal elements were added to the market square. The modelled area is shown in Figure 49.



Figure 48. Aerial photos from Sant Antoni Market in 2010 and 2019 (Google Maps, 2020)

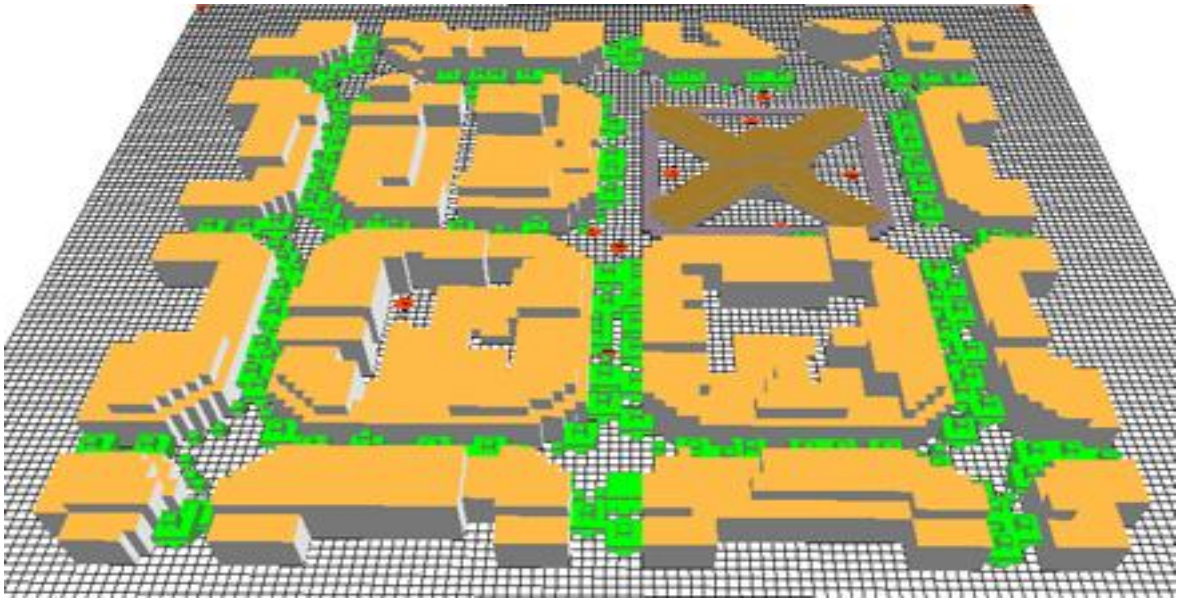


Figure 49. Model EM-SA-0: Sant Antoni before the implementation of the Superblock

Model EM-PN-0: Poblenou before Superblock

The 3D model shown in Figure 51 was elaborated with information from old aerial imagery extracted from Google Maps History tool (Google Maps, 2020). The main differences from the implemented urban project as seen in Figure 50 are the partially closing of the streets to cars by means of repainting of the asphalt and installing street furniture. A semi-public park was implemented in the central block where barren ground was. The modelled area is shown in Figure 51.

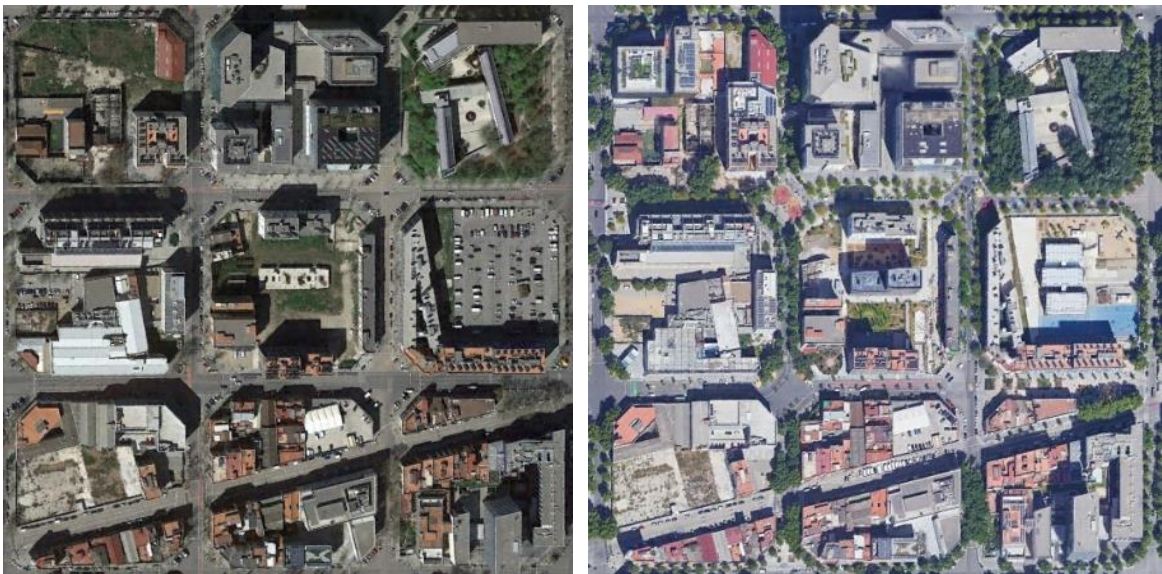


Figure 50. Aerial photos from Poblenou in 2015 and 2019 (Google Maps, 2020)

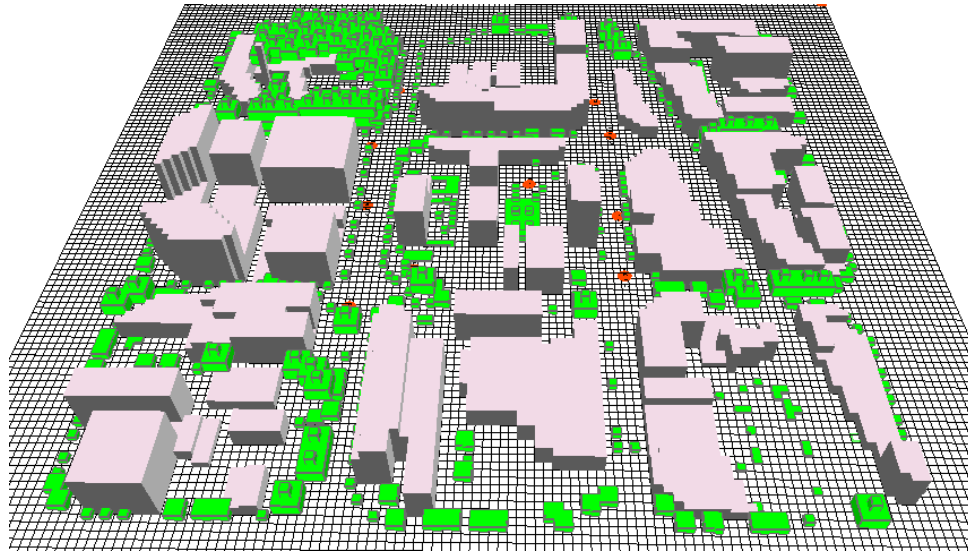


Figure 51. Model EM-PN-0: Poblenou before the implementation of the Superblock

Model EM-SA-1: Sant Antoni with Superblock

The 3D area model shown in Figure 52 was elaborated in accordance with the state of Sant Antoni's area in 2019 as seen in Figure 48.

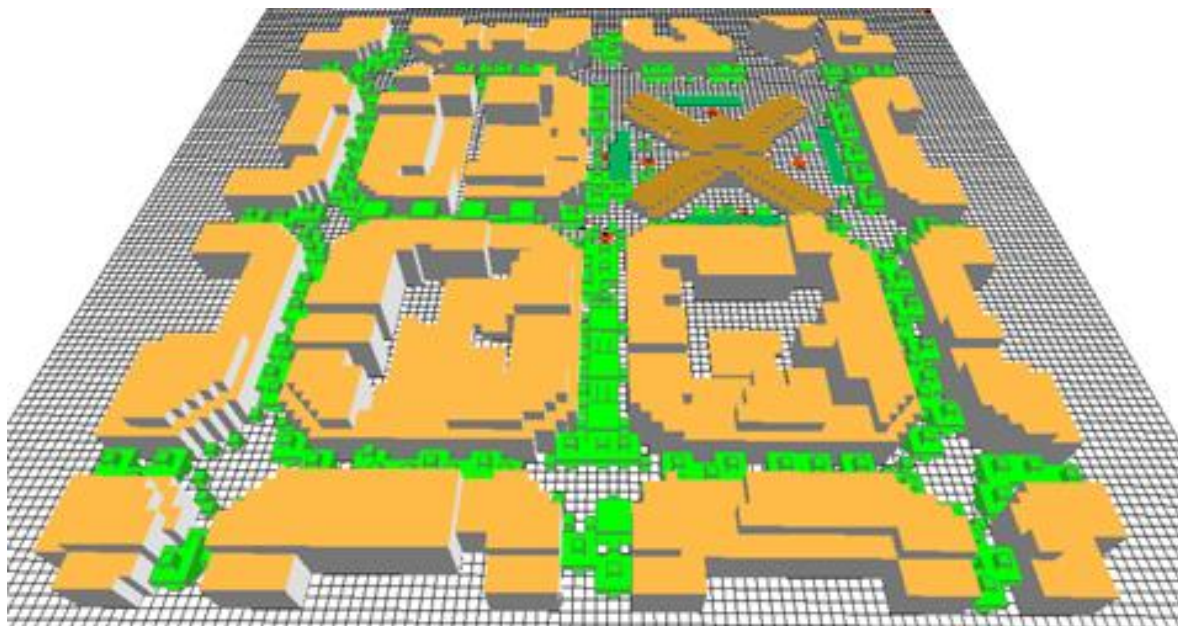


Figure 52. Model EM-SA-1: Sant Antoni after the implementation of the Superblock (ENVI-met)

Model EM-PN-1: Poblenou with Superblock

This 3D model shown in Figure 53 was modelled in accordance with the state of Sant Antoni's area in 2019 as seen in Figure 50.

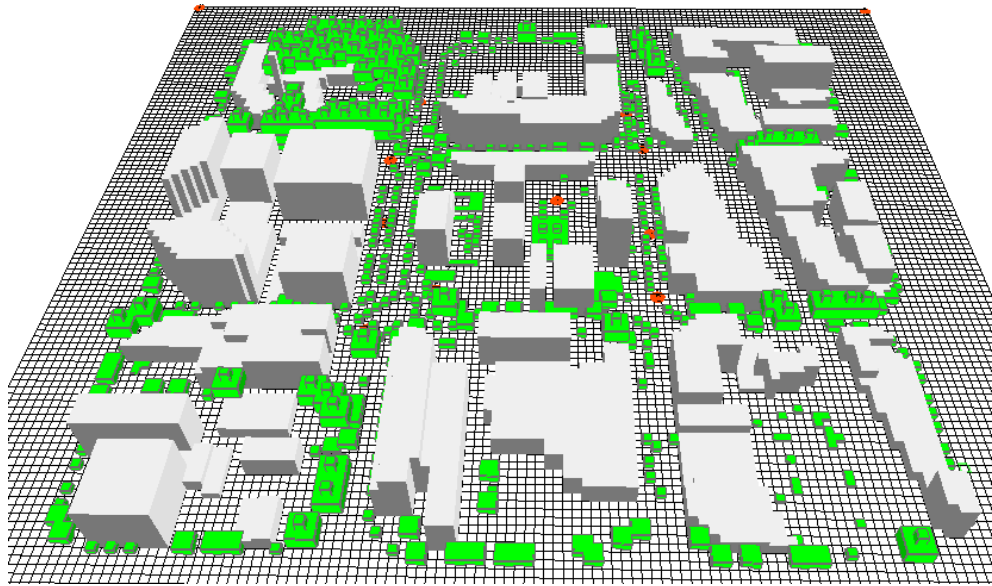


Figure 53. Model EM-PN-1: Poblenou after the implementation of the Superblock (ENVI-met)

2.2.3.1. Virtual Sensors

ENVI-met stores the data from the simulations in hourly steps for each of the climate variables of atmosphere, soil and building surfaces. This data can be later opened by the Leonardo module to create linear, 2D or 3D color graphs and the text data can be manually exported. To obtain data with a more refined time resolution it is necessary to create, prior to the simulation, virtual sensor in the 3D models. For the sensors, information time step is available in 10-minute steps. Figure 54 and Figure 55 show the location of those virtual sensors. As the Sant Antoni Superblock is smaller than the Poblenou Superblock, it contains less virtual sensors at its domains. In the other hand, virtual sensors were also placed at the outside of the Sant Antoni Superblock as it was possible to fit neighboring streets in the model.

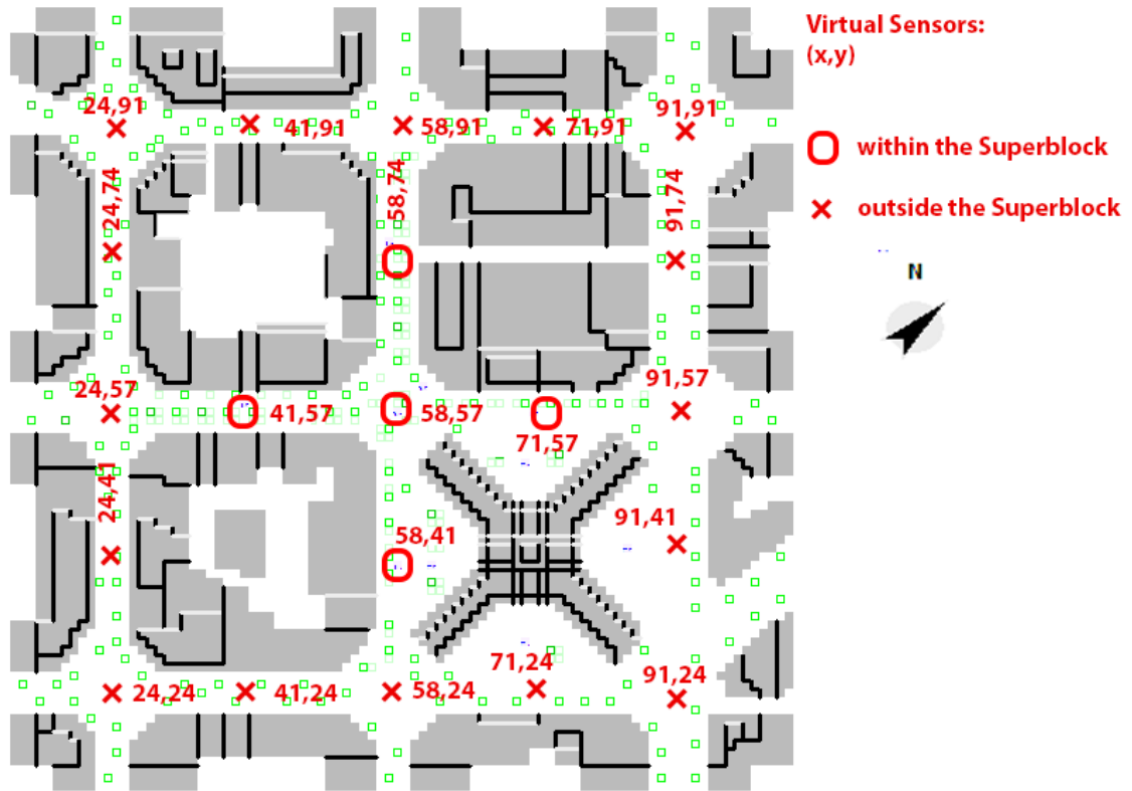


Figure 54. Locations of the virtual sensors in the Sant Antoni model

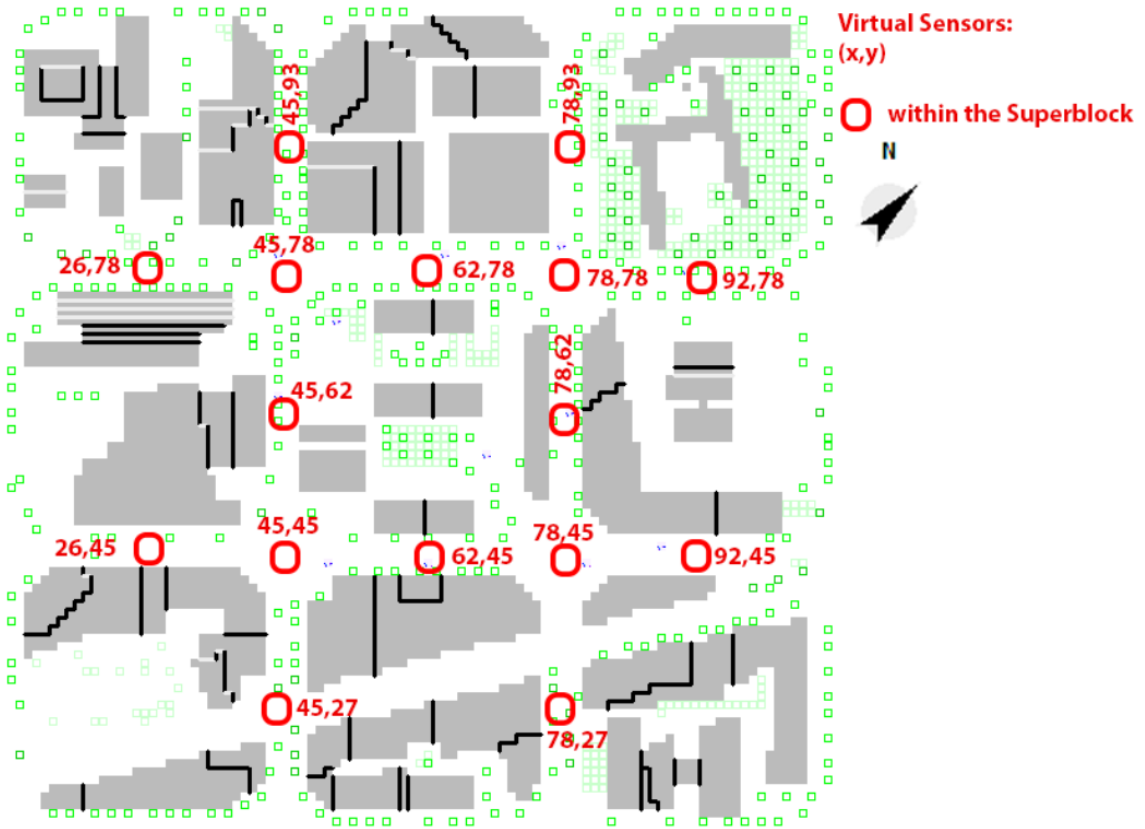


Figure 55. Locations of the virtual sensors in the Poblenou model

2.3 Urban Weather Generator

The Urban Weather Generator (UWG) was developed by Bueno et al. (2013) to assess the urban canopy temperature within an urban area. It uses as input the weather data of a nearby rural meteorological station and the topology and materials of a limited urban scape, such as a neighborhood. UWG performs the calculations shown in the diagrams in Figure 56 and Figure 57. The output is the predicted average hourly air temperature in the urban canyon.

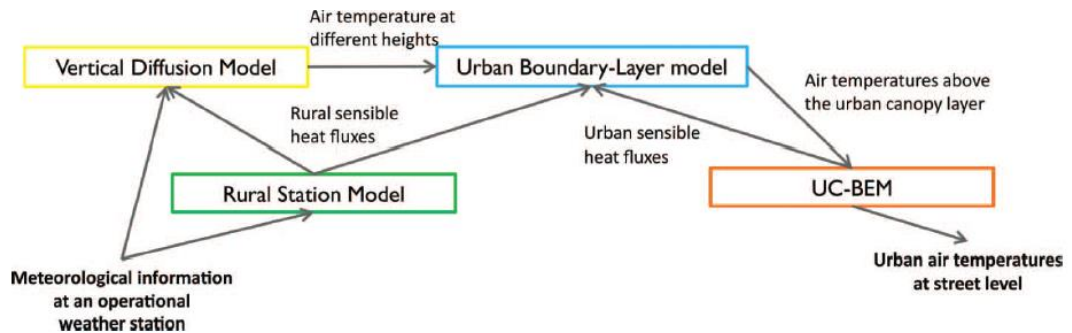


Figure 56. Schematic description of the calculations performed by the Urban Weather Generator (Bueno et al., 2013)

The UWG is offered by its developers in a variety of interfaces: a) standalone Python program, b) MATLAB program and c) Rhino 6.0 Grasshopper plug-in. The latter (c) was chosen to extract the urban characteristics from the geometrical data imported as shapes in Rhino software and that data was used in the UWG MATLAB version (b), which offers more detailed configuring with a more accessible programming code and editable output.

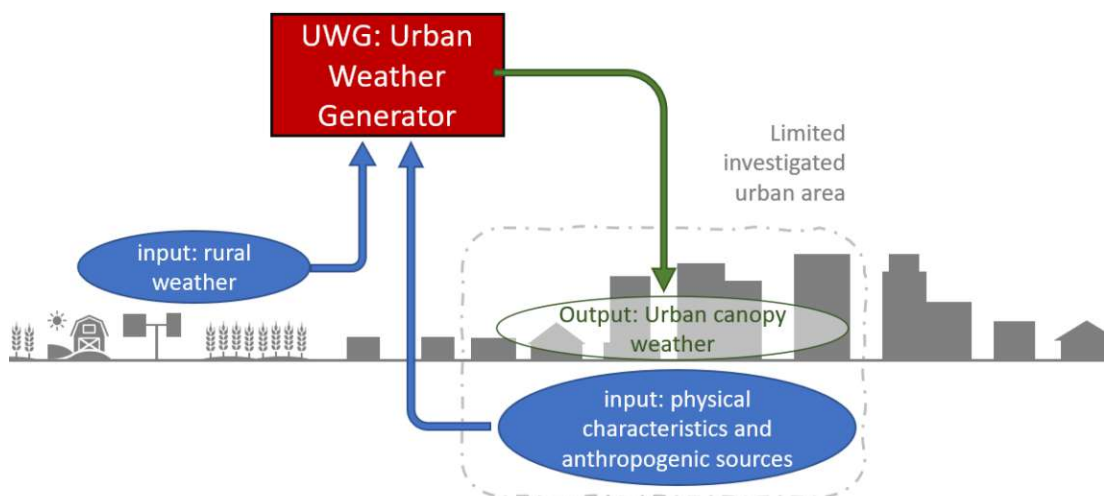


Figure 57. Schematic model of the Urban Weather Generator

2.3.1 Model Set up

In the software Rhino 6.0, a 3D geometric model of each of the two studied areas was created using the same sources as used for the ENVI-met model. It contains the building volumes clustered in groups with similar characteristics, such as usage and age. The size of the modelled areas to be evaluated as one Local Climate Zone (LCZ) comply with a side or diameter of 400 to 1,000 meters (Stewart and Oke, 2012).

2.3.2 Area Characteristics

The urban characteristic values calculated by UWG on Grasshopper using the area footprint and information about height of each building type was exported to UWG MATLAB and additional information about pavement albedo, proportion of green areas and tree canopies was inserted.

Using the same albedo values as applied to the ENVI-met model, the average albedo was estimated using the proportion of sidewalk (gray pavement) and road (asphalt) estimated using Google Maps aerial imagery (Google Maps, 2020). The same method was used to assess the area covered by grass and by the canopy of trees.

Sant Antoni area, urban characteristics:

Average building height: 19 m

Building density: 0.50

Vertical to horizontal ratio: 0.95

Other characteristics, before Superblock:

Average pavement albedo: 0.1710

Tree coverage: 11.43 %

Grass coverage: 0.60 %

After Superblock:

Average pavement albedo: 0.1961

Tree coverage: 12.83 %

Grass coverage: 1.05 %

Poblenou area, urban characteristics:

Average building height: 13 m

Building density: 0.37

Vertical to horizontal ratio: 0.62

Other characteristics, before Superblock:

Average pavement albedo: 0.2156

Tree coverage: 8.26 %

Grass coverage: 6.79 %

After Superblock:

Average pavement albedo: 0.2384

Tree coverage: 10.04 %

Grass coverage: 7.56 %

2.3.3 Building Characteristics

UWG automatically adjusts buildings, window/wall rate and thermal mass according to its age and usage, building albedos were manually adjusted to those values used in ENVI-met. The options for input are as bellow:

Usage options: Full-service restaurant, hospital, large hotel, large office, medium office, midrise apartment, outpatient, primary school, quick service restaurant, secondary school, small hotel, small office, stand-alone retail, strip mall, supermarket, and warehouse.

Age options: New construction, 1980's to present and Pre 1980's.

2.3.4 Anthropogenic heat gain: Traffic

The heat generated by traffic was taken from Bueno et al. (2013) for a mixed used area of Toulouse, because of the similarities with this area and the inner neighbourhoods of Barcelona where the studied areas are located. According to the author, 8 W/m² is a good approximation for the heat emitted by motor vehicles.

UWG applies the input value with a set schedule throughout the day with peaks on rush hour and proportional to the asphalt area.

Sant Antoni, before Superblock:

Asphalt area: 73,483 m²

Sant Antoni, after Superblock:

Asphalt area: 57,453 m²

Poblenou, before Superblock:

Asphalt area: 59,665 m²

Poblenou, after Superblock:

Asphalt area: 44,396 m²

2.3.5 Anthropogenic heat gain: Air conditioning

To calculate the heat generated by air conditioning, the following estimated values were input into the models:

Heating Setpoint: N/A (Summer simulation)

Cooling Setpoint: 26°C

Cooling period: Day for commercial and offices, and night for residential

Fraction of waste heat into the canyon:

Sant Antoni: 0.8 (mostly residential buildings with air split-system)

Poblenou: 0.5 (roughly half the buildings are large offices with central AHU installed over the roof)

2.3.6 Simulation Models – UWG

The 3D models used as input in the UWG tool were modelled with the same source of information that were used for the ENVI-met models from section 2.2.3. In UWG the 3D model is vectorized, so there is no need to choose a 3D resolution such as in ENVI-met. This way the models are more detailed, however, the UWG does not simulate using three-dimensional calculation but extract vertical and horizontal areas and volumes clustered in same building types and materials and use the total values in its calculations.

The models shown in Figure 58, Figure 59, Figure 60 and Figure 61 are equivalent to the 3D models elaborated for ENVI-met but more detailed.

Model UWG-SA-0: Sant Antoni before Superblock

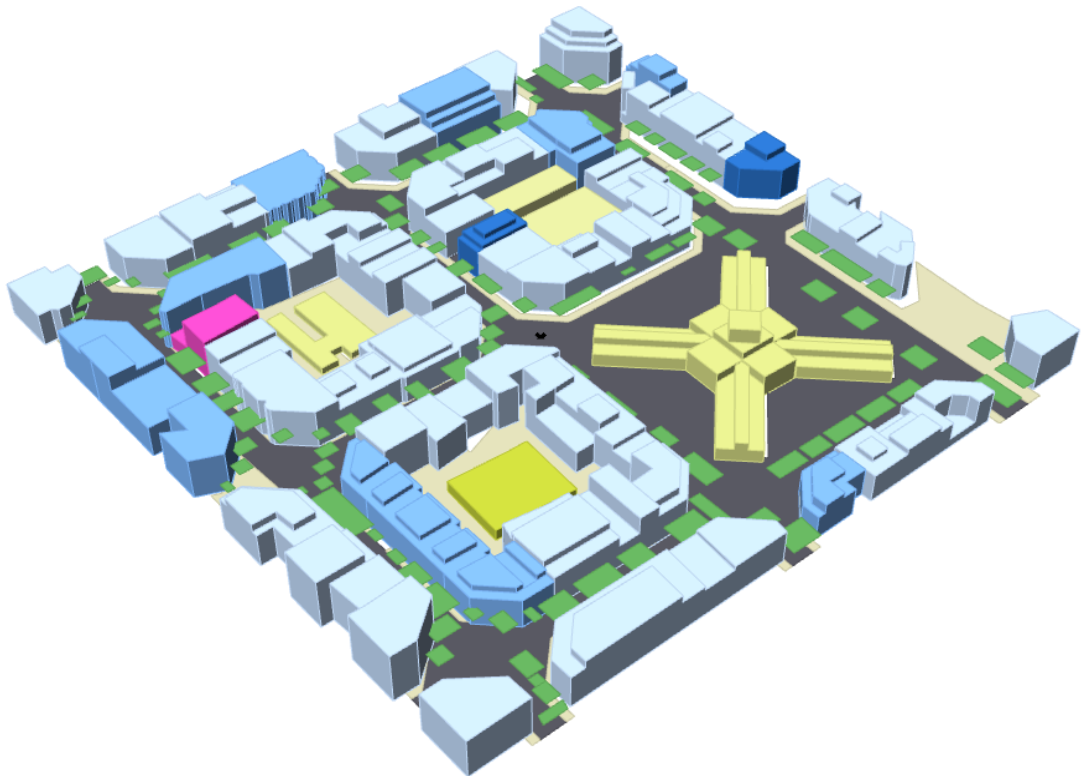


Figure 58. UWG Model Sant Antoni, before Superblock

Model UWG-SA-1: Sant Antoni with Superblock



Figure 59. UWG Model Sant Antoni, with Superblock

Model UWG-PN-0: Poblenou before Superblock



Figure 60. UWG Model Poblenou, before Superblock

Model UWG-PN-1: Poblenou with Superblock



Figure 61. UWG Model Poblenou, after Superblock

3 RESULTS

3.1 Overview

This chapter presents the results of the simulations for the two different tools: ENVI-met in section 3.2 and Urban Weather Generator in section 3.3.

3.2 ENVI-met

For each Superblock, the 2D color map results from ENVI-met and temporal and statistical graphs are displayed with results from before and after the implementation of Superblocks.

Only the output from the second day of the simulation is regarded as valid results, as the first 24 hours are considered the warm-up phase as evaluated and explained in section 2.2.1.2.

3.2.1 2D Results from ENVI-met

The 2D color maps shown in this section were created using the Leonardo and Biomet tools included in ENVI-met, air temperature of scenarios EM-SA-0, EM-SA-1, EM-PN-0 and EM-PN-1 are shown at heights of 1.5 m, to assess pedestrian level, and at 10 m, which is half of the height of the buildings in these areas. Temperatures are also shown in section plane diagrams.

The 2D color maps show air temperatures at 13:00 and 4:00 in degrees Celsius and the air temperature difference between scenarios in Kelvin which correspond to the areas before and after the implementation of the Superblocks. This difference is calculated as the subtraction of EM-SA-0 from EM-SA-1 (EM-SA-1 minus EM-SA-0) and the subtraction of EM-PN-0 from EM-PN-1 (EM-PN-1 minus EM-PN-0).

Ground surface temperature, air speed at pedestrian level as well as the resulting PET are shown in the 2D color maps for the hottest time of day, namely 13:00, to evaluate the effect of the Superblock implementation on the thermal comfort all through the studied areas.

Figure 62, Figure 63 and Figure 64 show the air temperature at different heights in Sant Antoni from 3D-models EM-SA-0 and EM-SA-1, at 13:00. Figure 65, Figure 66 and Figure 67 show the air temperature in Sant Antoni at 4:00. Figure 68 shows the wind speed at pedestrian level in Sant Antoni at 13:00. Figure 69 shows the surface

temperature of the ground in Sant Antoni at 13:00. Figure 70 shows the PET at pedestrian level in Sant Antoni at 13:00.

Figure 71, Figure 72 and Figure 73 show the air temperature at different heights in Poblenu from 3D-models EM-PN-0 and EM-PN-1, at 13:00. Figure 74, Figure 75 and Figure 76 show the air temperature in Poblenu at 4:00. Figure 77 shows the wind speed at pedestrian level in Poblenu at 13:00. Figure 78 shows the surface temperature of the ground in Poblenu at 13:00. Figure 79 shows the PET at pedestrian level in Poblenu at 13:00.

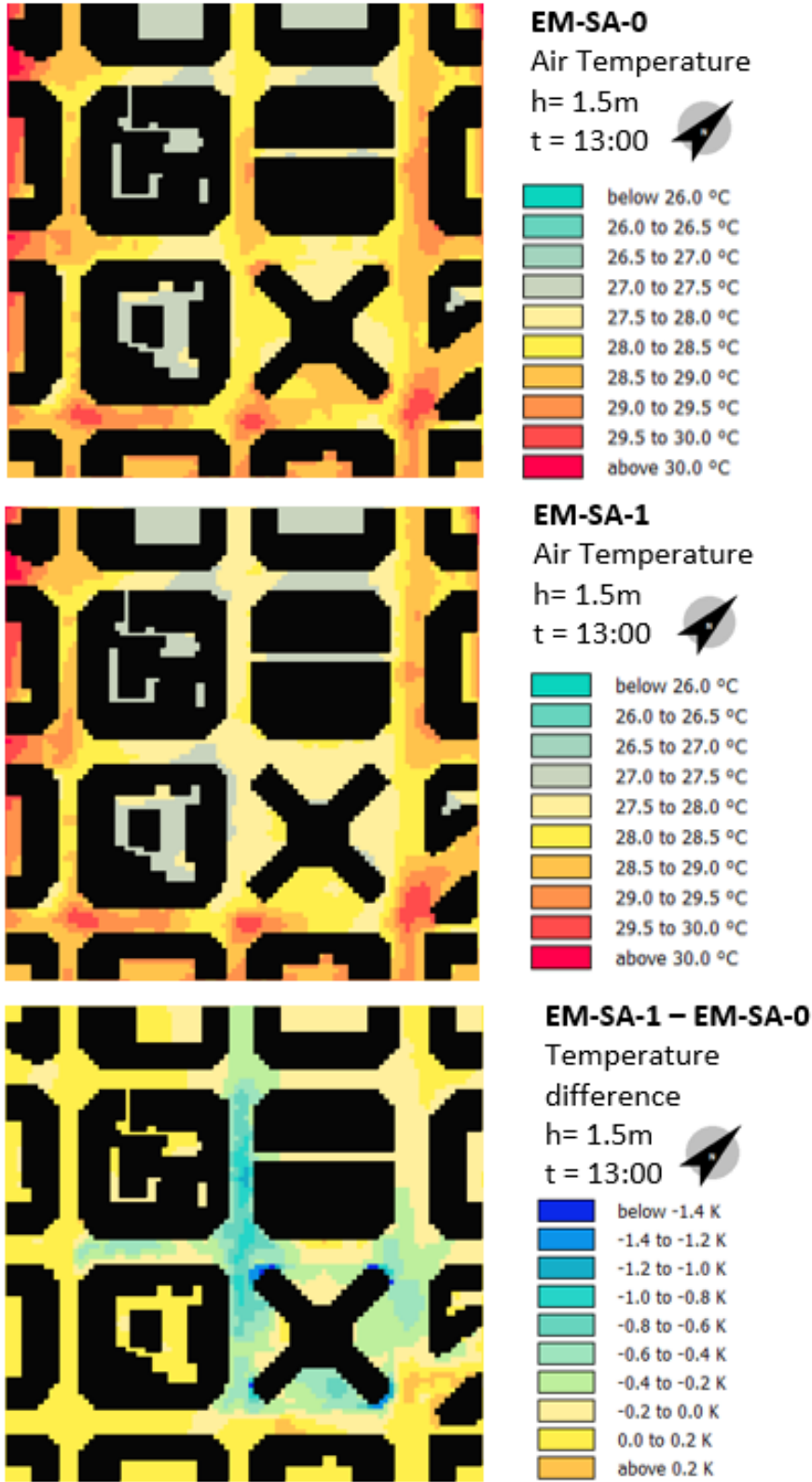


Figure 62. ENVI-met 2D temperature results for Sant Antoni at h = 1.5 m at 13:00

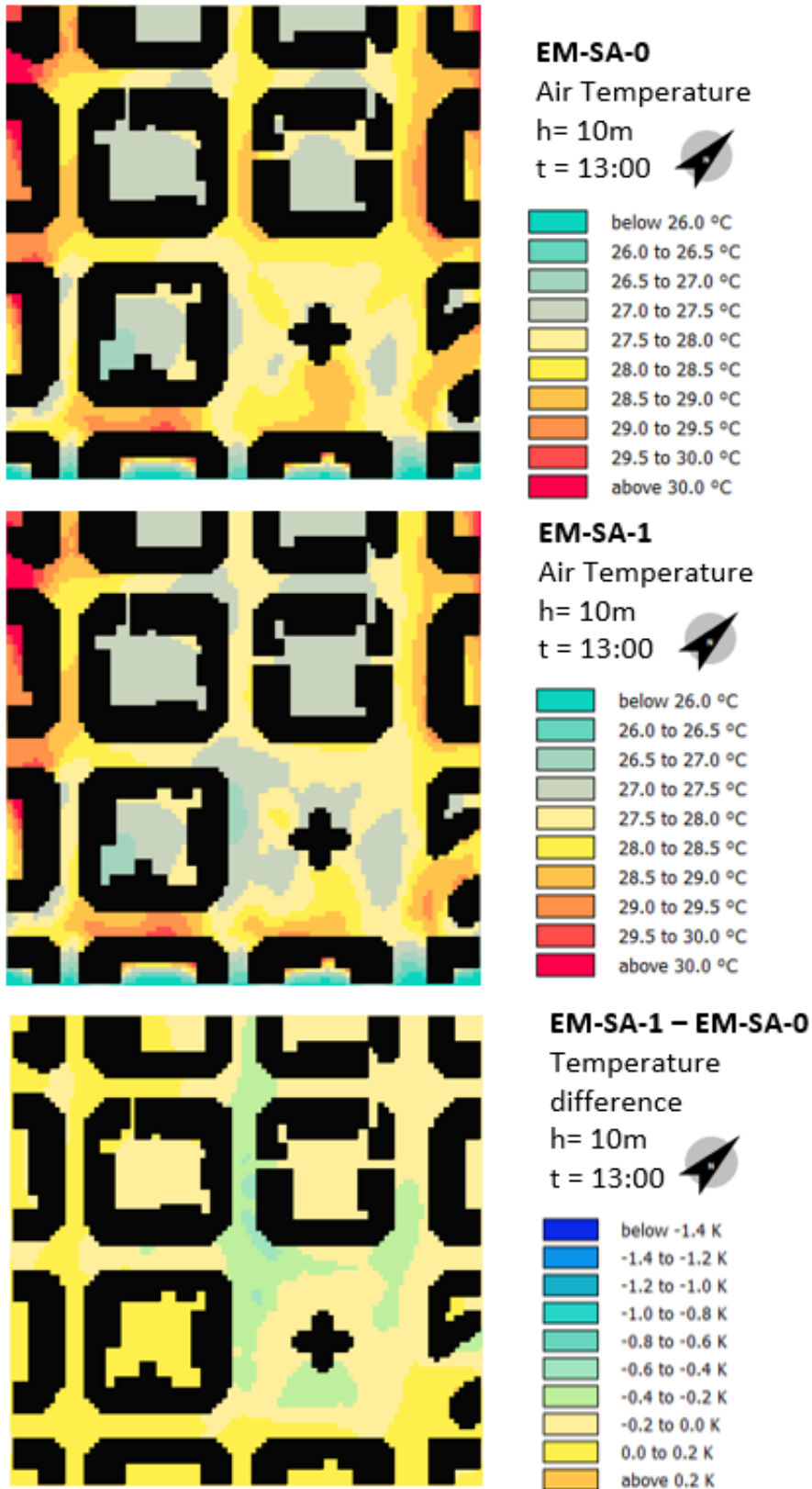
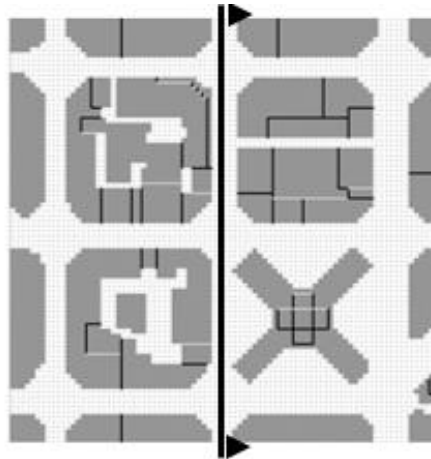


Figure 63. ENVI-met 2D temperature results for Sant Antoni at h = 10 m at 13:00

**Section
Diagram**
Height:
Up to 65m



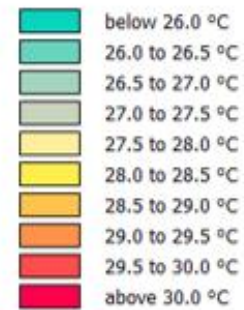
EM-SA-0

Air Temperature / t = 13:00



EM-SA-1

Air Temperature / t = 13:00



EM-SA-1 – EM-SA-0

Temperature difference / t = 13:00

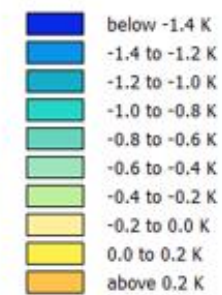


Figure 64. ENVI-met 2D temperature results for Sant Antoni section diagram at 13:00

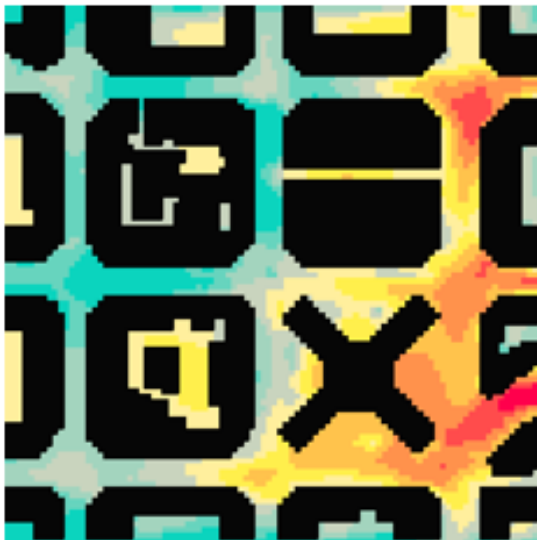
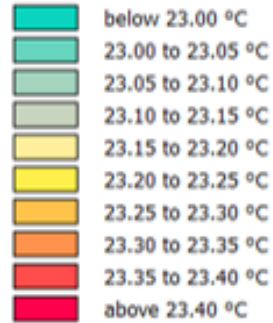


EM-SA-0

Air Temperature

h= 1.5m

t = 4:00

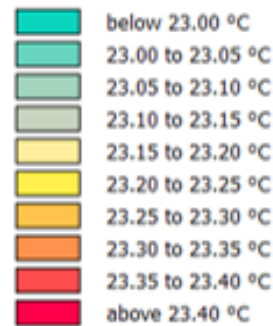


EM-SA-1

Air Temperature

h= 1.5m

t = 4:00



EM-SA-1 – EM-SA-0

Temperature

difference

h= 1.5m

t = 4:00

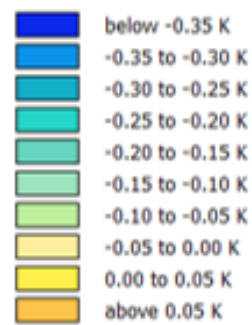


Figure 65. ENVI-met 2D temperature results for Sant Antoni at h = 1.5 m at 4:00

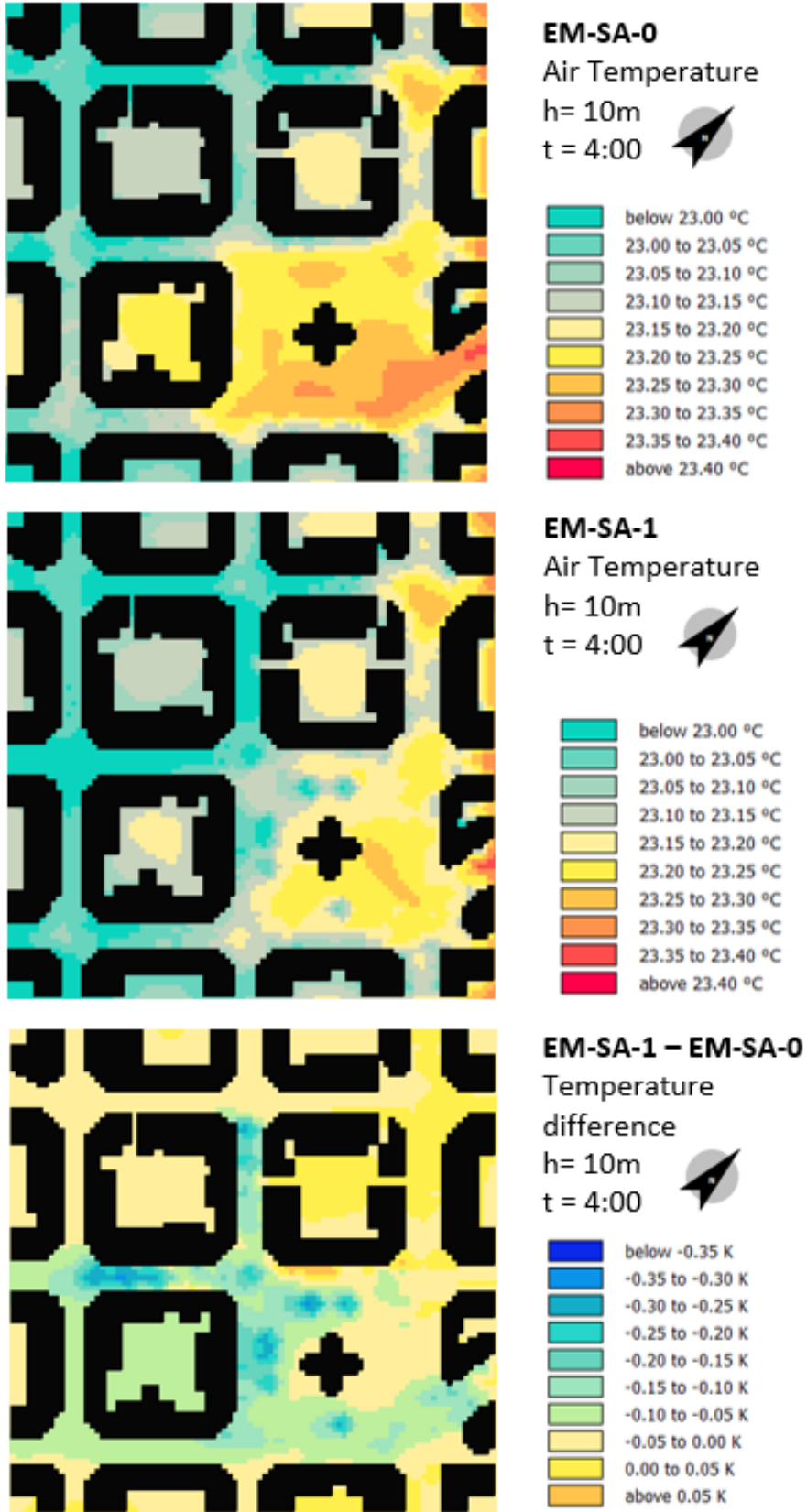
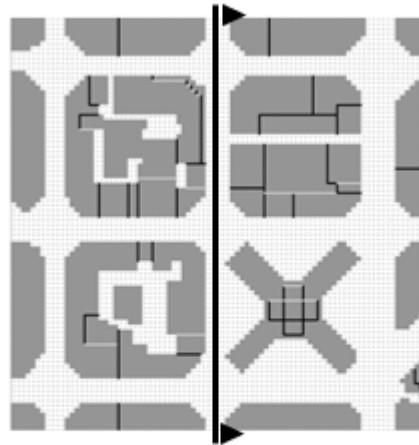


Figure 66. ENVI-met 2D temperature results for Sant Antoni at h = 10 m at 4:00

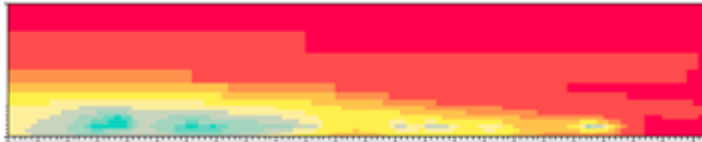
**Section
 Diagram**

Height:
 Up to 65m



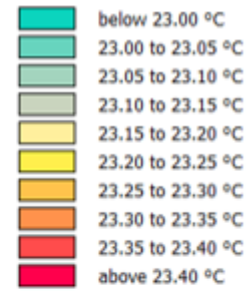
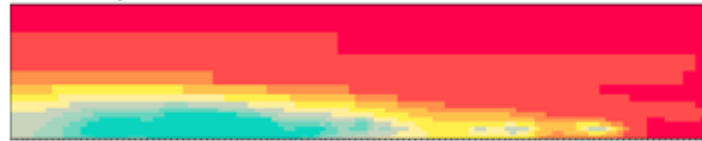
EM-SA-0

Air Temperature / t = 4:00



EM-SA-1

Air Temperature / t = 4:00



EM-SA-1 – EM-SA-0

Temperature difference / t = 4:00

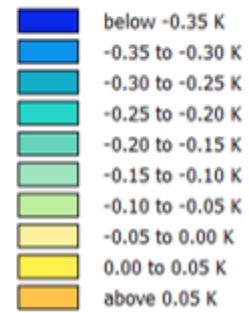
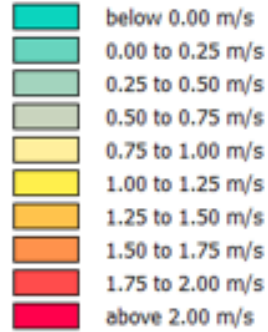


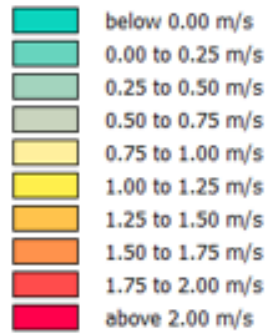
Figure 67. ENVI-met 2D temperature results for Sant Antoni section diagram at 4:00



EM-SA-0
 Air Speed
 h= 1.5m
 t = 13:00



EM-SA-1
 Air Speed
 h= 1.5m
 t = 13:00



EM-SA-1 – EM-SA-0
 Air Speed
 difference
 h= 1.5m
 t = 13:00

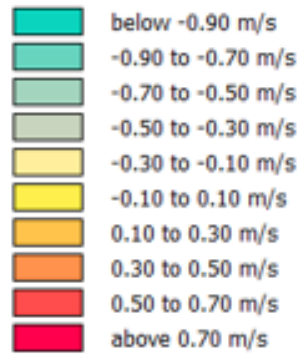


Figure 68. ENVI-met 2D air speed results for Sant Antoni at h = 1.5 m at 13:00

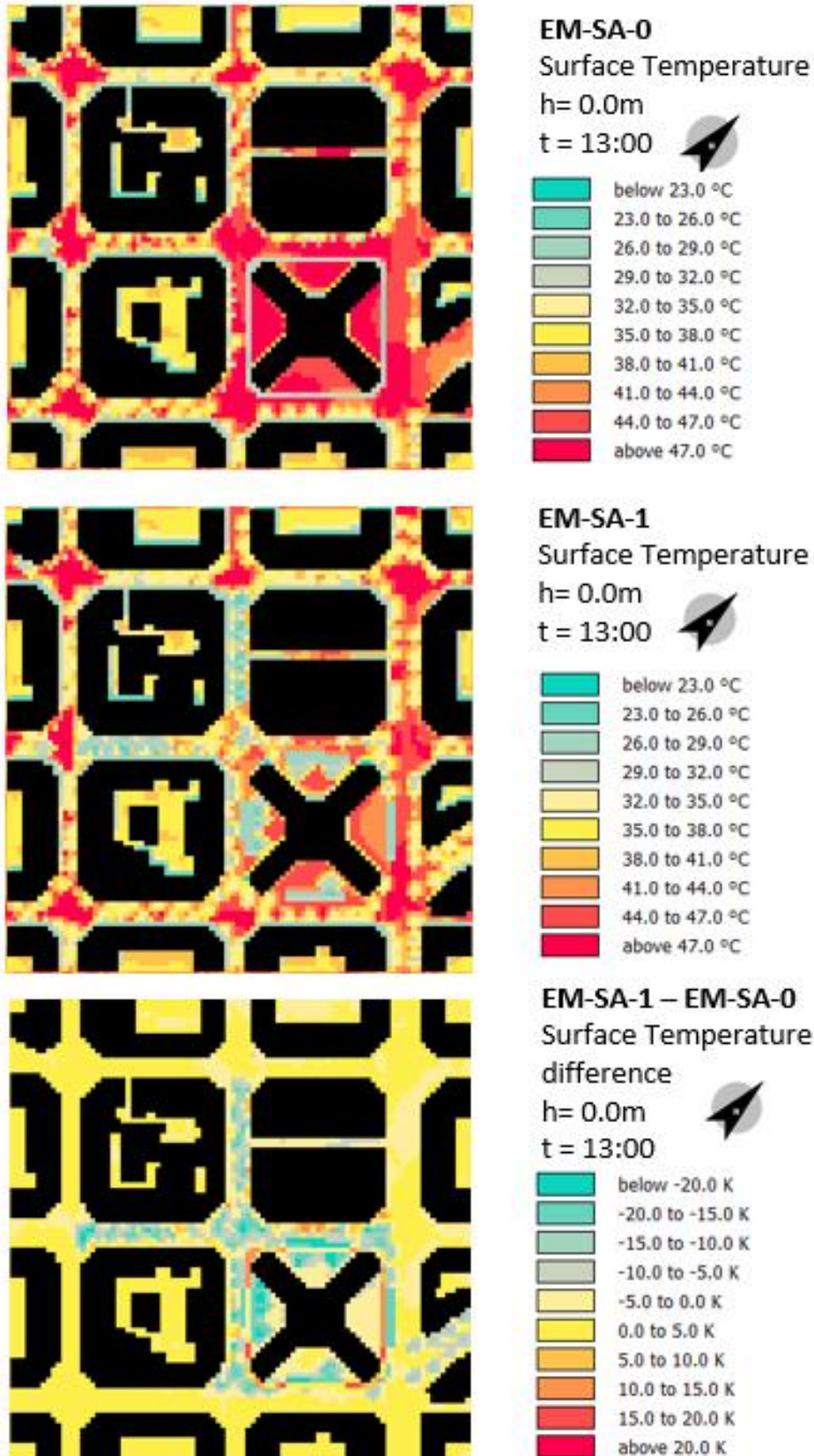


Figure 69. ENVI-met 2D surface temperature results for Sant Antoni at 13:00

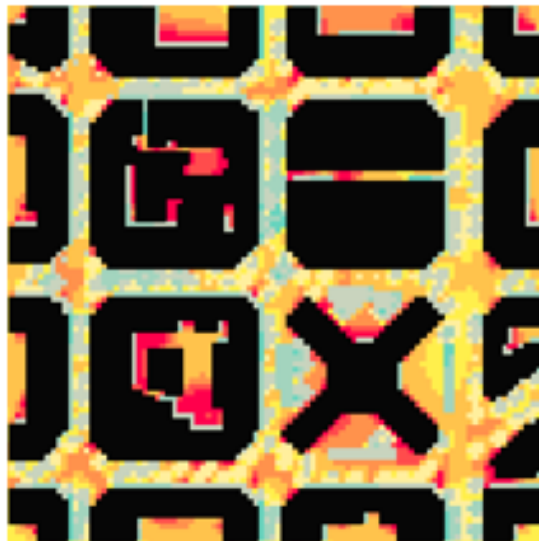
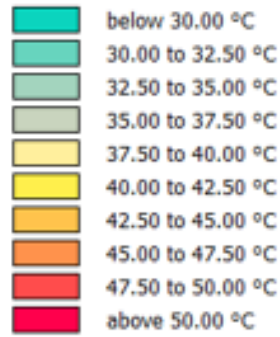


EM-SA-0

PET

h= 1.5m

t = 13:00

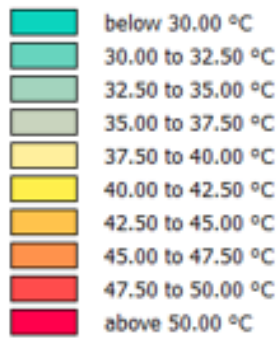


EM-SA-1

PET

h= 1.5m

t = 13:00



EM-SA-1 – EM-SA-0

PET difference

h= 1.5m

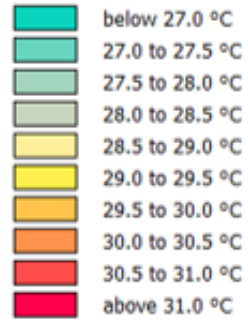
t = 13:00



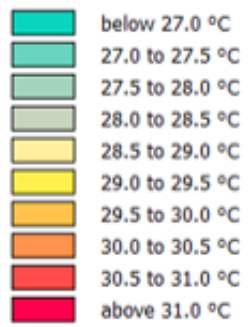
Figure 70. ENVI-met 2D PET results for Sant Antoni at h = 1.5 m at 13:00



EM-PN-0
 Air Temperature
 h= 1.5m
 t = 13:00



EM-PN-1
 Air Temperature
 h= 1.5m
 t = 13:00



EM-PN-1 – EM-PN-0
 Temperature difference
 h= 1.5m
 t = 13:00

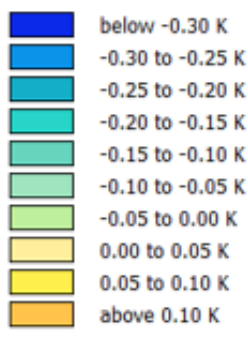


Figure 71. ENVI-met 2D temperature results for Poblenu at h = 1.5 m at 13:00

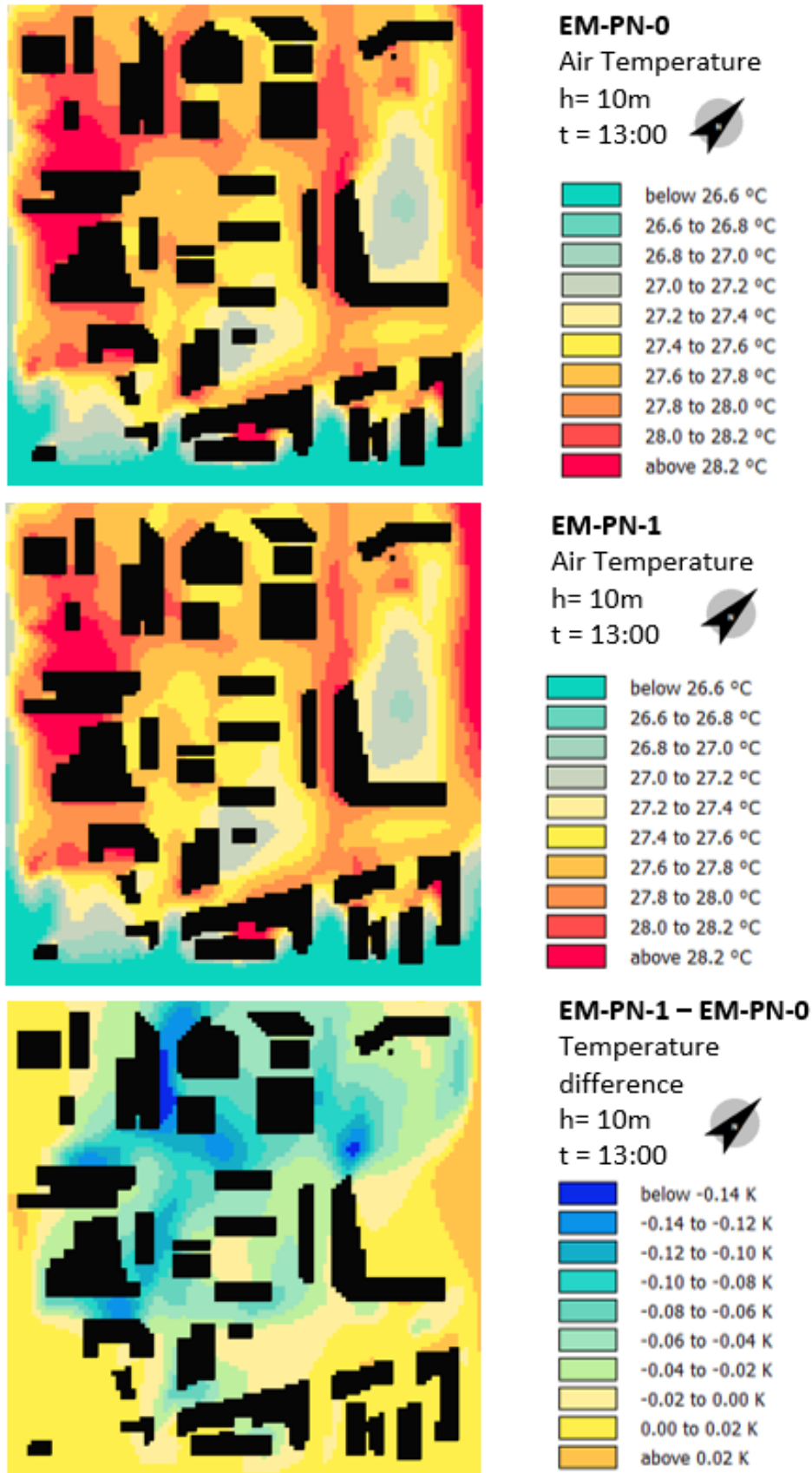


Figure 72. ENVI-met 2D temperature results for Poblenu at h = 10 m at 13:00

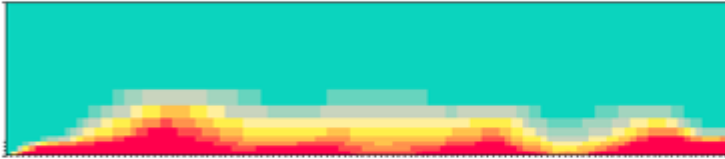
Section Diagram

Height:
Up to 70m



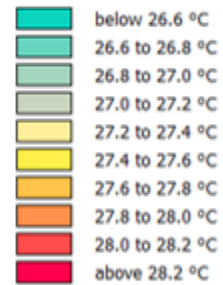
EM-PN-0

Air Temperature / t = 13:00



EM-PN-1

Air Temperature / t = 13:00



EM-PN-1 – EM-PN-0

Temperature difference / t = 13:00

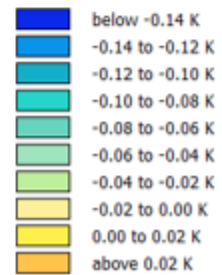


Figure 73. ENVI-met 2D temperature results for Poblenu section diagram at 13:00

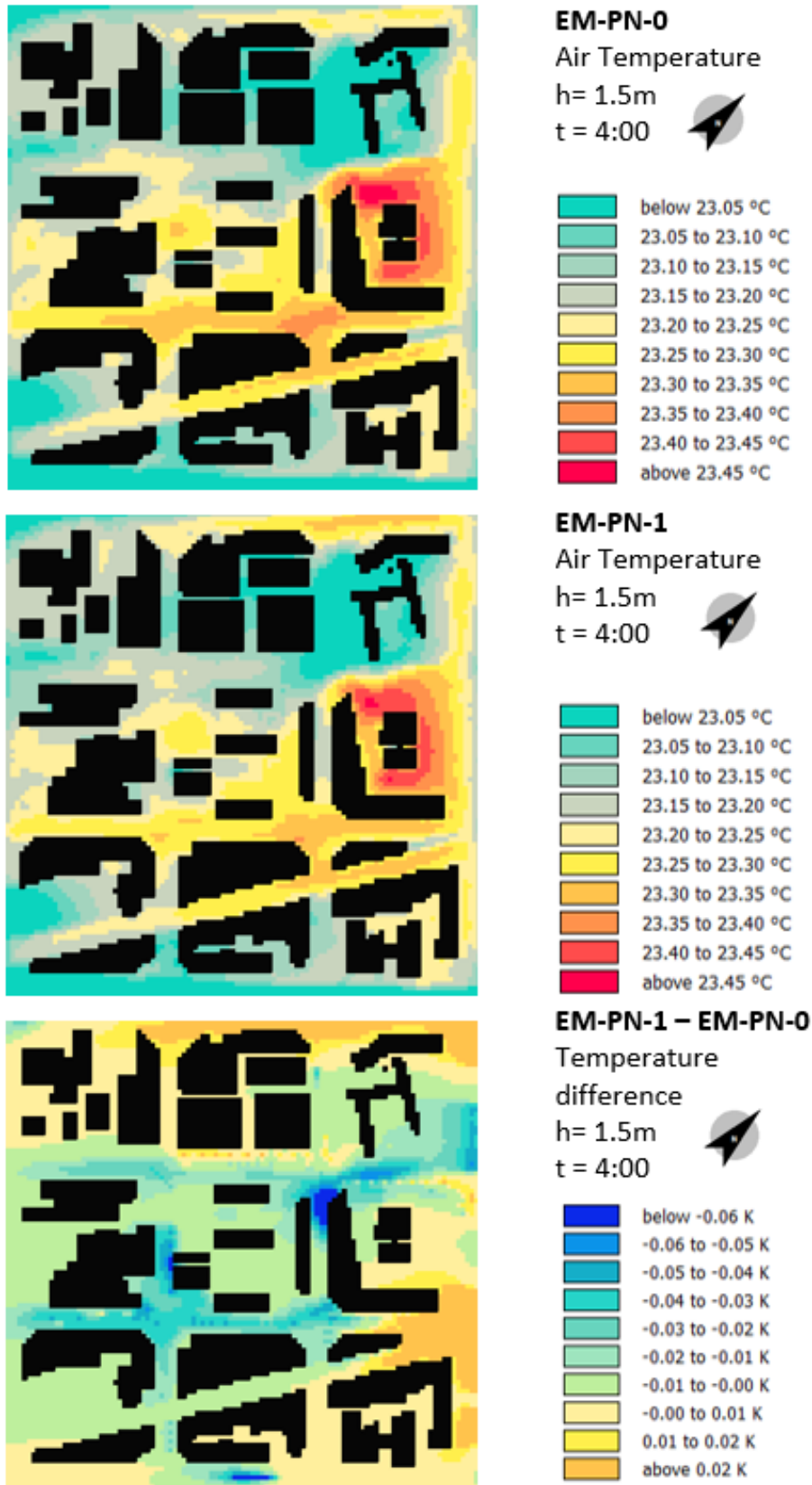


Figure 74. ENVI-met 2D temperature results for Poblenu at h = 1.5 m at 4:00

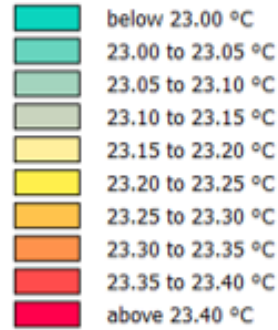


EM-PN-0

Air Temperature

h= 10m

t = 4:00

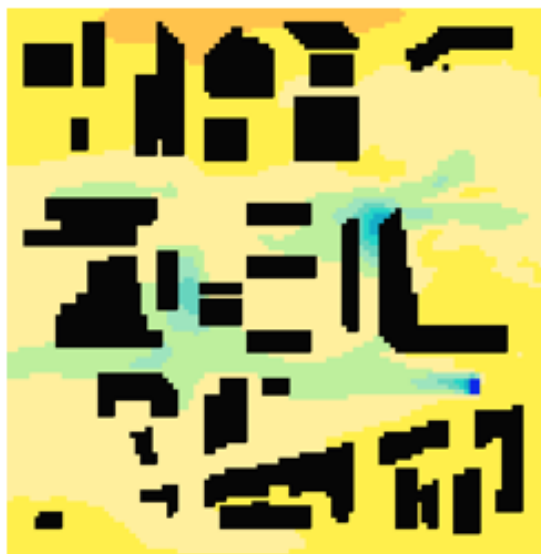
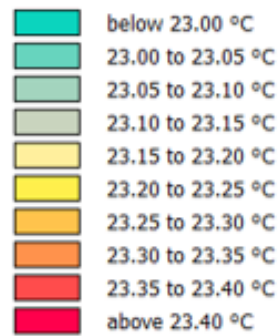


EM-PN-1

Air Temperature

h= 10m

t = 4:00



EM-PN-1 – EM-PN-0

Temperature difference

h= 10m

t = 4:00

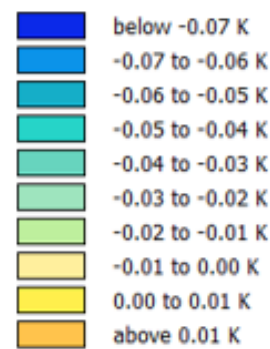


Figure 75. ENVI-met 2D temperature results for Poblenu at h = 10 m at 4:00

Section Diagram

Height:
Up to 70m



EM-PN-0

Air Temperature / t = 4:00



EM-PN-1

Air Temperature / t = 4:00



EM-PN-1 – EM-PN-0

Temperature difference / t = 4:00

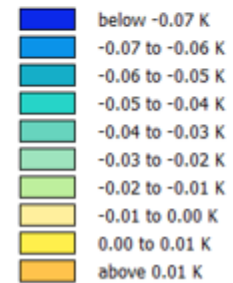
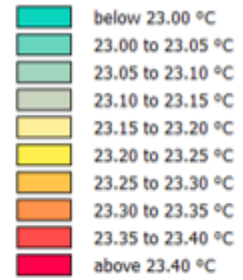
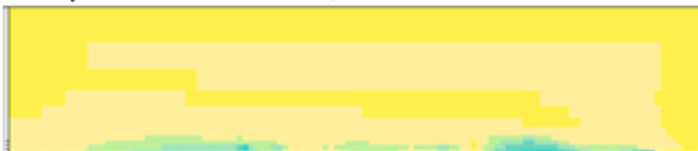


Figure 76. ENVI-met 2D temperature results for Poblenu section diagram at 4:00

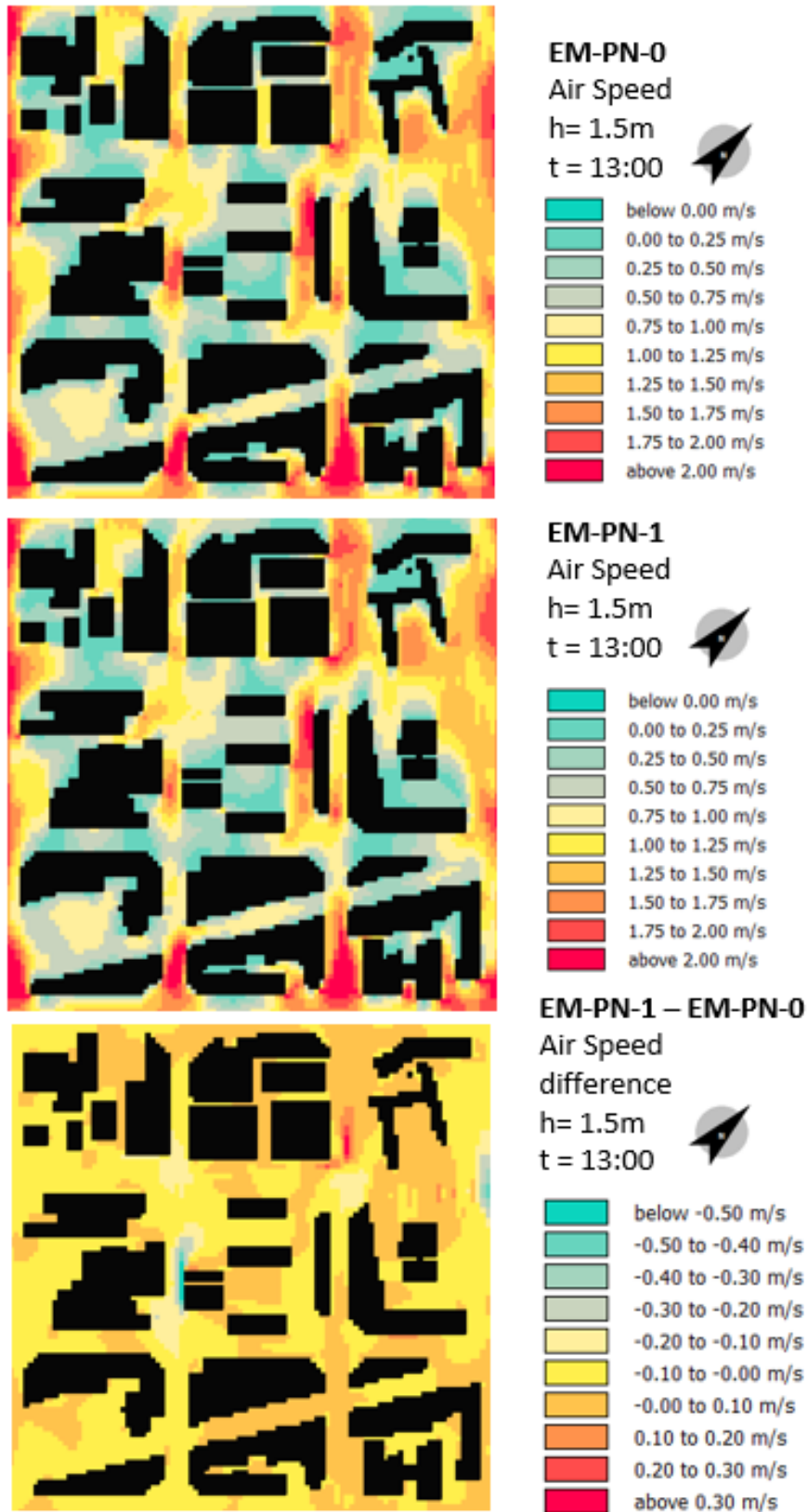


Figure 77. ENVI-met 2D air speed results for Poblenu at h = 1.5 m at 13:00

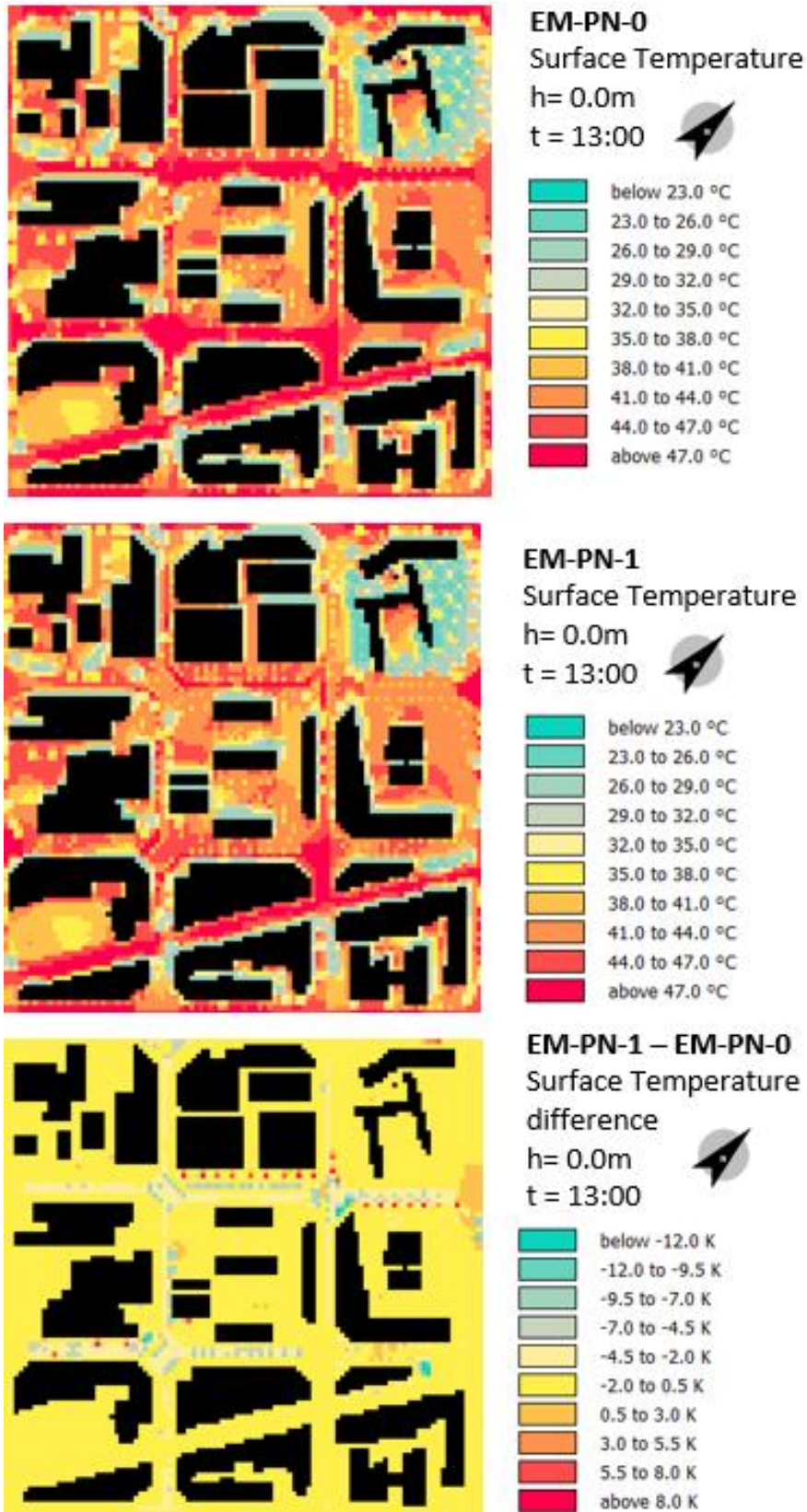


Figure 78. ENVI-met 2D surface temperature results for Poblenu at 13:00

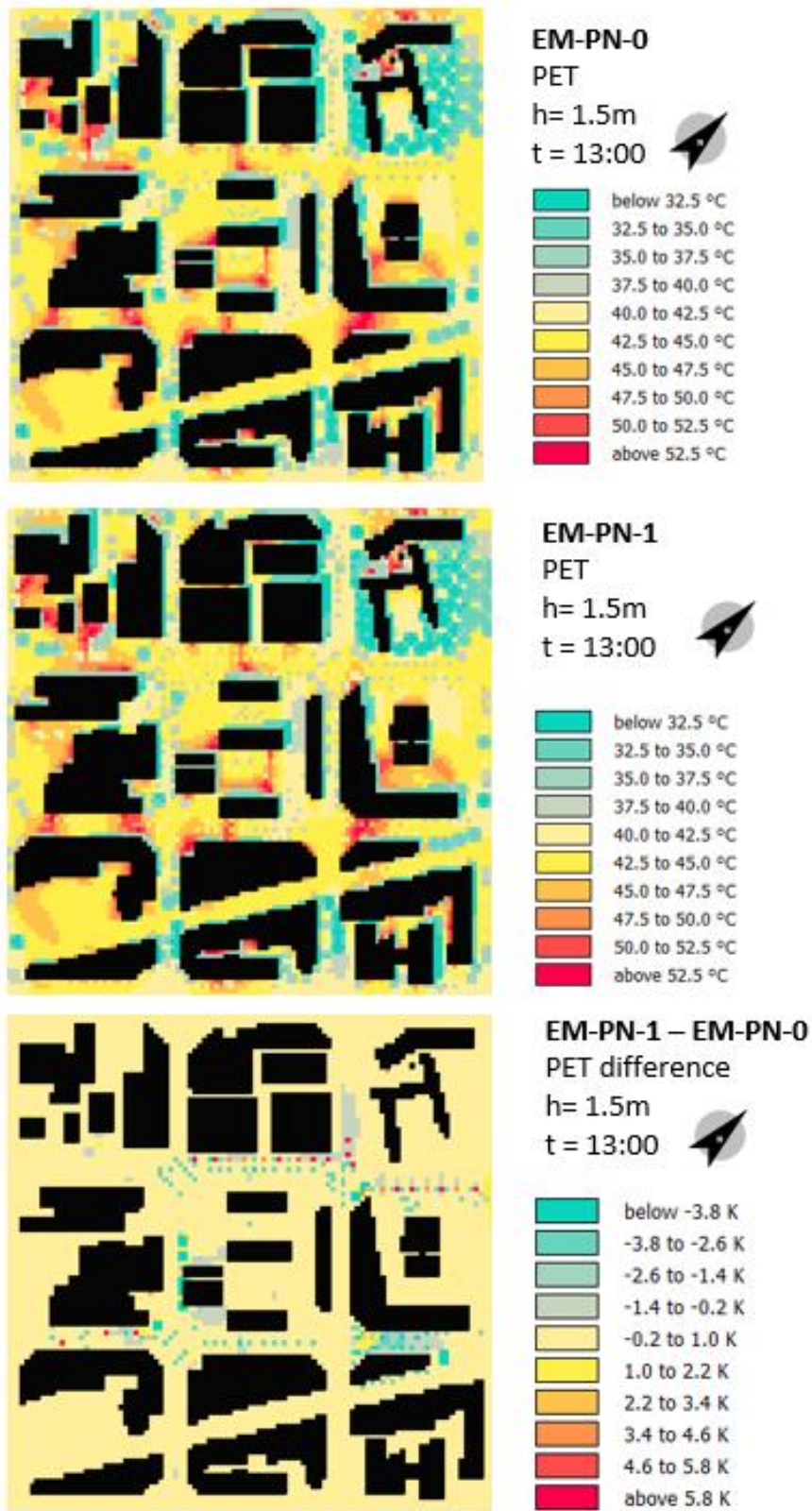


Figure 79. ENVI-met 2D PET results for Poblenu at h = 1.5 m at 13:00

3.2.2 Numerical Results – ENVI-met

In this section the plotted graphs of average air temperature at the virtual sensors, which were defined in section 2.2.3.1, show three different heights, namely 5 m, 10 m and 20 m. The measured temperature at Raval Weather Station, which was used as the Boundary Condition as described in 2.1, is also plotted. The difference in air temperature EM-SA-1 minus EM-SA-0 and EM-PN-1 minus EM-PN-0 are shown as well.

Hourly ground surface temperature, air speed at pedestrian level, as well as the resulting PET are plotted, and compared to the boundary conditions at the Raval Weather Station. The difference in these three variables between scenarios EM-SA-1 minus EM-SA-0 and EM-PN-1 minus EM-PN-0 are also shown.

Figure 80 shows the air temperature at different heights for the models EM-SA-0 and EM-SA-1 from Sant Antoni.

Figure 81 shows relative humidity, air speed and surface temperature for the models EM-SA-0 and EM-SA-1 from Sant Antoni.

Figure 82 shows absolute value of PET at pedestrian level in Sant Antoni and the difference between models EM-SA-0 and EM-SA-1.

Figure 83 shows the air temperature at different heights for the models EM-PN-0 and EM-PN-1 from Poblenou.

Figure 84 shows relative humidity, air speed and surface temperature for the models EM-PN-0 and EM-PN-1 from Poblenou.

Figure 85 shows absolute value of PET at pedestrian level in Poblenou and the difference between models EM-PN-0 and EM-PN-1.

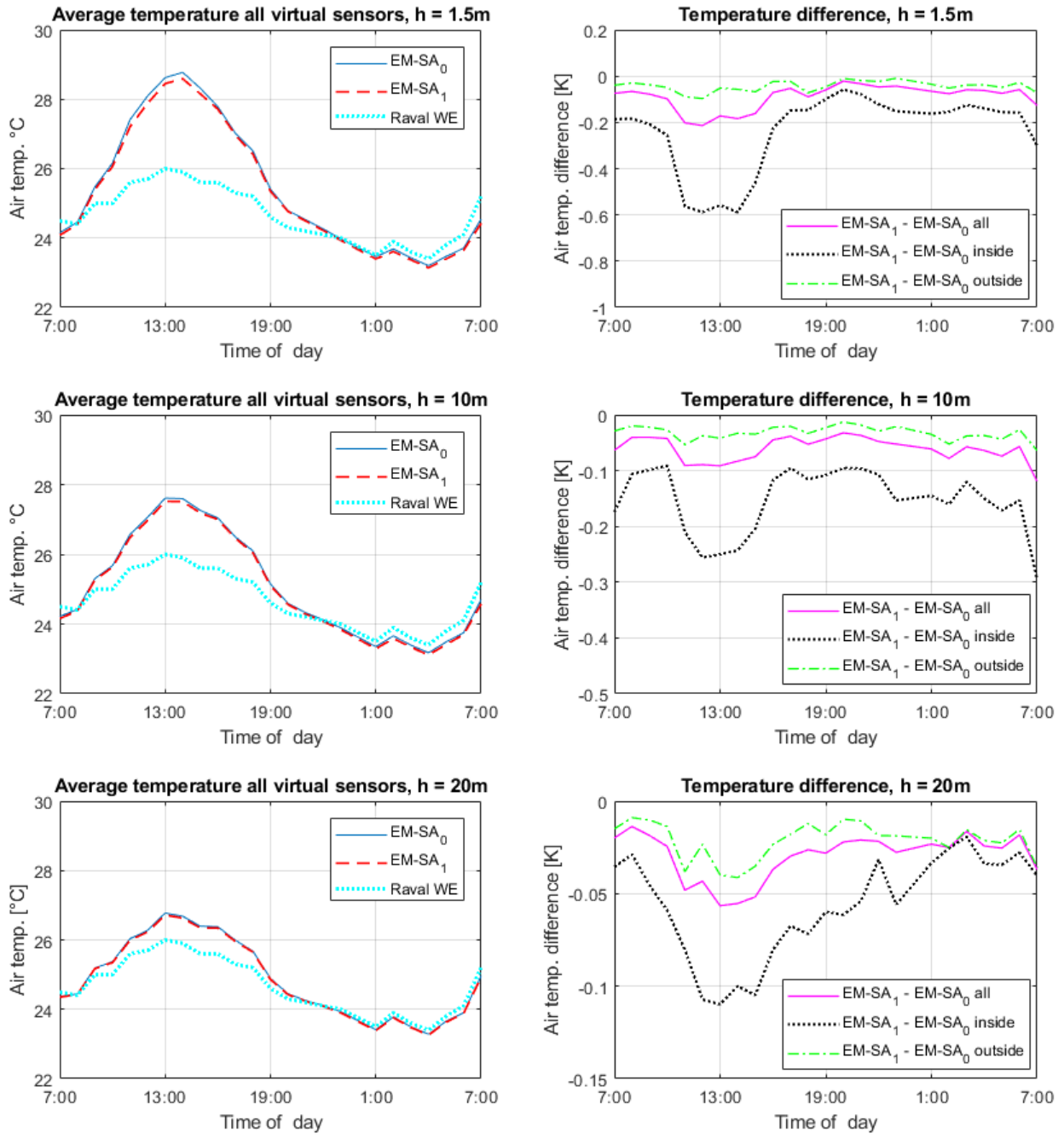


Figure 80. Hourly air temperature at different heights, Sant Antoni. Results from ENVI-met

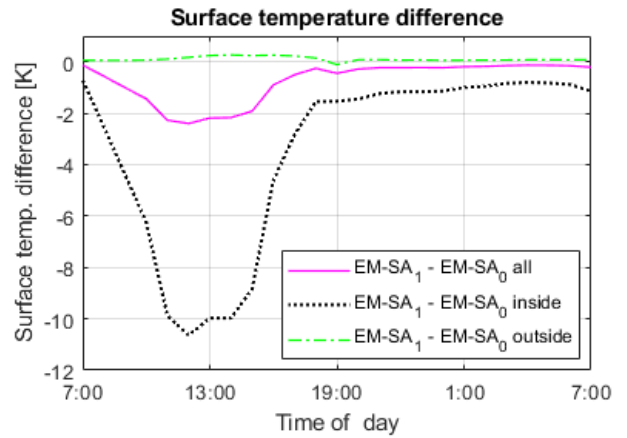
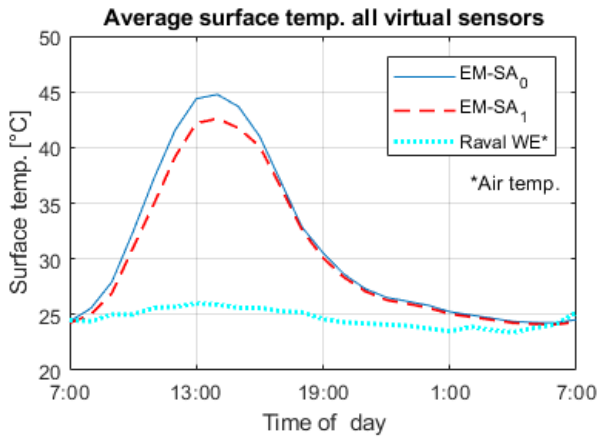
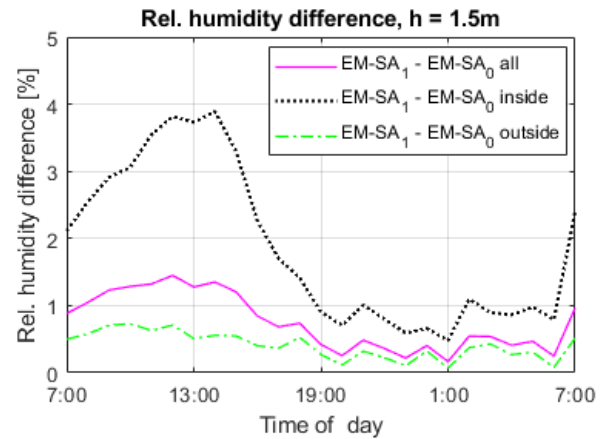
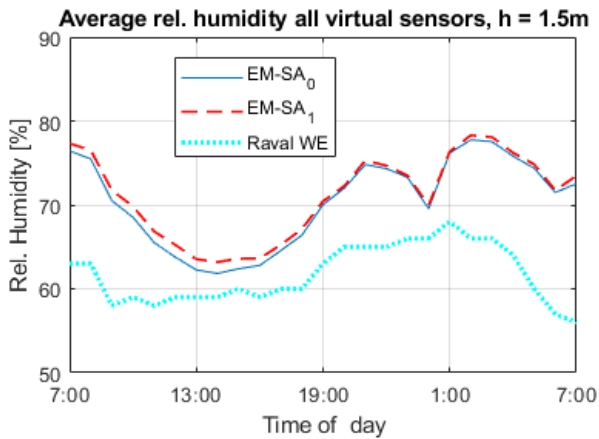
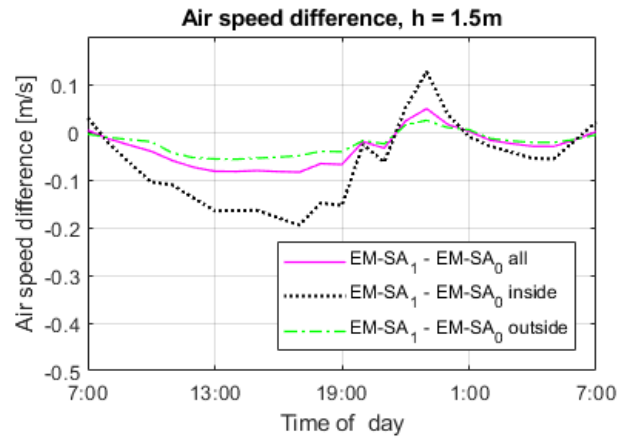
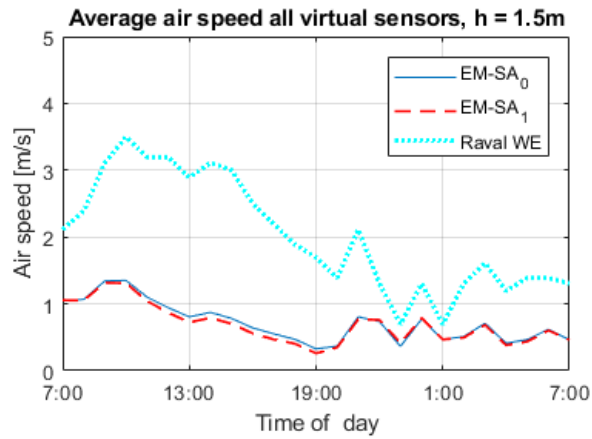


Figure 81. Hourly air speed, relative humidity and surface temperature, Sant Antoni. Results from ENVI-met

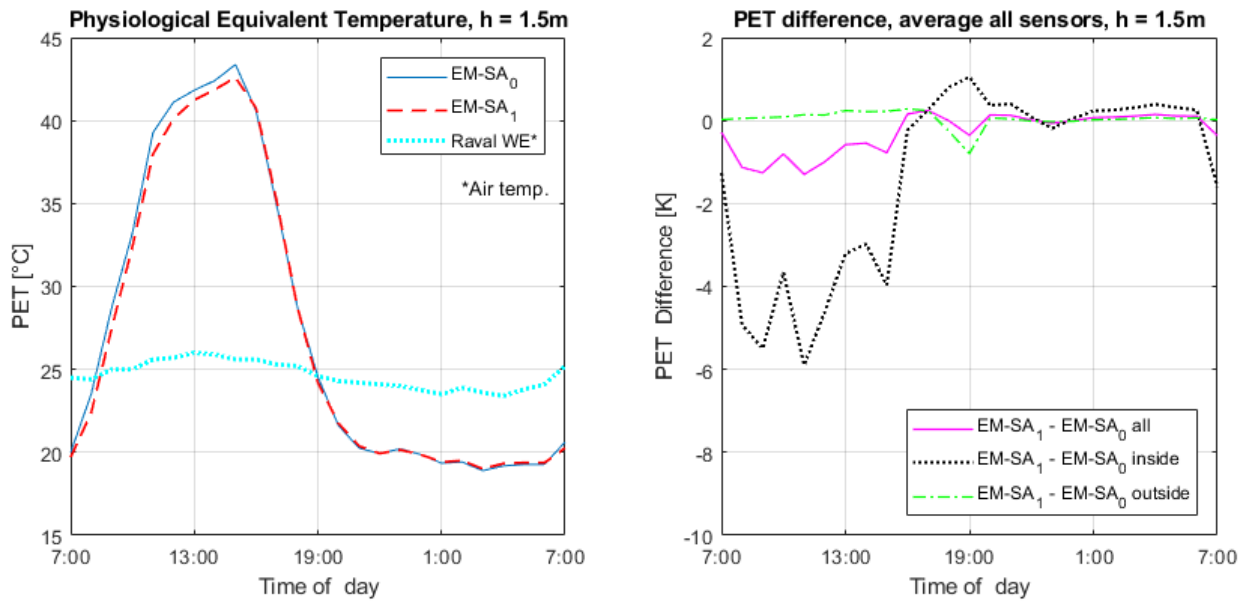


Figure 82. Hourly PET, Sant Antoni. Results from ENVI-met

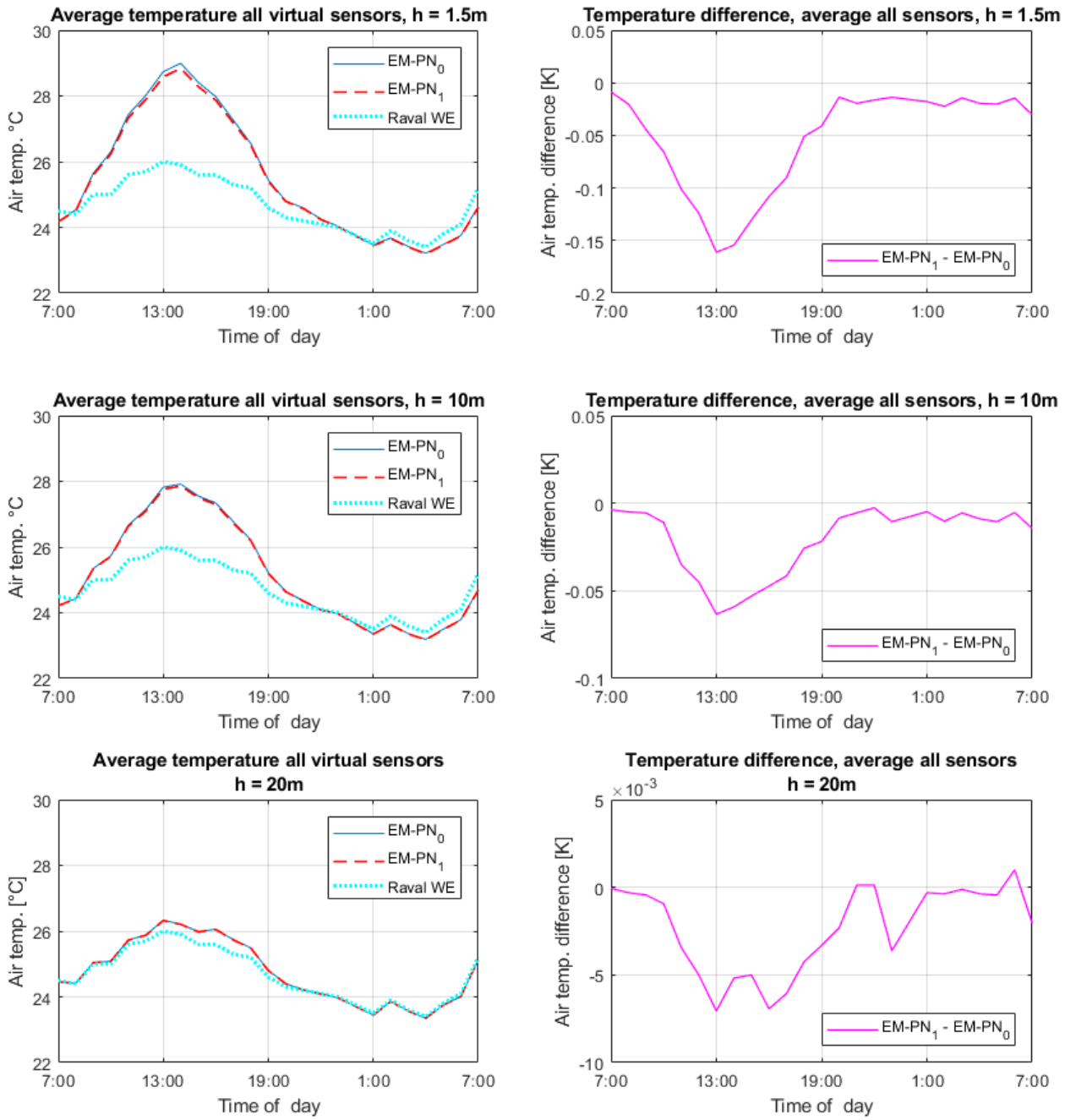


Figure 83. Hourly air temperature at different heights, Poblenu. Results from ENVI-met

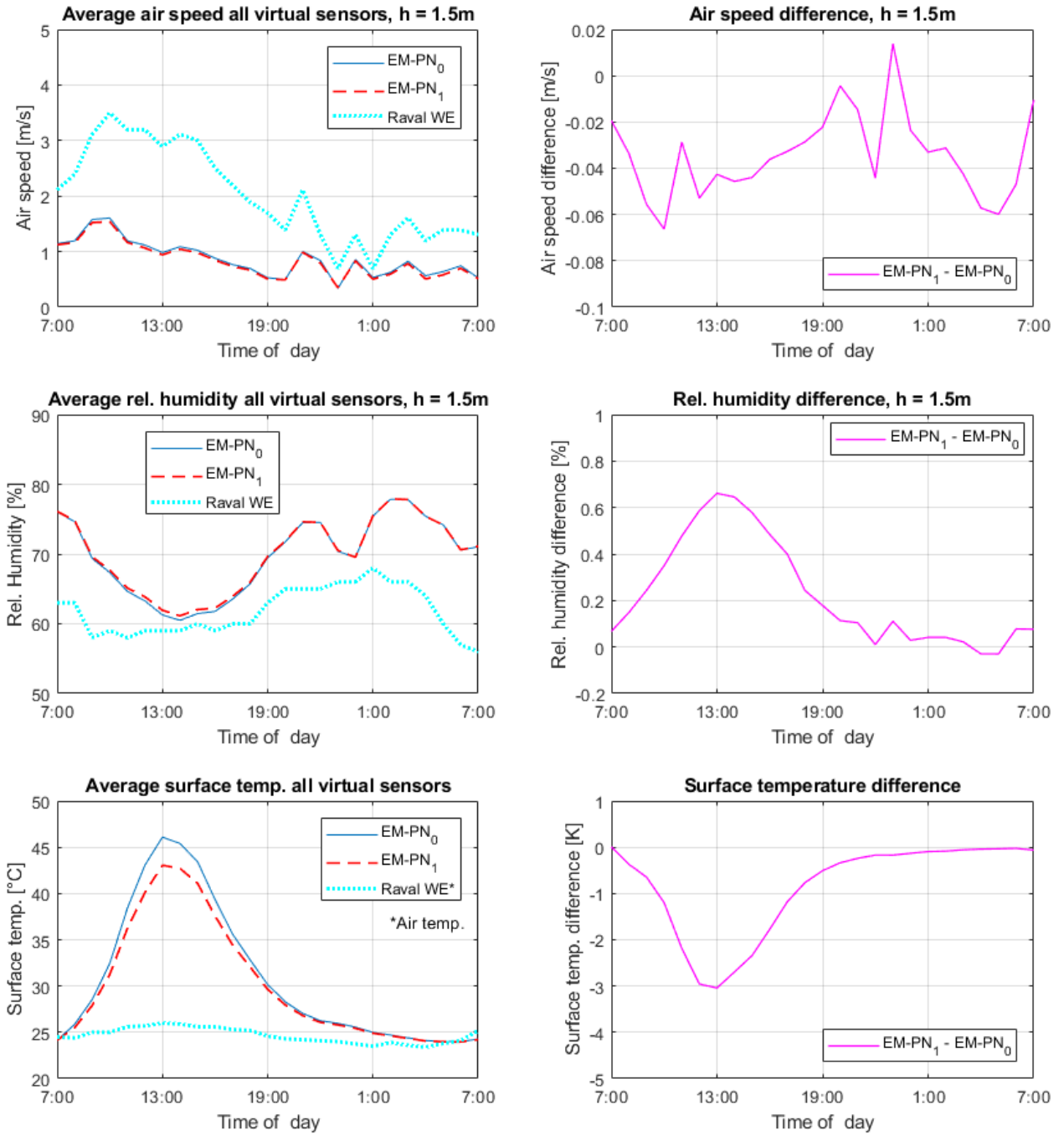


Figure 84. Hourly air speed, relative humidity, and surface temperature, Poblenu. Results from ENVI-met

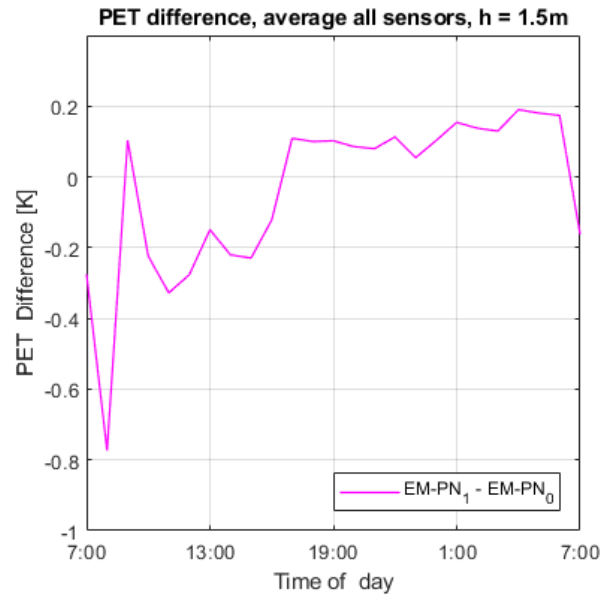
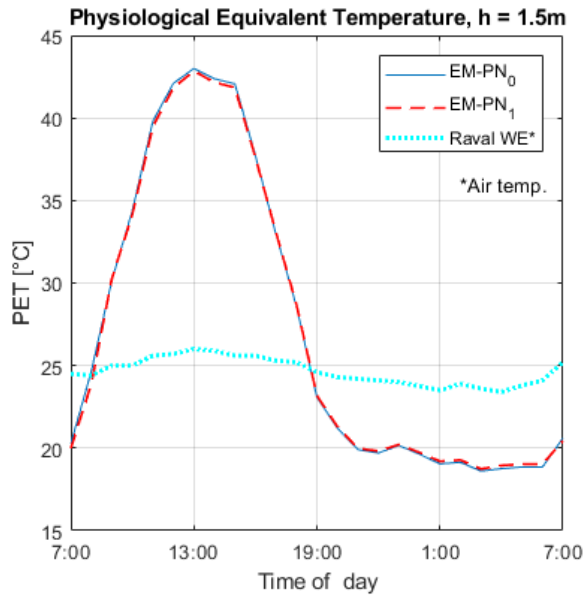


Figure 85. Hourly PET, Poblenu. Results from ENVI-met

3.3 Urban Weather Generator

The results from the UWG show the UHI effect for Sant Antoni and Poblenou before and after the implementation of the Superblock and are plotted in this section. The output of this tool is the average air temperature of urban canopy in all areas of the studied zone.

The results from the Urban Weather Generator tool in Figure 86, Figure 87 and Figure 88, were calculated from 1st of June until 31st of August.

The average urban canopy temperature was plotted for scenarios UWG-SA-0, UWG-SA-1, UWG-PN-0 and UWG-PN-1. The measured temperature at the Rural El Prat Weather Station, which was used as the Boundary Condition as described in 2.1, was also plotted.

Figure 86 shows urban canopy temperature without the addition of anthropogenic heat gains, whereas the results shown in Figure 87 consider them. Figure 88 shows the Urban Heat Island effect in all four scenarios, it was calculated by subtracting the rural air temperature to the urban air temperature.

Figure 89, Figure 90 and Figure 91 show the urban canopy temperature for the period between 31st of July at 7:00 and 1st of August at 7:00, which corresponds to the simulated period in ENVI-met.

The urban canopy temperature from the scenarios UWG-SA-0, UWG-SA-1, UWG-PN-0, UWG-PN-1, as well as the difference in urban canopy temperature were plotted. Results are shown both with and without anthropogenic heat gains in Figure 89 and Figure 90, respectively. Figure 91 shows the Urban Heat Island effect in all four scenarios for the selected period.

In Figure 92 and Figure 93, the box-plot graphs show the statistical distribution of urban canopy temperature difference of daily maximum and minimum temperatures between scenarios before and after Superblocks calculated by the UWG tool.

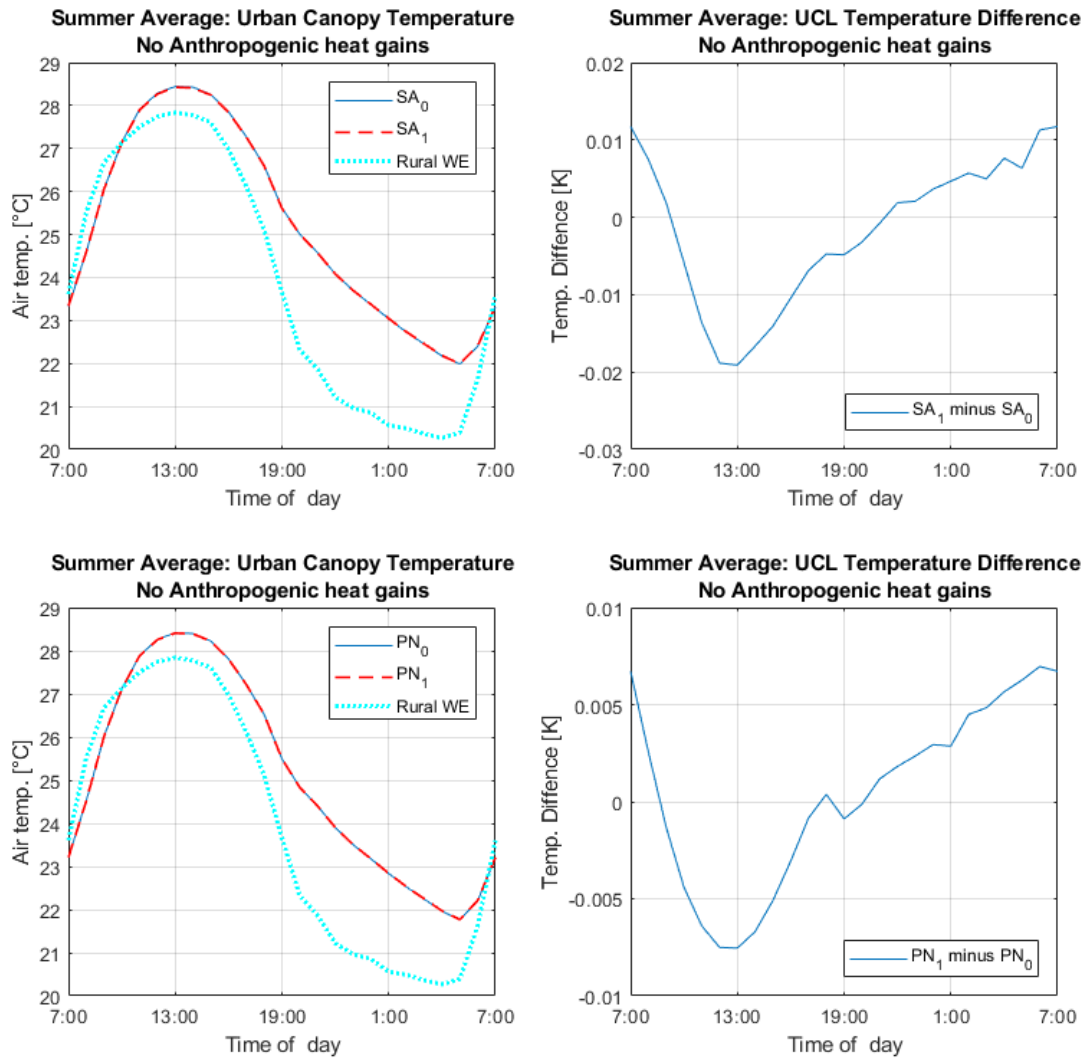


Figure 86. Hourly temperature, Summer average not considering anthropogenic gains.
 Results from UWG

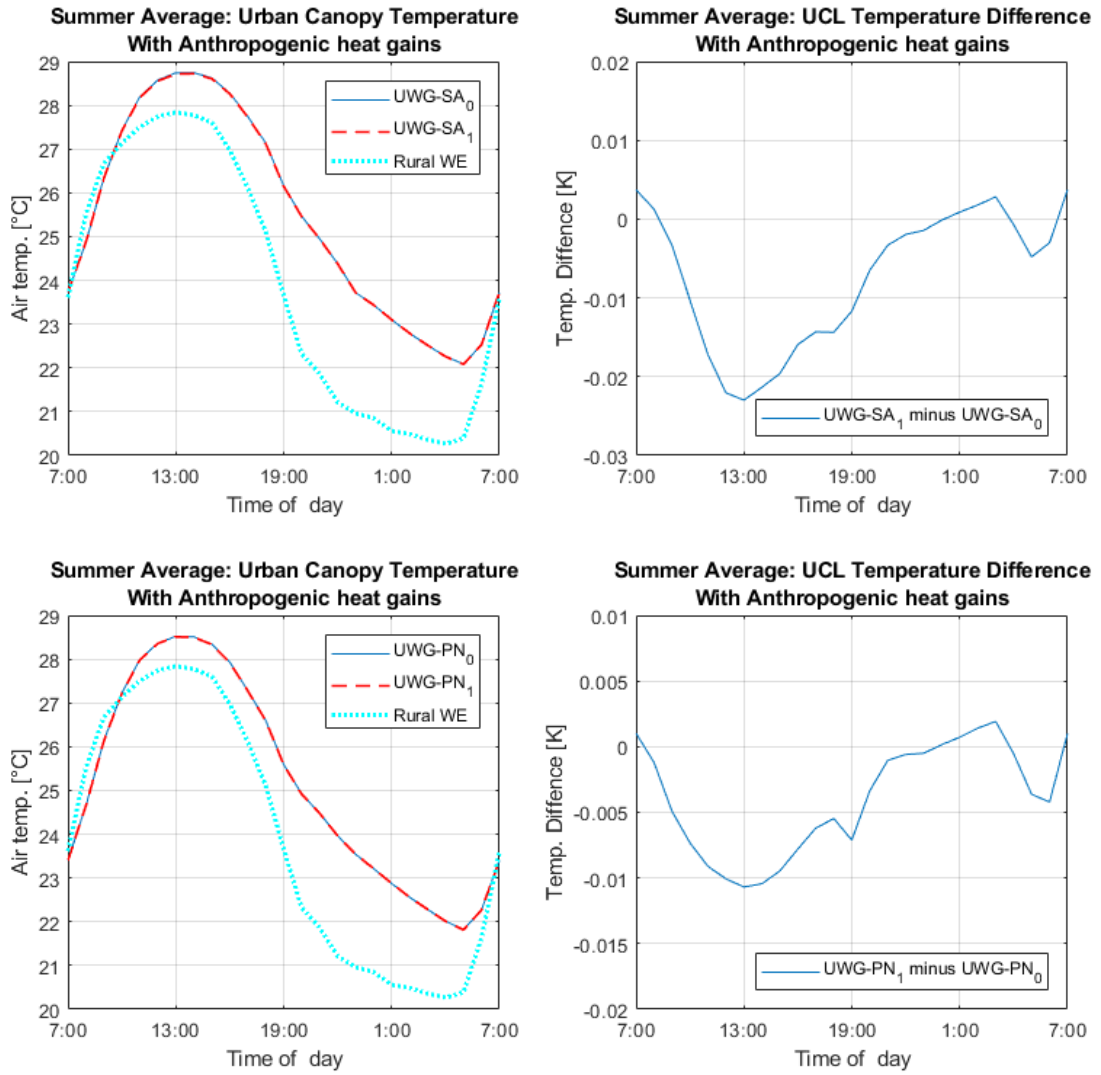


Figure 87. Hourly temperature, Summer average considering anthropogenic gains. Results from UWG

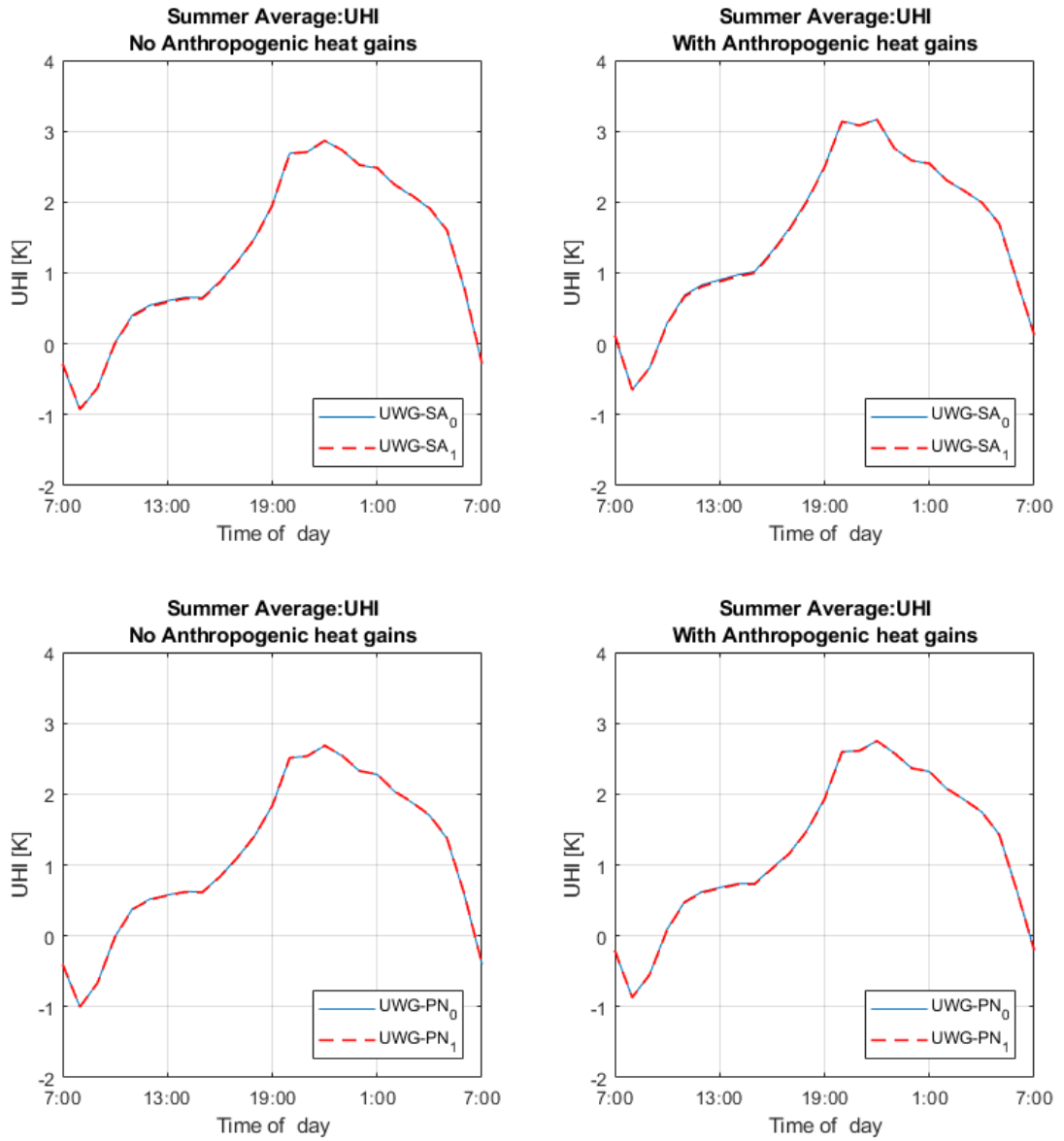


Figure 88. UHI, summer average. Results from UWG

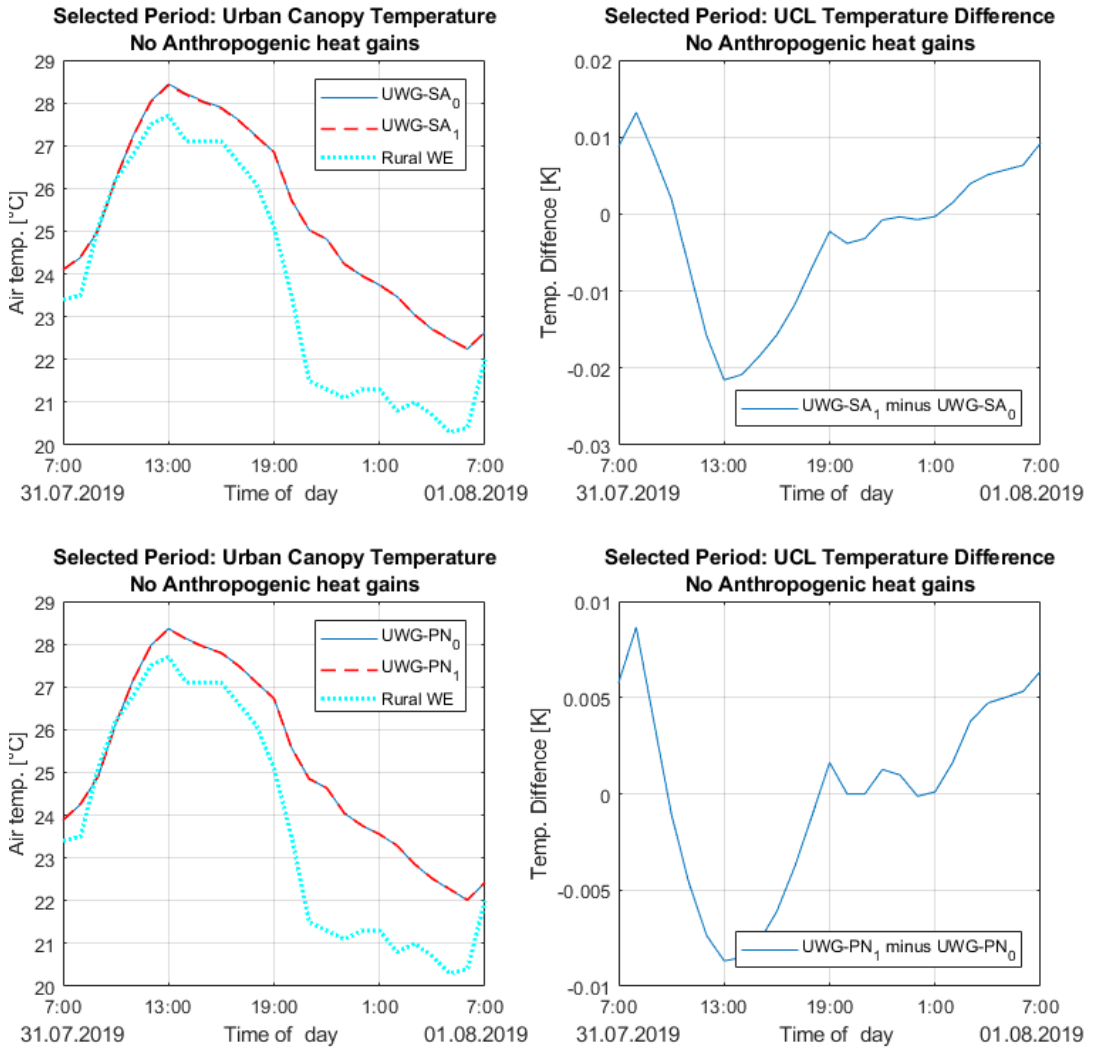


Figure 89. Hourly temperature, selected period not considering anthropogenic gains. Results from UWG

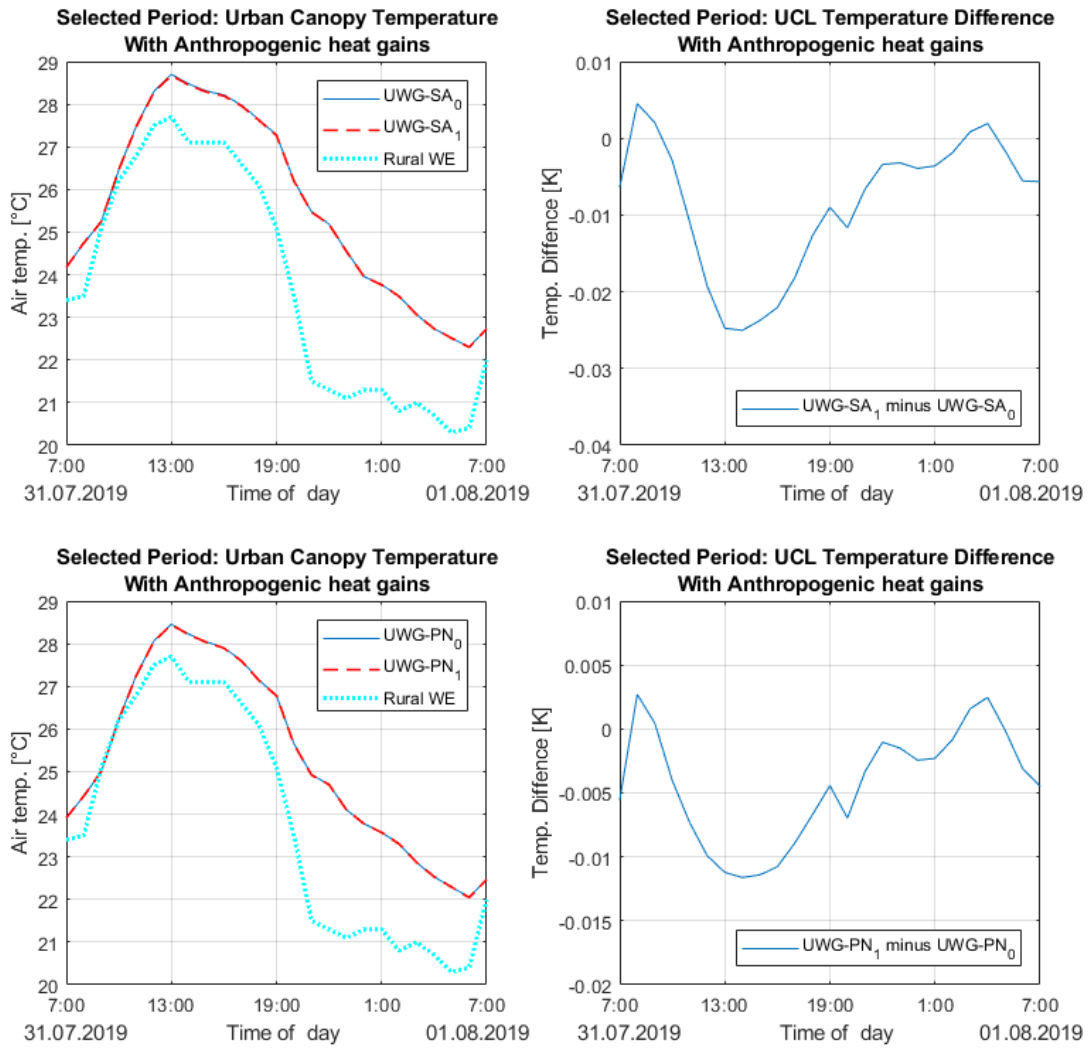


Figure 90. Hourly temperature, selected period considering anthropogenic gains. Results from UWG

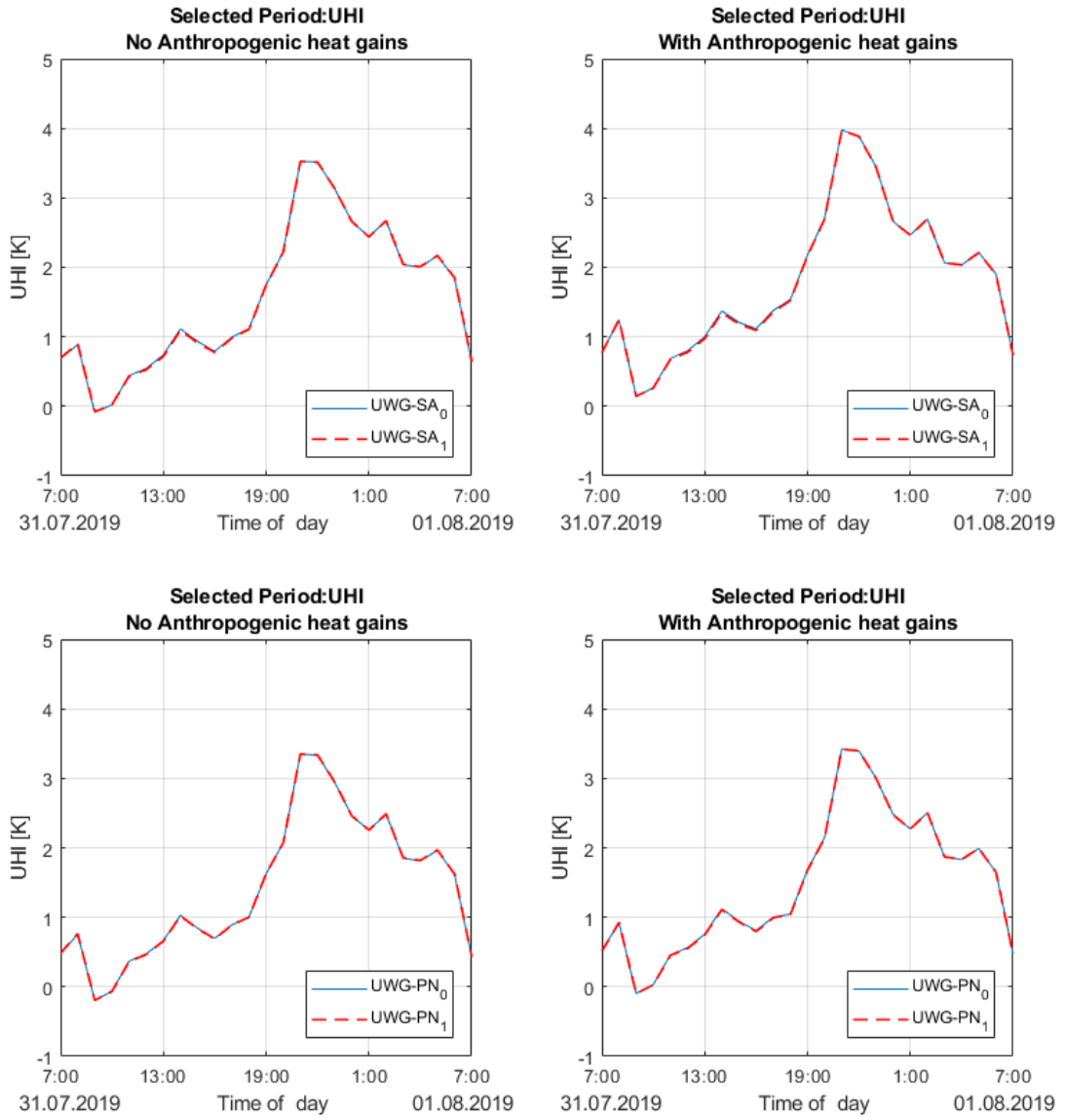


Figure 91. UHI, selected period. Results from UWG

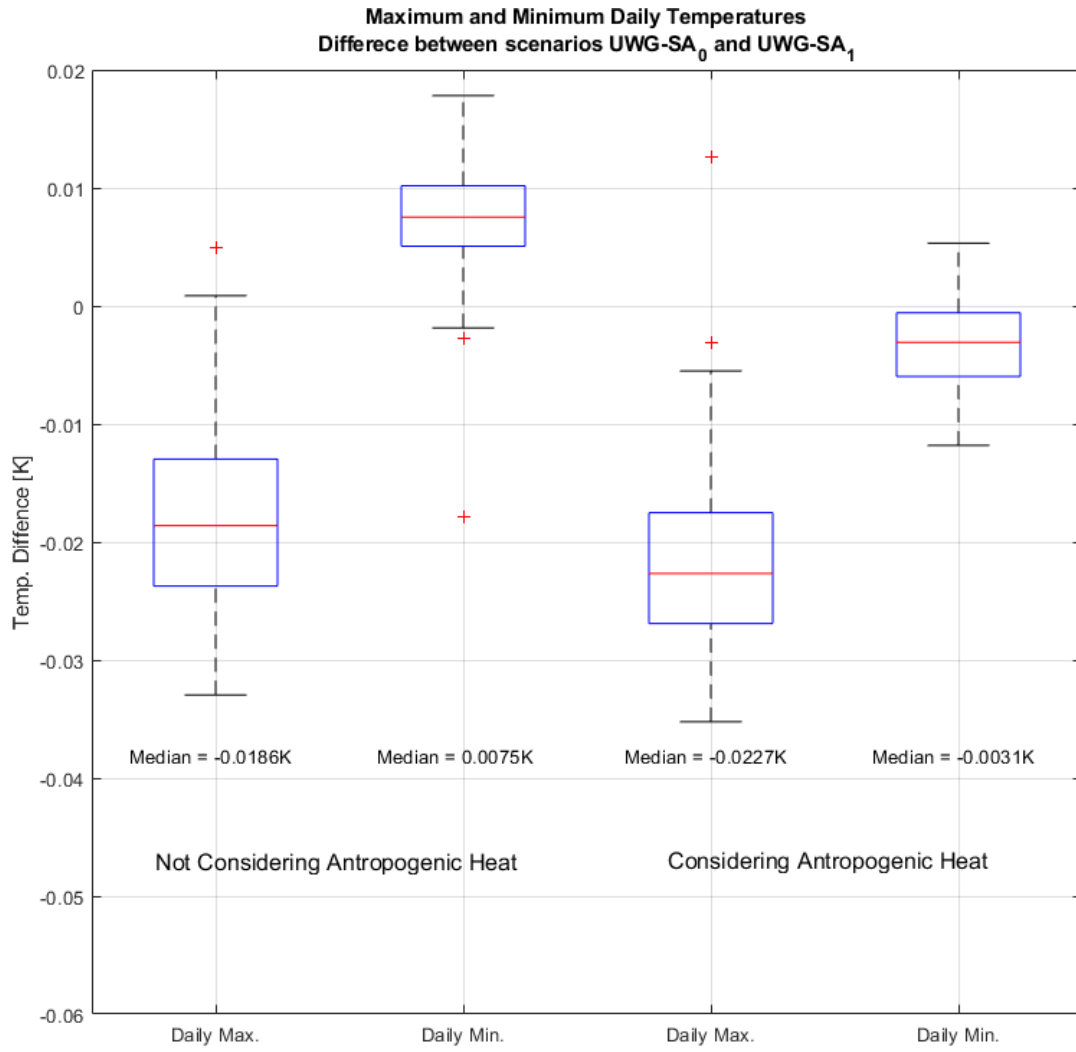


Figure 92. Temperature comparison before and after the implementation of the Superblock Sant Antoni. Boxplot of maximum and minimum temperature differences. Results from UWG

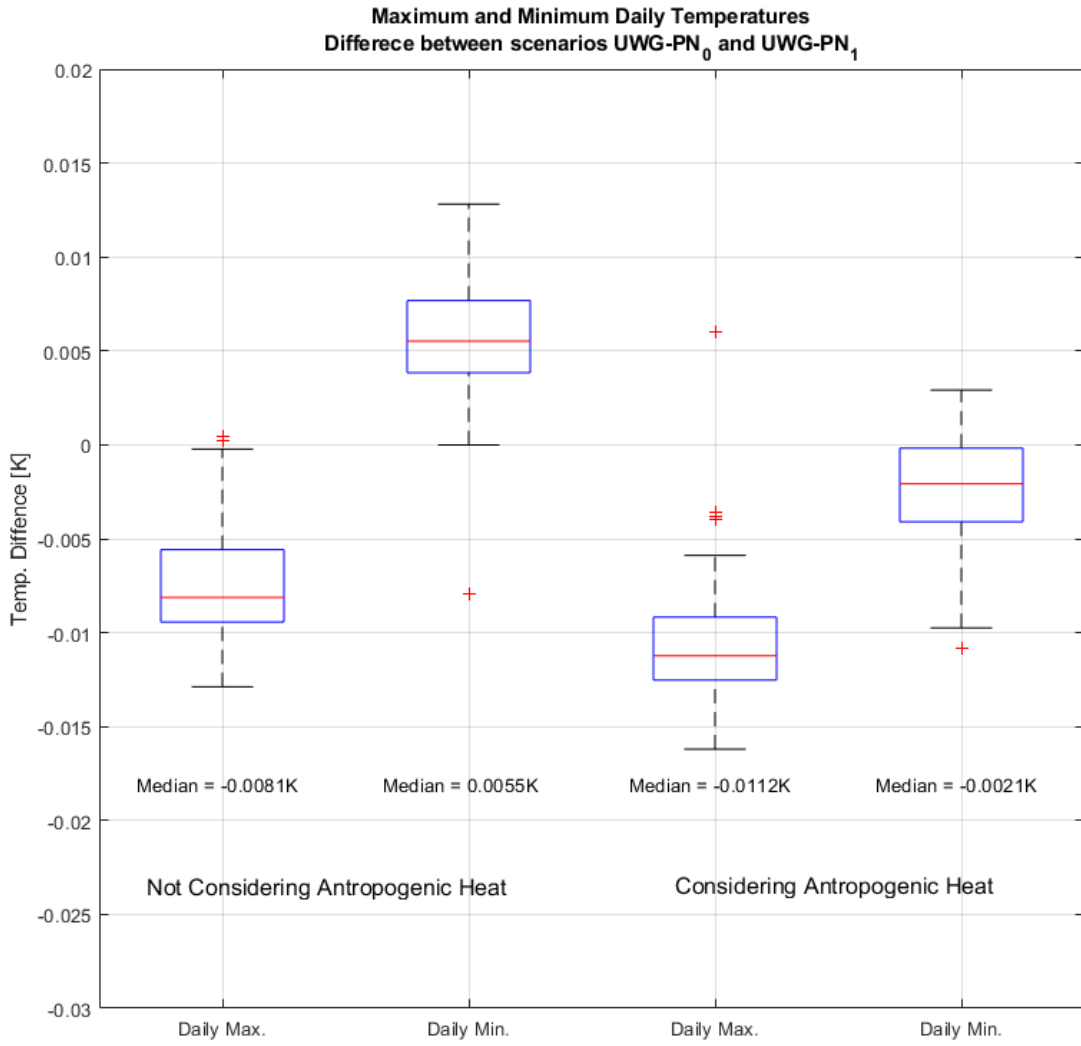


Figure 93. Temperature comparison before and after the implementation of the Superblock Poblenu. Boxplot of maximum and minimum temperature differences. Results from UWG

4 DISCUSSION

4.1 Overview

In this Discussion chapter, the results from the two evaluated tools will be first separately analyzed and then the results, and the tools, will be compared.

In section 4.2, the results from the CFD simulation from ENVI-met of the two studied areas before and after the implementation of Superblocks, will be discussed. In section 4.3, the results from the same areas and scenarios calculated by the Urban Weather Generator tool will be analyzed. Finally, in section 5, the results between both tools will be compared and divergences and convergences between them will be investigated.

4.2 ENVI-met

4.2.1 Sant Antoni

The 2D color map of temperature difference in Figure 62, from Sant Antoni, shows a decrease in temperature at pedestrian level during the day in the area where the Superblock was implemented, with a higher reduction on the perimeter of the market, where the dark parking roof was removed. At a height of 10 m, the decrease is significantly less evident (Figure 63), which is confirmed by the cross-section diagram from Figure 64. The graphs from Figure 80 show, at a height of 1.5m during the day, an average decrease of 0.6 K, which contrasts to a decrease of 0.25 K at 10 m and of 0.12 K at 20 m. At 4:00 the temperature decrease is less evident at all heights, starting at around 0.15 K at both 1.5 m and 10 m and decreasing to less than 0.05 K at 20 m.

Air speed also decreases with the implementation of the Superblock, especially on the central intersection, as seen in Figure 68, as this is the area where most new trees were planted. The peak decrease is of 0.9 m/s at 13:00 and at a height of 1.5 m. According to Figure 81, the average air speed decrease is around 0.18 m/s. The same figure shows that relative humidity increases up to 3.8% at 13:00.

Figure 69 shows that ground surface temperature at 13:00 decreases by up to 20 K where new shaded areas were created, and floor albedo is increased. In average, surface temperature dropped 10 K within the Superblock during daytime and 1 K during nighttime.

As a result of the implementation of the Sant Antoni Superblock, PET dropped up to 12 K at 13:00 at pedestrian level, with the color map coinciding closely to the surface temperature color map, as Figure 62 and Figure 70 show. In average, PET decreased around 5 K during daytime and had a slight increase of about 0.2 K during nighttime, as seen in Figure 82. The night increase in PET, even with a lower air temperature could be explained by lower air speed and higher humidity.

4.2.2 Poblenu

The temperature difference 2D color map at 13:00 at a height of 1.5 m in Figure 71 shows a decrease in temperature most streets where the Superblock was implemented, especially the western half, where most plant vases were installed. At a height of 10 m seen in Figure 72, the decrease is lower which is confirmed by the cross section diagram from Figure 73 and the graphs from Figure 83, which shows, at a height of 1.5 m, an average decrease of 0.15 K in contrast to a decrease of 0.05 K at 10 m and an even smaller one at 20m. At 4:00 the temperature decrease is less evident at all heights, and always lower than 0.05 K.

A decrease in air speed is almost not observed by the implementation of the Superblock, at about 0.06 m/s during the day at pedestrian level, as Figure 77 and Figure 84 show. Average relative humidity shows a slight increase of up to 0.6% during the day.

Figure 78 shows the punctual decrease in ground surface temperature where the plant vases were installed, this decrease was up to 12 K at 13:00 with an average decrease of 3 K.

The resulting reduction in PET at pedestrian level, thanks to of the implementation of the Poblenu Superblock, and seen in Figure 79, was estimated to be, at 13:00, up to 4 K where new shadows were created and, in average, 0.2 K.

A lower impact in PET from the Poblenu Superblock in comparison to the one in Sant Antoni is observed and one of the main factors should be the lower decrease in ground surface temperature in Poblenu. This Superblock was implemented with no flowerbeds, but vases, which can only accommodate small trees, that provide limited shaded areas, and have small, grassed area. Additionally, the Poblenu area is less densely built, which allow a greater ventilation and its microclimate is less dependent to local albedo and shading. Furthermore, the market area of Sant Antoni was covered with a light gray pavement while the pedestrianized portions of Poblenu Superblock are mainly marked with painted asphalt, with a lower albedo.

4.3 Urban Weather Generator

As revealed in Figure 88, the summer average calculated UHI in Sant Antoni, not counting Anthropogenic gains, is around 0.7 K at daytime and up to 2.8K during nighttime. The UHI in Poblenou with the same conditions was calculated to be 0.6 K at daytime and up to 2.6K during nighttime. Considering anthropogenic gains, the UHI was 1.0 K and 3.2 K in Sant Antoni during day and night, respectively. The UHI considering anthropogenic gains in Poblenou was 0.7 K during daytime and 2.7 K during nighttime.

The effect of anthropogenic gains in UHI, when it is considered, on the Sant Antoni region is considerable higher due to the higher proportion of the air conditioning waste heat being released to the street canyon.

The urban canopy temperature difference during the day, comparing the scenarios before and after the implementation of the Superblock, was in average 0.019 K and 0.0075 K during the summer for Sant Antoni and Poblenou, respectively, without the consideration of anthropologic gains. Considering these gains, the temperature difference of the urban canopy was 0.022K and 0.011 K for Sant Antoni and Poblenou. The urban canopy temperature difference increased as anthropogenic gains were considered thanks to the smaller road area to which traffic heat emissions were applied with the Superblocks.

As expected, the UHI effect during the night in all scenarios is higher as the thermal mass of the built environment stores heat during the day that is released at nighttime. In the early hours of the day, when the temperature is quickly rising, the rural temperature rises faster, as the urban centers have a higher thermal mass, and the low morning sun has difficulty to reach between the building.

5 CONCLUSION

In the course of this work, two very different tools were used to assess the impact in microclimate generated by the implementation of the studied Superblocks. These tools have very different methodologies and complexities of implementation and the output variables are also distinct.

The workflow of modeling with ENVI-met in version 4.4.3 was not optimal, because the implementation of the 3D model in blocks was manual, and a vectorized 3D model could not be automatically converted to ENVI-met. Additionally, once an area was modelled using a chosen resolution, it was impossible to convert to another resolution without starting the whole modelling process again. The new module *Monde* could help with that conversion, but it only works where there is a complete open-source 3D model available in Open-Source Maps, which is not the case for Barcelona and many other cities outside the USA.

ENVI-met simulation also showed very costly in terms of computational resources and time when done in a standard personal computer, such numerical complexity is typical to CFD simulations. The interface to export the raw numerical results to other programs was not ideal, the output files are saved in a proprietary format and must be manually converted to excel point by point. However, the output is very rich in details, spatially and concerning the number of output variables. It also presents a detailed map of the microclimate in the studied area and could be a very useful tool evaluate landscaping and architectural projects.

The results from ENVI-met in Sant Antoni show, with the implementation of the Superblock, a reduction in air temperature from pedestrian level until a height of 10 m, both during the day and at night. The same cannot be said at higher altitudes or just outside the project area. A noticeable decrease in perceived temperature in the pedestrian level was also revealed by the simulation, mostly due to a reduction of direct sun radiation and despite the increase in relative humidity and decrease in wind speed.

The results from the ENVI-met simulation show that the implementation of the Poblenou Superblock has an impact in air temperature and PET at pedestrian level about four times and two times lower than that of Sant Antoni, respectively. Sant Antoni Superblock has a more robust and permanent new infrastructure, with larger trees and more extensive flowerbeds, more asphalt converted into pedestrian paths, and a lighter new pavement than that of Poblenou. The distinct typologies of both

neighborhoods could also have played a whole in the different results, Sant Antoni is more densely occupied with little space for ventilation which could render its microclimate more susceptible to the local urban characteristics. Even with a measurable effect at ground level, the studied Superblocks fail to have a measurable impact on the higher parts of the urban canopy and outside of it.

The Urban Weather Generator has the advantage to be easy to implement once a 3D model is generated and, because of the nature of its calculation, is very fast and only takes a few minutes. The output regarding the building variables is very detailed but not as extensive regarding atmospheric variables.

Regarding the results from UWG, the little impact in the overall urban canopy temperature shows that the Superblocks, at least when a small portion of the urban fabric is altered, have limited consequence in the local UHI and in the air temperature throughout the day. This disproves one of the original questions about the impact of Superblocks in UHI and in the local air-conditioning usage. For the scale of the models calculated by UWG, the proposed changes by the Superblocks proved to be too limited, as the effect in the urban canopy temperature of the studied urban renewals was negligible. A possible explanation is that there is little change to building typology and building type or perhaps the original areas of intervention contained already many mature trees, and the percentage change was relatively small.

The Superblock is an urban solution that gained momentum during the year of 2020 as the COVID-19 pandemic brought the urge for more open public spaces as means of avoiding public agglomeration. This interest was added to the already critical need to address UHI and climate change. Additionally, the city of Barcelona is determined to expand the size of the Superblock project to the scale of the whole metropolis as the pilot projects were deemed successful. In fact, in the year 2020, similar urban renovations were implemented around the world in cities such as of Cordoba, Argentina and Montreal, Canada. Therefore, future studies could focus on the analysis of Superblocks when done in a metropolitan scale, and in this case the use of UWG could be recommended.

6 INDEX

6.1 List of Figures

Figure 1. Global temperature anomaly 1880-2018 (NASA, 2019).....	2
Figure 2. Barcelona average temperatures, 1971-2000 (Agencia, 2011)	6
Figure 3. Barcelona average precipitation and maximum daily precipitation, 1971-2000 (Agencia, 2011).....	6
Figure 4. Histogram of the absolute number of months in each decade with an average daily temperature above 24°C	7
Figure 5. Histogram of the absolute number of months in each decade with an average high temperature above 29°C	7
Figure 6. Cumulative Histogram per decade 1970 to 2010 of average monthly temperature. 8	
Figure 7. Cumulative Histogram per decade 1970 to 2010 of average monthly temperature. Months from June to September.....	8
Figure 8. Projection of the average temperature increase [K] for Barcelona (Agencia, 2011) 9	
Figure 9. Projection of the length of heatwaves in days for Barcelona (Agencia, 2011)	10
Figure 10. Projection of the increase in warm nights (above 20°C) in percentage for Barcelona (Agencia, 2011).....	10
Figure 11. Schematic temperature profile of an urban area showing the UHI effect (EPA, 2008)	11
Figure 12. The variables affecting thermal comfort and the PMV scale (Kumar, 2019).....	12
Figure 13. The relation between PPD and PMV (ASHRAE, 2011).....	13
Figure 14. PET index threshold and corresponding sensation categories and levels of physical stress (Kántor, 2016).....	14
Figure 15. Schematic representation of the street traffic before and after the implementation of Superblocks (Rueda, 2016)	14
Figure 16. The current street network of Barcelona, with its total length and surface area (Rueda, 2016)	15
Figure 17. Proposed street network of Barcelona, after the implementation of all planned Superblocks, with its total length and surface area (Rueda, 2016)	15
Figure 18. Schematic isometric view of an urban intersection, before and after the implementation of a Superblock (Rueda, 2016).....	16
Figure 19. Location of the two studied Superblocks, the old town of Barcelona is highlighted in red (Google Maps, 2020)	17
Figure 20. The intervention area of the Sant Antoni Superblock (Google Maps, 2020).....	18
Figure 21. Urban and landscape project of the Sant Antoni Superblock (Barcelona, 2019b) 19	
Figure 22. Sections of the street canyon comparing the original situation to the Superblock design (Barcelona, 2019b).....	19

Figure 23. Tamarit Street before the implementation of the Sant Antoni Superblock in 2014 (Google Maps, 2020) 20

Figure 24. Tamarit Street after the implementation of the Sant Antoni Superblock in 2019 . 20

Figure 25. Corner of Tamarit Street and Comte Borrell streets before the implementation of the Sant Antoni Superblock in 2009 (Google Maps, 2020)..... 21

Figure 26. Corner of Tamarit Street and Comte Borrell streets after the implementation of the Sant Antoni Superblock in 2019 (Google Maps, 2020)..... 21

Figure 27. The intervention area of the Poblenou Superblock (Google Maps, 2020) 22

Figure 28. Details of the implementation of the Poblenou Superblock (Barcelona, 2019b) .. 23

Figure 29. Corner of Roc de Boronat and Sancho de Ávila streets, before the implementation of the Poblenou Superblock in 2014 (Google Maps, 2020) 23

Figure 30. Corner of Roc de Boronat and Sancho de Ávila streets, after the implementation of the Poblenou Superblock in 2019 24

Figure 31. Location of the weather station relative to the studied areas (Google Maps, 2020) 25

Figure 32. More detailed view of the Raval weather station (Salvati et al., 2017) 26

Figure 33. El Prat de Llobregat weather station (Servei, 2019)..... 26

Figure 34. Location of the installed sensor-logger (Google Maps, 2020) 27

Figure 35. Installation of the sensor-logger..... 27

Figure 36. ENVI-met Model Architecture (ENVI-met, 2019) 28

Figure 37. Schematic model of ENVI-met..... 29

Figure 38. Sant Antoni ENVI-met models with 3 different resolutions 31

Figure 39. Poblenou ENVI-met models with 3 different resolutions 31

Figure 40. Scatter graph comparing the divergence in simulated air temperatures at 1.5 m between the medium resolution model (3 x 3 meters) and large resolution model (4 x 4 meters) for Sant Antoni 32

Figure 41. Scatter graph comparing the divergence in simulated air temperatures at 1.5 m between the medium resolution model (3 x 3 meters) and large resolution model (4 x 4 meters) for Poblenou 33

Figure 42. Scatter graph comparing the divergence in simulated air temperatures at 1.5 m according to the duration of the simulation for Sant Antoni 35

Figure 43. Scatter graph comparing the divergence in simulated air temperatures at 1.5 m according to the duration of the simulation for Poblenou..... 35

Figure 44. Measured and simulated air temperatures, with two different Full-forcing methods 36

Figure 45. Scatter graph comparing simulated using different Full-forcing methods and measured temperature 37

Figure 46. Measured weather station data during the evaluated period 38

Figure 47. Graph showing the measured direct solar radiation and its approximation to a parabolic curve 39

Figure 48. Aerial photos from Sant Antoni Market in 2010 and 2019 (Google Maps, 2020) .	40
Figure 49. Model EM-SA-0: Sant Antoni before the implementation of the Superblock.....	41
Figure 50. Aerial photos from Poblenou in 2015 and 2019 (Google Maps, 2020)	41
Figure 51. Model EM-PN-0: Poblenou before the implementation of the Superblock	42
Figure 52. Model EM-SA-1: Sant Antoni after the implementation of the Superblock (ENVI- met)	42
Figure 53. Model EM-PN-1: Poblenou after the implementation of the Superblock (ENVI-met)	43
Figure 54. Locations of the virtual sensors in the Sant Antoni model.....	44
Figure 55. Locations of the virtual sensors in the Poblenou model	44
Figure 56. Schematic description of the calculations performed by the Urban Weather Generator (Bueno et al., 2013)	45
Figure 57. Schematic model of the Urban Weather Generator	45
Figure 58. UWG Model Sant Antoni, before Superblock	49
Figure 59. UWG Model Sant Antoni, with Superblock	49
Figure 60. UWG Model Poblenou, before Superblock.....	50
Figure 61. UWG Model Poblenou, after Superblock.....	50
Figure 62. ENVI-met 2D temperature results for Sant Antoni at h = 1.5 m at 13:00	53
Figure 63. ENVI-met 2D temperature results for Sant Antoni at h = 10 m at 13:00	54
<i>Figure 64. ENVI-met 2D temperature results for Sant Antoni section diagram at 13:00</i>	<i>55</i>
Figure 65. ENVI-met 2D temperature results for Sant Antoni at h = 1.5 m at 4:00	56
Figure 66. ENVI-met 2D temperature results for Sant Antoni at h = 10 m at 4:00	57
<i>Figure 67. ENVI-met 2D temperature results for Sant Antoni section diagram at 4:00</i>	<i>58</i>
Figure 68. ENVI-met 2D air speed results for Sant Antoni at h = 1.5 m at 13:00	59
Figure 69. ENVI-met 2D surface temperature results for Sant Antoni at 13:00.....	60
Figure 70. ENVI-met 2D PET results for Sant Antoni at h = 1.5 m at 13:00.....	61
Figure 71. ENVI-met 2D temperature results for Poblenou at h = 1.5 m at 13:00.....	62
Figure 72. ENVI-met 2D temperature results for Poblenou at h = 10 m at 13:00.....	63
<i>Figure 73. ENVI-met 2D temperature results for Poblenou section diagram at 13:00</i>	<i>64</i>
Figure 74. ENVI-met 2D temperature results for Poblenou at h = 1.5 m at 4:00.....	65
Figure 75. ENVI-met 2D temperature results for Poblenou at h = 10 m at 4:00.....	66
<i>Figure 76. ENVI-met 2D temperature results for Poblenou section diagram at 4:00</i>	<i>67</i>
Figure 77. ENVI-met 2D air speed results for Poblenou at h = 1.5 m at 13:00	68
Figure 78. ENVI-met 2D surface temperature results for Poblenou at 13:00	69
Figure 79. ENVI-met 2D PET results for Poblenou at h = 1.5 m at 13:00	70
Figure 80. Hourly air temperature at different heights, Sant Antoni. Results from ENVI-met	72
Figure 81. Hourly air speed, relative humidity and surface temperature, Sant Antoni. Results from ENVI-met	73
Figure 82. Hourly PET, Sant Antoni. Results from ENVI-met.....	74
Figure 83. Hourly air temperature at different heights, Poblenou. Results from ENVI-met...	75

Figure 84. Hourly air speed, relative humidity, and surface temperature, Poblenu. Results from ENVI-met	76
Figure 85. Hourly PET, Poblenu. Results from ENVI-met	77
Figure 86. Hourly temperature, Summer average not considering anthropogenic gains. Results from UWG	79
Figure 87. Hourly temperature, Summer average considering anthropogenic gains. Results from UWG	80
Figure 88. UHI, summer average. Results from UWG	81
Figure 89. Hourly temperature, selected period not considering anthropogenic gains. Results from UWG	82
Figure 90. Hourly temperature, selected period considering anthropogenic gains. Results from UWG.....	83
Figure 91. UHI, selected period. Results from UWG	84
Figure 92. Temperature comparison before and after the implementation of the Superblock Sant Antoni. Boxplot of maximum and minimum temperature differences. Results from UWG	85
Figure 93. Temperature comparison before and after the implementation of the Superblock Poblenu. Boxplot of maximum and minimum temperature differences. Results from UWG	86

6.2 List of Tables

Table 1. Running time and error of each simulation from the resolution test	33
Table 2. Running time and error of each simulation from the warm-up test.....	34
Table 3. Meteorological conditions of the simulated days	38
Table 4. Material Albedos	40

6.3 List of Equations

(1) Root mean square error.....	32
(2) Coefficient of variation	32

7 LITERATURE

Achour-Younsi, S. and Kharrat, F., 2016. 'Outdoor Thermal Comfort: Impact of the Geometry of an Urban Street Canyon in a Mediterranean Subtropical Climate – Case Study Tunis, Tunisia', *Procedia - Social and Behavioral Sciences*, vol. 216, pp. 689–700.

Agencia, 2011 (Agencia Estatal de Meteorología). *Iberian Climate Atlas: Air Temperature and Precipitation (1971-2000)* [Online]. Available at http://www.aemet.es/documentos/es/conocermas/recursos_en_linea/publicaciones_y_estudios/publicaciones/Atlas-climatologico/Atlas.pdf (Accessed 3 October 2019).

Aleksandrowicz, O., Vuckovic, M., Kiesel, K. and Mahdavi, A., 2017. 'Current trends in urban heat island mitigation research: Observations based on a comprehensive research repository', *Urban Climate*, vol. 21, pp. 1–26.

Ambrosini, D., Galli, G., Mancini, B., Nardi, I. and Sfarra, S., 2014. 'Evaluating Mitigation Effects of Urban Heat Islands in a Historical Small Center with the ENVI-Met® Climate Model', *Sustainability*, vol. 6, no. 10, pp. 7013–7029.

ASHRAE, 2011 (American Society of Heating, Refrigerating and Air-Conditioning Engineers). *55: Thermal Environmental Conditions for Human Occupancy*, Atlanta, USA.

Barcelona, 2019a (City of Barcelona). *Know your neighborhood Website* [Online]. Available at <https://ajuntament.barcelona.cat/> (Accessed 4 November 2019).

Barcelona, 2019b (City of Barcelona). *Superilles: Fem Junts el Programa Superilles* [Online]. Available at <http://ajuntament.barcelona.cat/superilles/ca/> (Accessed 20 October 2019).

Barcelona, 2013 (City of Barcelona). *Pla del verd i de la biodiversitat de Barcelona 2020*. [Online], Barcelona, Medi Ambient i Serveis Urbans - Hàbitat Urbà. Available at <https://ajuntament.barcelona.cat/ecologiaurbana/sites/default/files/Pla%20del%20verd%20i%20de%20la%20biodiversitat%20de%20Barcelona%202020.pdf> (Accessed 5 May 2019).

Barcelona, 2015 (City of Barcelona). *Compromís de Barcelona per Clima* [Online], Barcelona. Available at https://ajuntament.barcelona.cat/premsa/wp-content/uploads/2015/11/Compromis_Bcn_Clima.pdf (Accessed 4 May 2019).

Barcelona, 2016 (City of Barcelona). *Omplim de Vida el Carrer: La implantació de les Superilles* [Online], Barcelona, City of Barcelona Comissió d'Ecologia, Urbanisme i Mobilitat. Available at <https://bcnroc.ajuntament.barcelona.cat/jspui/bitstream/11703/97356/1/mesuradegovernomplimdevidaelscarrerslaimplantacidelessuperi-160518111846.pdf> (Accessed 12 June 2019).

Bueno, B., Norford, L., Hidalgo, J. and Pigeon, G., 2013. 'The urban weather generator', *Journal of Building Performance Simulation*, vol. 6, no. 4, pp. 269–281.

EEA, 2019 (European Environmental Agency). *Global and European Temperature: Will the increase in global average temperature stay below 2 °C above pre-industrial levels?* [Online]. Available at <https://www.eea.europa.eu/data-and-maps/indicators/global-and-european-temperature-9/assessment> (Accessed 15 August 2019).

ENVI-met, 2019. *ENVI-met Model Architecture* [Online]. Available at <http://envi-met.info/doku.php?id=intro:modelconcept> (Accessed 20 September 2019).

EPA, 2008 (American Environmental Protection Agency). *Reducing Urban Heat Islands: Compendium of Strategies: Urban Heat Island Basics* [Online]. Available at <https://www.epa.gov/sites/production/files/2014-06/documents/basicscompendium.pdf> (Accessed 12 August 2019).

Eurostat, 2016. *Urban Europe — statistics on cities, towns, and suburbs — life in cities* [Online]. Available at https://ec.europa.eu/eurostat/statistics-explained/index.php/Urban_Europe_%E2%80%94_statistics_on_cities,_towns_and_suburbs_%E2%80%94_life_in_cities (Accessed 20 September 2019).

Google Maps, 2020. *Google Maps* [Online]. Available at <https://www.google.at/maps> (Accessed 5 May 2020).

Höppe, P., 1999. 'The physiological equivalent temperature - a universal index for the biometeorological assessment of the thermal environment', *International journal of biometeorology*, vol. 43, no. 2, pp. 71–75.

IEA, 2018 (International Energy Agency). *The Future of Cooling: Opportunities for energy-efficient air conditioning* [Online]. Available at <https://webstore.iea.org/the-future-of-cooling> (Accessed 20 October 2019).

IPCC, 2019 (Intergovernmental Panel on Climate Change). *Scenario Process for AR5* [Online]. Available at https://sedac.ciesin.columbia.edu/ddc/ar5_scenario_process/index.html (Accessed 6 December 2019).

Julià, P. M., 2017. *Evaluación de proyectos urbanos: El caso de las supermanzanas de Barcelona*, Final Master Thesis for Ingeniería de caminos, canales y puerto, Barcelona, UPC Barcelona.

Kántor, N., 2016. 'Differences between the evaluation of thermal environment in shaded and sunny position', *Hungarian Geographical Bulletin*, vol. 65, no. 2, pp. 139–153.

Kumar, P., 2019. *Role of CFD in evaluating occupant thermal comfort* [Online]. Available at <https://www.simulationhub.com/blog/role-of-cfd-in-evaluating-occupant-thermal-comfort> (Accessed 10 November 2020).

López-Cabeza, V. P., Galán-Marín, C., Rivera-Gómez, C. and Roa-Fernández, J., 2018. 'Courtyard microclimate ENVI-met outputs deviation from the experimental data', *Building and Environment*, vol. 144, pp. 129–141.

Mendes, F. H., 2014. *Tutorial Para Iniciantes: Software ENVI-met versão 3.1* [Online]. Available at http://cmq.esalq.usp.br/wiki/lib/exe/fetch.php?media=publico:projetos:envi-met31_tutorial_iniciantes.pdf (Accessed 6 July 2019).

NASA, 2019 (National Aeronautics and Space Administration). *2018 fourth warmest year in continued warming trend: Global Climate Change* [Online]. Available at <https://climate.nasa.gov/news/2841/2018-fourth-warmest-year-in-continued-warming-trend-according-to-nasa-noaa/> (Accessed 21 October 2019).

Prado, R. T. A. and Ferreira, F. L., 2005. 'Measurement of albedo and analysis of its influence the surface temperature of building roof materials', *Energy and Buildings*, vol. 37, no. 4, pp. 295–300.

Richard, C., Doré, G., Lemieux, C., Bilodeau, J.-P. and Haure-Touzé, J., 2015. 'Albedo of Pavement Surfacing Materials: In Situ Measurements', *Cold Region Engineering*, pp. 181–192.

Roberts, D., 2019. *Barcelona's radical plan to take back streets from cars: Introducing Superblocks* [Online]. Available at <https://www.vox.com/energy-and-environment/2019/4/9/18300797/barcelona-spain-superblocks-urban-plan> (Accessed 19 August 2019).

Rueda, S. 2016. *La Supermanzana, nueva célula urbana para la construcción de un nuevo modelo funcional y urbanístico de Barcelona* [Online], Barcelona. Available at <http://www.bcnecologia.net/es/proyectos/la-supermanzana-nueva-celula-urbana-para-la-construccion-de-un-nuevo-modelo-funcional-y> (Accessed 3 May 2019).

Salvati, A., Roura, H. C. R. and Cecere C., 2017. 'Assessing the urban heat island and its energy impact on residential buildings in Mediterranean climate: Barcelona case study', *Energy and Buildings*, vol. 146, pp. 38–54.

Salvati, A., Roura Helena C. and Cecere, C., 2016. 'Urban heat island prediction in the mediterranean context: an evaluation of the urban weather generator model', *ACE: Architecture, City and Environment*.

Servei, 2019 (Servei Meteorològic de Catalunya). *Dades de l'estació automàtica Barcelona - el Raval* [Online]. Available at <http://www.meteo.cat/observacions/xema/dades?codi=X4&dia=2018-08-22T00:00Z> (Accessed 25 October 2019).

Stewart, I. D. and Oke, T. R., 2012. 'Local Climate Zones for Urban Temperature Studies', *Bulletin of the American Meteorological Society*, vol. 93, no. 12, pp. 1879–1900.

Tsoka, S., Tsikaloudaki, K. and Theodosiou, T., 2017. 'Urban space's morphology and microclimatic analysis: A study for a typical urban district in the Mediterranean city of Thessaloniki, Greece', *Energy and Buildings*, vol. 156, pp. 96–108.

UNSD, 2018 (United Nations Statics Division). *Energy Statistics Pocketbook 2018* [Online], New York. Available at <https://unstats.un.org/unsd/energy/pocket/2018/2018pb-web.pdf> (Accessed 15 July 2019).

Vuckovic, M., Kiesel, K. and Mahdavi, A., 2015a. 'Toward Advanced Representations of the Urban Microclimate in Building Performance Simulation', *Energy Procedia*, vol. 78, pp. 3354–3359.

Vuckovic, M., Maleki, A., Kiesel, K. and Mahdavi, A., 2015b. 'Simulation-Based Assessment of UHI Mitigation in Central European Cities', *14th International Conference of the International Building Performance Simulation Association*, Hyderabad, India, Dec. 7-9, 2015., pp. 971–978.

Walther, E. and Goestchel, Q., 2018. 'The P.E.T. comfort index: Questioning the model', *Building and Environment*, vol. 137, pp. 1–10.